



저작자표시-비영리-변경금지 2.0 대한민국

이용자는 아래의 조건을 따르는 경우에 한하여 자유롭게

- 이 저작물을 복제, 배포, 전송, 전시, 공연 및 방송할 수 있습니다.

다음과 같은 조건을 따라야 합니다:



저작자표시. 귀하는 원저작자를 표시하여야 합니다.



비영리. 귀하는 이 저작물을 영리 목적으로 이용할 수 없습니다.



변경금지. 귀하는 이 저작물을 개작, 변형 또는 가공할 수 없습니다.

- 귀하는, 이 저작물의 재이용이나 배포의 경우, 이 저작물에 적용된 이용허락조건을 명확하게 나타내어야 합니다.
- 저작권자로부터 별도의 허가를 받으면 이러한 조건들은 적용되지 않습니다.

저작권법에 따른 이용자의 권리는 위의 내용에 의하여 영향을 받지 않습니다.

이것은 [이용허락규약\(Legal Code\)](#)을 이해하기 쉽게 요약한 것입니다.

[Disclaimer](#)

공학박사 학위논문

**Development of Bacterial Quorum Quenching Sheet Media  
and Application of Cellulose Degrading Bacteria for  
Biofouling Control in MBR for Wastewater Treatment**

정족수감지 억제 미생물 고정화 판형담체 개발과 셀룰로오스 분해  
미생물의 적용을 통한 하폐수처리용 분리막 생물반응기에서의  
생물막오염 제어

2017 년 2 월

서울대학교 대학원

화학생물공학부

남 창 현



## **Abstract**

# **Development of Bacterial Quorum Quenching Sheet Media and Application of Cellulose Degrading Bacteria for Biofouling Control in MBR for Wastewater Treatment**

Chang Hyun Nahm

School of Chemical and Biological Engineering

The Graduate School

Seoul National University

Although a membrane bioreactor (MBR) has been widely applied for advanced wastewater treatment over the past two decades, membrane biofouling (i.e., biofilm formation on the membrane surface) still remains a major drawback that limits the widespread use. Recently, quorum quenching (QQ) has emerged as an effective biological control strategy for membrane biofouling in MBR. In particular, the use of QQ bacteria entrapping media (QQ-media) was proven to be efficient and economically feasible biofouling control in MBR. However, few studies have been conducted to explore how to increase the performance of QQ-media for biofouling control in MBR with different membrane types. In addition, because QQ is not effective in biofouling control after biofilm was formed, further

studies are required to develop a new bacterium targeting degradation of already formed biofilm. In this study, QQ bacteria entrapping sheets (QQ-sheets) were developed as a new shape of moving QQ-media for alleviating in biofouling in MBR with a hollow fiber module. Moreover, cellulolytic bacteria were applied to mitigate biofouling in MBR by degrading cellulose-induced biofilm as an alternative biological control strategy to QQ-based control.

Firstly, QQ-sheets as a new shape of moving QQ-media were developed to overcome the limitation of previously reported QQ-beads, particularly in MBR with a hollow fiber (HF) module. In a lab-scale MBR, QQ-sheets with a thickness of 0.5 mm exhibited a greater physical washing effect than did QQ-beads with a diameter of 3.5 mm because the former collided with membrane surfaces at the inner as well as the outer part of HF bundles, whereas the latter only made contact with the outer part. Moreover, QQ-sheets showed 2.5-fold greater biological QQ activity than did QQ-beads due to their greater total surface area at a fixed volume of QQ-media. Taking into account dense structure of HF bundles, these combined merits of QQ-sheets bring the QQ technology to practical applications in MBRs with commercial HF modules.

Secondly, cellulase was introduced to MBR as a cellulose-induced biofilm control strategy. For practical application of cellulase to MBR, a cellulolytic (i.e., cellulose-degrading) bacterium, *Undibacterium* sp. DM-1, was isolated from a lab-scale MBR for wastewater treatment. Prior to its application to MBR, it was confirmed that the cell-free supernatant of DM-1 was capable of inhibiting biofilm formation and of detaching the mature biofilm of activated sludge and cellulose-producing bacteria. This suggested that cellulase could be an effective anti-

biofouling agent for MBRs used in wastewater treatment. *Undibacterium* sp. DM-1 entrapping beads (i.e., cellulolytic-beads) were applied to a continuous MBR to mitigate membrane biofouling 2.2-fold, compared to an MBR with vacant-beads as a control. Subsequent analysis of cellulose content in biofilm formed on the membrane surface revealed that this mitigation was associated with an approximately 30% reduction in cellulose by cellulolytic-beads in MBR.

### **Keywords**

Membrane bioreactor (MBR), Biofouling control, Bacteria entrapping media, Quorum quenching, Cellulase, Hollow fiber membrane, Bead, Sheet

*Student Number:* 2013-20969



# Table of Contents

<b>Abstract</b>	<b>i</b>
<b>Table of Contents</b> .....	<b>v</b>
<b>List of Figures</b> .....	<b>ix</b>
<b>List of Tables</b> .....	<b>xvii</b>
<b>Chapter I</b> .....	<b>1</b>
<b>I.1. Backgrounds</b> .....	<b>3</b>
<b>I.2. Objectives</b> .....	<b>5</b>
<b>Chapter II</b> .....	<b>7</b>
<b>II.1. Membrane Bioreactor (MBR)</b> .....	<b>9</b>
II.1.1. Overview: MBR for Advanced Wastewater Treatment .....	9
II.1.2. Membrane Modules .....	1 8
II.1.3. Trend in MBR Market .....	2 4
II.1.4. Membrane Fouling in MBR .....	2 7
II.1.5. Fouling Control in MBR .....	3 2
<b>II.2. Quorum Sensing (QS)</b> .....	<b>3 9</b>
II.2.1. Definition and Mechanism .....	3 9
II.2.2. Mechanism .....	4 1
II.2.2.1. Gram-Negative Bacteria QS .....	4 1
II.2.2.2. Gram-Positive Bacteria QS .....	4 7
II.2.2.3. Interspecies QS communication .....	4 9



II.2.2.4. Other QS System.....	5	1
II.2.3. Role of QS in Biofilm Formation.....	5	6
II.2.4. Detection of AHL Signal Molecules.....	6	0
<b>II.3. Quorum Quenching (QQ).....</b>	<b>6</b>	<b>6</b>
II.3.1. QS Control Strategy.....	6	6
II.3.1.1. Blockage of AHL Synthesis.....	6	8
II.3.1.2. Interference with Signal Receptors.....	7	0
II.3.1.3. Degradation of AHL Signal Molecules.....	7	1
II.3.2. Application of QQ to Control Biofouling in Membrane Process.....	7	6
II.3.2.1. Enzymatic QQ Application.....	7	6
II.3.2.2. Bacterial QQ.....	8	1
<b>II.4. Immobilization Technique for biocatalyst.....</b>	<b>9</b>	<b>5</b>
II.4.1. Whole-Cell Immobilization Method.....	9	5
II.4.2. Hydrogel.....	9	8
II.4.3. Nanofiber (Electrospun).....	1	0
<b>II.5. Extracellular Polymeric Substances (EPS).....</b>	<b>1</b>	<b>0</b>
II.5.1. Role of EPS in Biofilm Matrix: House of Biofilm Cells.....	1	0
II.5.2. Polysaccharides: Key Elements of EPS for Biofilm Formation....	1	0
II.5.3. Control of Membrane Biofouling by Disruption of EPS.....	1	1
<b>Chapter III.....</b>	<b>1</b>	<b>1</b>
<b>III.1. Introduction.....</b>	<b>1</b>	<b>2</b>
<b>III.2. Materials and Methods.....</b>	<b>1</b>	<b>2</b>
III.2.1. Preparation of QQ-media.....	1	2
III.2.2. Fabrication of Hollow Fiber Modules.....	1	2
III.2.3. Fabrication of Polyacrylic Stick Modules.....	1	2

III.2.4. Assessment of Physical Washing Effect .....	1 2 8
III.2.5. Assessment of QQ Activity .....	1 2 9
III.2.6. MBR Operation .....	1 3 0
III.2.7. Analytical Methods .....	1 3 3
<b>III.3. Results and Discussion .....</b>	<b>1 3 4</b>
III.3.1. Comparison of QQ Efficiency using QQ-beads between Single- and Multi-layer HF Modules .....	1 3 4
III.3.2. Development of Sheet-shaped Media .....	1 3 9
III.3.3. Evaluation of Biofouling Control by QQ-sheets in MBRs with Single- and Multi-layer HF Modules .....	1 4 8
III.3.4. Direct Comparison of Biofouling Mitigation between QQ-sheets and QQ-beads in MBR with HF Module .....	1 5 2
<b>III.4. Conclusions .....</b>	<b>1 5 4</b>
<b>Chapter IV.....</b>	<b>1 5 5</b>
<b>IV.1. Introduction .....</b>	<b>1 5 7</b>
<b>IV.2. Material and Methods.....</b>	<b>1 5 9</b>
IV.2.1. Bacterial Strains and Culture Conditions .....	1 5 9
IV.2.2. Visualization of Cellulose and Biofilms of Activated Sludge.....	1 5 9
IV.2.3. Isolation of Cellulolytic Microorganisms and Cellulose-producing Bacteria from MBR .....	1 6 1
IV.2.4. Assay for Biofilm Formation and Detachment.....	1 6 4
IV.2.5. Preparation of Beads for MBR Application.....	1 6 5
IV.2.6. Biostability of Cellulolytic-beads in MBR .....	1 6 6
IV.2.7. MBR Operation .....	1 6 6
IV.2.8. Analysis of Cellulose and EPS in Biofilm in MBR.....	1 6 9
<b>IV.3. Results and Discussion .....</b>	<b>1 7 0</b>

IV.3.1. Effect of Cellulase on Biofilm Formation of Activated Sludge in MBR	1 7 0
IV.3.2. Isolation and Identification of Cellulolytic Microorganism .....	1 7 4
IV.3.3. Anti-biofouling Activity of <i>Undibacterium</i> sp. DM-1.....	1 7 6
IV.3.4. Effect of Cellulolytic-beads on Mitigation of Membrane Biofouling .....	1 8 0
IV.3.5. The Correlation between Cellulose, EPS and Membrane Biofouling in MBR .....	1 8 2
IV.3.6. Biostability of Cellulolytic-beads .....	1 8 7
<b>IV.4. Conclusions .....</b>	<b>1 9 0</b>
<b>Chapter V .....</b>	<b>1 9 1</b>
<b>국문초록 .....</b>	<b>1 9 5</b>
<b>Reference .....</b>	<b>1 9 7</b>

# List of Figures

Figure II- 1. Schematic diagrams of conventional activated sludge (CAS) and membrane bioreactor (MBR) process. (Source: <a href="http://env.kubota.co.jp">http://env.kubota.co.jp</a> ) .....	1 0
Figure II- 2. MBR configurations (a) Submerged/immersed MBR, (b) Side-stream/ external MBR (Chang et al., 2002b) .....	1 5
Figure II- 3. Pictures of Zeeweed-hollow fiber modules (manufactured by GE-Zenon) used in real wastewater treatment plants . .....	2 1
Figure II- 4. Global MBR market revenue and volume for wastewater treatment (Frost&Sullivan, 2013).....	2 5
Figure II- 5. Idealised view of fouling on membrane surface (Source: <a href="https://sites.google.com/site/algaeultrafiltration/current-issues/fouling-and-flux-optimisation">https://sites.google.com/site/algaeultrafiltration/current-issues/fouling-and-flux-optimisation</a> ).....	2 9
Figure II- 6. MBR fouling mechanism for operating at constant flux (Gkotsis et al., 2014) .....	3 0
Figure II- 7. The number of published research on MBR and fouling since 1993 (Source: Web of science) .....	3 1
Figure II- 8. UF permeability on application of <i>P. aeruginosa</i> and <i>Acinetobacter johnsonii</i> simultaneously with/without their lytic phages (Yoon, 2015).....	3 6
Figure II- 9. Population density-dependent gene regulation. Increasing number of bacterial cells may due to clonal growth. Filled dots indicates the intercellular signal molecule (Federle and Bassler, 2003) .....	4 0
Figure II- 10. Structures of different QS signal molecules. (Saghi et al., 2015).....	4 3
Figure II- 11. General model of AHL QS process in Gram-negative bacteria (Fetzner, 2015). .....	4 4

Figure II- 12. General model for peptide QS in Gram-positive bacteria. (Akin, 1987b).	4 8
Figure II- 13. QS circuits in <i>V. harveyi</i> bacteria (Mc Grath and van Sinderen, 2007).....	5 0
Figure II- 14. Structure of DSF family and related signal molecules from a range of bacteria (Ryan and Dow, 2011).....	5 4
Figure II- 15. An extracellular enzyme from <i>X. campestris</i> can disperse the aggregates light microscopy of (a) cultures of an <i>rpf</i> mutant after growth and (b) the same culture after treatment of DSF .....	5 5
Figure II- 16. (Top) epifluorescence photomicrographs of the wild type (PA01) and the <i>lasI</i> mutant (PA0-JP1) grown with or without the autoinducer, 3OC12-HSL added to the medium. (Bottom) views of Z series of wild-type and <i>lasI</i> mutant biofilms (with or without 3OC12-HSL) acquired by scanning confocal laser microscopy.....	5 8
Figure II- 17. Occurrence of AHL signals in biocake during continuous MBR operation: (a) 22 h, (b) 46 h, (c) 58 h, and (d) 72 h (Yeon et al., 2008). .....	5 9
Figure II- 18. Construction and use of a bacterial AHL biosensor. The exogenous AHL interact with a LuxR family protein inside the bacterial biosensor (non-AHL producer), which results in the transcription of a reporter gene from a LuxR family-AHL regulated promoter as shown by the open triangle. The LuxR family gene is usually expressed from a constitutive promoter as shown with a filled triangle. The properties of biosensor can be dependent on report gene (s) (Steindler and Venturi, 2007) ....	6 2
Figure II- 19. Three major AHL QS control strategies: (1) Blockage of AHL synthesis, (2) Interference with signal receptor, and (3) AHL inactivation .....	6 7
Figure II- 20. (a) Mechanism of AHL production by LuxI-type AHL syntheses. (b) Structure of acyl-SAM analogs and SAM analogs (Cheong et al., 2013). .....	6 9
Figure II- 21. (A) Possible linkage degraded by quorum quenching enzymes in quorum sensing molecule <i>N</i> -acyl homoserine lactone and (B) corresponding degradation	

mechanism of quorum quenching enzymes. (Mashburn and Whiteley, 2005) .....	7 2
Figure II- 22. Schematic diagram showing the preparation of the MEC through layer-by-layer (LBL) deposition of PSS-chitosan on MIEX resin and enzyme immobilization via glutaraldehyde treatment. (Yeon et al., 2009).....	7 9
Figure II- 23. Schematic diagram of acylase immobilization onto the nanofiltration membrane surface by forming a chitosan-acylase matrix (Kim et al., 2011) .....	8 0
Figure II- 24. Reconstructed CLSM images of biofilm formed on the (a) raw and (b) Acyl-NF membranes after a 38-hour operation of the continuous NF of <i>P.aeruginosa</i> and then stained with SYTO 9 and ConA. (Kim et al., 2011). .....	8 0
Figure II- 25. Image of a microbial -vessel (MV) (Oh et al., 2012) .....	8 3
Figure II- 26. Schematic diagram of the ceramic microbial-vessel under the inner flow feeding mode (Cheong et al., 2014). .....	8 5
Figure II- 27. Images of live/dead QQ bacteria from the lumens of the used CMVs. (A) MBR-B with the CMV under the inner flow feeding mode, (B) MBR-C with the CMV under the normal feeding mode. Green color: live cell; red color: dead cell (Cheong et al., 2014).....	8 5
Figure II- 28. Comparison of SEM images of Vacant-Beads and QQ-Beads: cross section of a vacant bead (a) $\times 25$ , (b) $\times 1000$ , and (c) $\times 6000$ and of a CEB (d) $\times 25$ , (e) $\times 1000$ , and (f) $\times 6000$ . (Kim et al., 2013b) .....	8 7
Figure II- 29. Concept of QQ-Beads with combined effect of both biological QQ and physical washing effect (Kim et al., 2013b).....	8 8
Figure II- 30. Preparation scheme of a macrocapsule coated with a membrane layer through the phase inversion method. (Kim et al., 2015).....	9 0
Figure II- 31. (a) Photographs of an alginate bead and PSf, PES, PVDF coated macrocapsules. (b) SEM images of the outer surface, inner surface and cross-section	

of each macrocapsule coated with PSf, PES, and PVDF, respectively. (Kim et al., 2015)	9 1
.....	9 1
Figure II- 32. Fluorescence images of bead cross-sections entrapped with JB525 (an AHL reporter strain) only (a, near surface; a', center) and with both JB525 and BH4 (b, near surface; b', center).	9 3
.....	9 3
Figure II- 33. TMP profiles of MBRs with no media (Conventional MBR, black line), QQ-hollow cylinder (QQ-HC-MBR, red line), Vacant-hollow cylinder (Vacant-HC-MBR, blue line), and QQ-bead (QQ-bead-MBR, yellow line)	9 4
.....	9 4
Figure II- 34. Chemical structures of natural polymer and their derivatives which were blended with PVA hydrogel to form wound dressing materials, such as (a) sodium alginate, (b) chitosan, (c) dextran, (d) N-O-carboxymethyl chitosan, (e) hydroxyethyl starch (HES), and (f) (1,3), (1,6)- $\beta$ -glucan. (Kamoun et al., 2015)	1 0 0
.....	1 0 0
Figure II- 35. Schematic diagram for an electrospinning experiment with a perpendicular arrange (Manefield et al., 1999)	1 0 3
.....	1 0 3
Figure II- 36. Handheld device for the electrospinning of wound dressings. Inset: PEO fibers electrospun from aqueous solution onto a hand (Manefield et al., 1999)..	1 0 4
.....	1 0 4
Figure II- 37. An image of fluorescent <i>E. coli</i> cells (the red spots) embedded in electrospun PVA-polymer nanofibres. Both a large fibre and individual nanofibres with embedded fluorescent cells are shown (Eberl et al., 1996).	1 0 5
.....	1 0 5
Figure II- 38. Bacterial cells embedded in the matrix of biofilm (Xiong and Liu, 2010)	1 0 7
.....	1 0 7
Figure II- 39. Microcolonies in the mature biofilm are characterized by an extracellular polymeric substances (EPS) matrix, composed of extracellular DNA (eDNA), polysaccharides, proteins, amyloid fibres and bacteriophages (McDougald et al., 2012)	1 0 7
.....	1 0 7

Figure II- 40. Biofilm of <i>M. tuberculosis</i> overexpressing GFP were developed in standing culture by exposure to TRS and then stained with specific fluorophores: PYPRO Ruby for staining the proteins (Trivedi et al., 2016). .....	1 1 1
Figure II- 41. Evolution of the hydraulic resistance during the cleaning of Carbosep M5 membranes with Alcalase (1.40 units/L, 8.7 initial pH) (Argüello et al., 2002)..	1 1 5
Figure II- 42. Optical images images: (a) device (PBS treated), (b) device treated with dispersin B.....	1 1 7
Figure III- 1. Preparation scheme of QQ-media, (a) QQ-beads and (b) QQ-sheets ....	1 2 5
Figure III- 2. Schematic diagrams of (a) single-layer hollow fiber module (S-HF), (b) multi-layer hollow fiber module (M-HF), (c) single-layer polyacrylic stick module, and (d) multi-layer polyacrylic stick module. Hollow fiber modules and polyacrylic stick modules were used for MBR operation and batch experiment for assessment of physical washing effect, respectively. ....	1 2 7
Figure III- 3. Schematic diagram of the two MBRs (MBR A and MBR B) operated in parallel in six phases.....	1 3 1
Figure III- 4. TMP profiles of Vacant-bead-MBR and QQ-bead-MBR equipped with a) S-HF (phase S1) and b) M-HF (phase M1). Vacant-Beads ( $D = \sim 3.5$ mm, $N = 568$ ) and QQ-beads ( $D = \sim 3.5$ mm, $N = 550$ ) were used in the corresponding MBRs.....	1 3 7
Figure III- 5. (a) Images of a $10 \times 10$ mm QQ-sheet with a thickness of 0.5 mm, and (b) cross-sectional SEM images of a Vacant-sheet and a QQ-sheet (Magnifications are $150\times$ and $2000\times$ for the images on the left and right sides, respectively.) .....	1 4 0
Figure III- 6. (a) Comparison of physical washing effect of Vacant-beads ( $D = 3.5$ mm, $N = 550$ ) and Vacant-sheets ( $T = 0.5$ mm, $N = 260$ ) in a single layer polyacrylic fiber module and (b) visual comparison of the crystal violet stained region in the acrylic	



fibers. Error bar: standard deviation ( $n = 3$ ). Physical washing effect of Vacant-sheets and Vacant-beads was presented in the percentage of biofilm reduced relative to the control reactor..... 1 4 2

Figure III- 7. Comparison of the physical washing effect between Vacant-beads ( $D = 3.5$  mm,  $N = 545$ ) and Vacant-sheets ( $T = 0.5$  mm,  $N = 267$ ) in a multi-layer polyacrylic fiber module. (a) Differentiation of inner part (9 fibers) from outer part (16 fibers) in M-HF. Comparison of biofilm formed in control reactor with no media, reactor with Vacant-beads and reactor with Vacant-sheets at (b) the inner and (c) outer part of the multi-layer module. .... 1 4 4

Figure III- 8. QQ activity as a function of total surface area of QQ-sheets and QQ-beads. The QQ activity was defined as the number of nanomoles of degraded C8-HSL per min, which was measured after 30 min in the presence of QQ-media. The prepared QQ-media were as follows: QQ-beads ( $D = 3.5$  mm,  $N = 45$ ), thick QQ-sheets ( $W = 10$ mm,  $L = 10$  mm,  $T = 1.0$  mm,  $N = 9$ ), medium QQ-sheets ( $W = 10$ mm,  $L = 10$  mm,  $T = 0.7$  mm,  $N = 13$ ), and thin QQ-sheets ( $W = 10$ mm,  $L = 10$  mm,  $T = 0.5$  mm,  $N = 21$ ).D, L, N, W, and T represent diameter, length, number, width, and thickness of the media, respectively. Two QQ-media shown in red points were used in MBR operation. Error bar: standard deviation ( $n = 3$ ). .... 1 4 7

Figure III- 9. TMP profile of Vacant-sheet-MBR and QQ-sheet-MBR equipped (a) with S-HF (phase S2) and (b) with M-HF (phase M2). Vacant-sheets ( $T = 0.5$  mm,  $N = 260$ ) and QQ-sheets ( $T = 0.5$  mm,  $N = 265$ ) were inserted in each corresponding MBR. .... 1 5 0

Figure III- 10. Comparison of EPS content in the biofilm formed on the membrane surface in Vacant-sheet-MBR and QQ-sheet-MBR. Error bar: standard deviation ( $n = 3$ ) .... 1 5 1

Figure III- 11. TMP profile of QQ-bead-MBR and QQ-sheet-MBR equipped (a) with S-HF

(phase S3) and (b) with M-HF (phase M3). QQ-beads ( $D = 3.5$  mm,  $N = 540$ ) and QQ-sheets ( $T = 0.5$  mm,  $N = 255$ ) were used in each corresponding MBR..... 1 5 3

Figure IV- 1. Schematic diagram and operating conditions of vacant- and cellulolytic-MBR ..... 1 6 8

Figure IV- 2. Reconstructed 3D CLSM images: (a) distribution of cellulose enmeshed in the biofilm of activated sludge; (b) distribution of microorganisms in the biofilm before (Cellulase-) and after (Cellulase+) the addition of cellulase in the activated sludge; and (c) distribution of cellulose in the biofilm before (Cellulase-) and after (Cellulase+) the addition of cellulase in the activated sludge. .... 1 7 3

Figure IV- 3. Cellulolytic-activity from cell-free supernatant of six cellulolytic isolates grown for 48 h. Congo red staining (red) indicates presence of CMC and light orange regions are the NaCl-destained zones which indicate hydrolysis of CMC. ((a) *Undibacterium* sp. DM-1; (b) *Bacillus* sp. DM-2; (c) *Bacillus* sp. DM-3; (d) *Microbacterium* sp. DM-4; (e) *Aspergillus* sp. DM-5; and (f) *Trichosporon* sp. DM-6). ..... 1 7 5

Figure IV- 4. Test of (a) biofilm formation inhibitory and (b) biofilm detachment activity of the supernatant of DM-1 and commercial cellulase on test organisms: 1. *Enterobacter* sp. CPB-1; 2. *Rhodococcus* sp. CPB-2; and 3. Activated sludge. Error bar: standard deviation ( $n = 6$  as the technical replicates)..... 1 7 8

Figure IV- 5. TMP profiles of vacant- and cellulolytic-MBRs in (a) Phase 1 and (b) Phase 2, and  $T_{TMP}$  of the two MBRs in Phase 1. .... 1 8 1

Figure IV- 6. (a) Cellulose and (b) EPS content in the biofilm formed on the membrane surface in vacant- and cellulolytic-MBRs. Error bar: standard deviation ( $n = 3$ ). 1 8 5

Figure IV- 7. X-ray diffraction (XRD) patterns of extracted biofilm samples from the vacant- and cellulolytic-MBRs ..... 1 8 6

Figure IV- 8. (a) Cross-sectional images of cellulolytic- and vacant-beads; (b) viability of cellulolytic-beads during MBR ( $n = 4$ ); and (c) cellulolytic activity of fresh and used (i.e., 50 days of operation) cellulolytic-bead. Error bar: standard deviation ( $n = 3$ ).

..... 1 8 9

# List of Tables

Table II- 1. Key facets of the MBR configurations. (Judd, 2004) .....	1 6
Table II- 2. Summary of commercial MBR membrane module (Santos and Judd, 2010) 1	7
Table II- 3 Advantages and disadvantages of three major membrane configurations, hollow fiber membrane, flat sheet membrane, and tubular membrane. (Source:  <a href="http://dynatecsystems.com">http://dynatecsystems.com</a> ) .....	2 2
Table II- 4. Major manufacturing company for flat sheet and hollow fiber membrane  (Santos et al., 2011).....	2 3
Table II- 5. The 16 Largest-scale MBR plants in the world (Judd, S., the MBR site,  <a href="http://www.thembrsite.com">http://www.thembrsite.com</a> ).....	2 6
Table II- 6. General model of AHL QS process in Gram-negative bacteria. (Matthyse and  McMahan, 1998) .....	4 5
Table II- 7. AHL QS signal reporter stain.....	6 3
Table II- 8. List of QQ enzymes involved in the degradation of AHL QS signals .....	7 3
Table II- 9. General requirement for whole-cell immobilization.....	9 7
Table II- 10. Methods for synthesizing physical and chemical hydrogels (Steindler and  Venturi, 2007) .....	9 9
Table III- 1. MBR operating conditions (for all of the operation phases).....	1 3 2
Table III- 2. Average number of days required for on TMP jump, $T_{TMP}$ , to occur in MBR A  and B in each of the six phases.....	1 3 8
Table IV- 1. Biovolumes of microbial biofilm and cellulose formed by activated sludge in  the absence and presence of cellulase. LAS AF software was employed to calculate the	

biovolume. Parenthesis: Standard deviation ( $n = 4$ ).....	1 6 0
Table IV- 2. List of (a) cellulolytic microorganisms and (b) cellulose-producing bacteria isolated from the activated sludge in the lab-scale MBR operated in this study..	1 6 3

# **Chapter I**

## **Introduction**



## **I.1. Backgrounds**

Over the past two decades, a membrane bioreactor (MBR) has been widely used for an advanced wastewater treatment technology offering significant advantages such as small footprint and high effluent quality (Hentzer et al., 2001, Barber et al., 1997). For these reasons, the global market for MBR system grew to \$838.2 million in 2011 and forecast to reach up to \$3.44 billion by 2018. This represents a compound annual growth rate (CAGR) of 22% over this period (Hai et al., 2013). Nonetheless, the main drawback that hinders the wider spread of MBRs is membrane biofouling, which is mainly caused by biofilm formation on the membrane surface that increases operation and maintenance costs. Since the introduction of MBR technology, the countless studies have been conducted to reduce membrane biofouling but most of them were limited to physical and chemical strategies (Drews, 2010).

Recently, novel biological strategies have attracted considerable attention because they essentially consider fundamental reasons for natural biofilm formation. In particular, quorum quenching (QQ) have emerged as effective biological control strategies to uproot the biofilm formation and the consequent membrane biofouling in MBR (Xiong and Liu, 2010). Motivated by the discovery of quorum sensing (QS) involved in bacterial biofilm formation (Bassler et al., 1993), Yeon et al., identified that QS also plays a key role in membrane biofouling in MBR (Yeon et al., 2008). Earlier in the research, the enzymatic decomposition of QS signal molecules called *N*-acyl homoserine lactones (AHLs) (i.e., enzymatic QQ) was initiated to inhibit membrane biofouling in MBR (Yeon et al., 2009, Kim et al., 2011). In a follow-up study to overcome the limitation of enzymatic QQ such



as high cost and instability of enzyme, *Rhodococcus* sp. BH4 which produces AHL-degrading enzyme was isolated from a wastewater treatment plant and applied as a novel QQ bacterium (Oh et al., 2012). Mitigation of biofouling in MBR was achieved by bacterial QQ through microbial vessels encapsulating BH4 bacteria (QQ-vessels) (Oh et al., 2013, Weerasekara et al., 2014). The success of bacterial QQ shifted to develop more efficient QQ-media. As a result, spherical BH4 entrapping beads (QQ-beads) (Kim et al., 2013b), cylinder-shaped moving QQ-media (QQ-Cylinder (Lee et al., 2016b) and QQ-Hollow Cylinder (Lee et al., 2016c)) were developed as moving QQ-media to have both biological (QQ) and physical washing (friction) effect on mitigation of biofouling in MBR.

However, all previous studies on QQ-media have focused on improving anti-biofouling capabilities without full consideration of membrane module types. In particular, the QQ-media suitable for hollow fiber (HF) module has not been developed although HF modules are employed in MBR as a major membrane type. In addition, because QQ-media cannot completely control biofouling as well as degrade the already-formed biofilm, another bacteria entrapping media capable of degrading the biofilm is required for effective biofouling control. Especially, cellulose, one component in extracellular polymeric substances (EPS) (Kjelleberg and Givskov, 2007), has been shown to be involved in biofilm formation for several bacterial species (Robledo et al., 2012, Spiers et al., 2013, Serra et al., 2013). However, cellulose-degrading enzyme (i.e., cellulase) in biofouling control in MBR has not been investigated. Therefore, further development of bacteria entrapping media in physical and biological ways is required for more effective biofouling control in MBR and thus for widespread application of MBR technology.

## **I.2. Objectives**

The objective of this study was to develop bacteria entrapping media for effective biofouling control in MBR. This study focused on the supplementation of previously reported media in two aspects, i.e., modification of the media shape and change of microorganism targeting other biofilm formation pathway besides QQ. The specific objectives of this study are as follows:

### **(1) Development of QQ Bacteria Entrapping Sheets (QQ-Sheets) for Biofouling Control in MBR with a Hollow Fiber Module**

QQ-sheets were developed as a new shape of QQ-media to enhance the anti-biofouling performance in a QQ-MBR with a hollow fiber (HF) module. QQ-sheets were compared with QQ bacteria entrapping beads (QQ-beads) in terms of biological QQ activity and physical washing effect. The enhanced anti-biofouling performance of QQ-sheets was also evaluated in continuous laboratory scale MBR with a HF module in comparison with QQ-beads.

### **(2) Application of Cellulose-degrading Bacteria Entrapping Beads (Cellulolytic-Beads) for Biofouling Control in MBR**

The effect of cellulose, one of polysaccharides, on biofilm formation of activated sludge in MBR was investigated. A cellulolytic (i.e., cellulose-producing) bacterium, *Undibacterium* sp. DM-1, was isolated from a laboratory-scale MBR for reducing the cellulose-induced biofouling in MBR. The ability of DM-1 to reduce biofilms was investigated in activated sludge and in two different cellulose-producing bacteria, *Enterobacter* sp. CPB-1 and *Rhodococcus* sp. CPB-2.



# **Chapter II**

## **Literature Review**



## **II.1. Membrane Bioreactor (MBR)**

### **II.1.1. Overview: MBR for Advanced Wastewater Treatment**

A membrane bioreactor (MBR) is an advanced wastewater treatment process where a biological activated sludge process is combined with membrane filtration equipment (Hentzer et al., 2001). As depicted in Figure II- 1, the system of MBRs is similar to that of conventional activated sludge (CAS) with exception that the biomass including microorganisms responsible for removing the contaminants of concern are retained within the bioreactor component of the system using membrane rather than secondary clarifier. Elimination of the need for secondary clarifiers brings many advantages over conventional wastewater treatment processes. First, the integrated process can produce exceptional effluent quality capable of meeting the most stringent water quality requirements. In addition, it allows for efficient performance with a smaller foot prints and less sludge production, and easy retrofit of previous wastewater treatment plants.

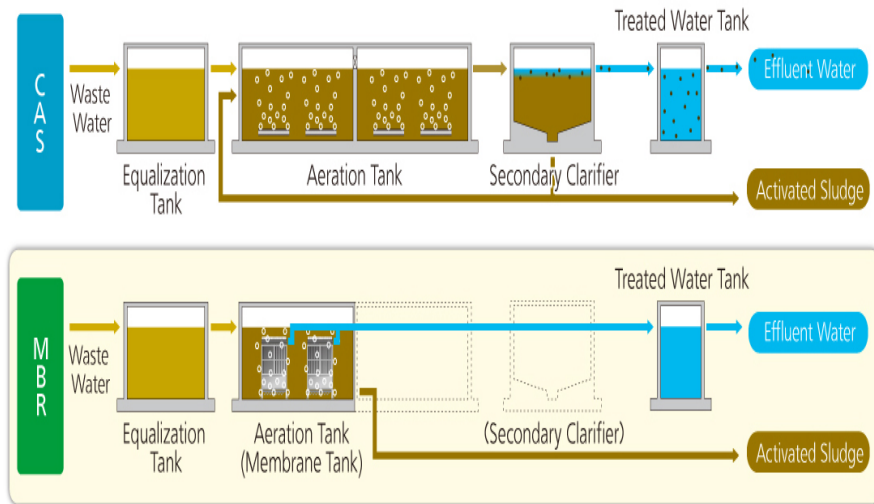


Figure II- 1. Schematic diagrams of conventional activated sludge (CAS) and membrane bioreactor (MBR) process. (Source: <http://env.kubota.co.jp>)

### **II.1.1.1. Advantages and Disadvantages of MBR**

There are four main advantages of MBR process in comparison with CAS process (Chang et al., 2002a)

(i) High quality effluent - The small pore size (less than 0.5  $\mu\text{m}$ ) of the membrane means that the treated effluent has very high quality and significantly reduced pathogen concentration. MBR processes provide a substantially clarified and disinfected effluent of high enough quality to be discharged to sensitive receiving bodies or to be reclaimed for applications such as urban irrigation, utilities or toilet flushing

(ii) Small footprint - The retention of the solids and the increase in SRT to generate higher biomass solids concentrations also impacts on the plant footprint. The increased concentrations mean that the same total mass of solids is contained in a smaller volume, such that the footprint is smaller.

(iii) Better biotreatment - concentration of biomass can be increased by increasing solids retention time (SRT) since SRT is an independent parameter in MBR. The longer SRT tends to provide better biotreatment overall and usually yields better quality of effluent. MBRs are especially effective at the biological removal of ammonia (i.e. nitrification)

(iv) Simple maintenance - settleability of sludge or microscopic observation of microorganism is not necessary. All that is required is check of trans-membrane pressure (TMP) and basic water quality analysis such as chemical oxygen demand (COD), total nitrogen (TN), or total phosphorus (TP) removal efficiency.

Although MBR process many advantages compared to a CAS process,



MBRs still remains some constraints to be solved (Chang et al., 2002a).

(i) Higher equipment and operating cost – although the capital cost of smaller size of the land could be saved by removing a settling tank, membrane module itself is not a cheap application. Also, a fouling on membrane results in loss of membrane permeability, forcing an operator to clean membrane once in a while. Also, operating MBR requires extra energy consumption such as electricity cost. MBR is known to usually use over 10 times higher energy cost than CAS dose. (Yamamoto et al., 1989)

(ii) Greater process complexity – because membrane separation process is supplemented, it requires additional operating protocols relating to the maintenance of membrane

### **II.1.1.2. MBR Configuration**

The basic need of MBR consideration is to design the suitable membrane system and the combination of biochemical effect parameters such as organic and hydraulic loading, sludge age and so on. As shown in Figure II- 2, there two basic types of MBR configurations based on the integration of membrane modules for wastewater treatment: 1) submerged/ immersed MBR and 2) side-stream/ external MBR (Chang et al., 2002b). And, the key facets of each configuration are summarized in Table II- 1.

Yamamoto et al. was the first introduce submerged MBR in an aeration tank for filtration (Drews, 2010). Submerged MBRs are common in municipal wastewater treatment processes due to its compatibility with biological activated sludge process. Membrane modules are directly immersed in the reactor. By the application of negative pressure, permeate flux is drawn through the membranes thus leaving biomass within the reactor which can be easily wasted (Chang et al., 2002b)..

In external configuration, membrane modules are fixed outside the reactor. External MBRs are usually used in industries for high strength wastewater with poor filterability. However, due to the high cost of pumping and recirculating of activated sludge from separate unit process back to bioreactor dissipates more energy (Chang et al., 2002b).

The performance of submerged and external MBR in terms of water treatment are similar, but overall operating and capital costs for submerged MBRs are typically much lower than those for external MBRs, and comparable to those for CAS process (Jefferson et al., 2000). Due to the absence of a high flow

recirculation pump, submerged MBRs consume much lower power than external MBRs. Thus, more than 99% of MBRs around the globe rely on submerged membranes based on the treated water volume, and this trend is expected to continue in the future (Yoon, 2015). In submerged MBR, perhaps a roughly equal number of hollow fiber and flat sheet membrane supplier exist. Some of the membrane manufacturers are summarized in Table II- 2. Especially, Kubota, Evoqua (formerly Siemens), Asahi Kasei, and GE are the major suppliers playing globally and the number of membranes are based on PVDF in the MBR market.

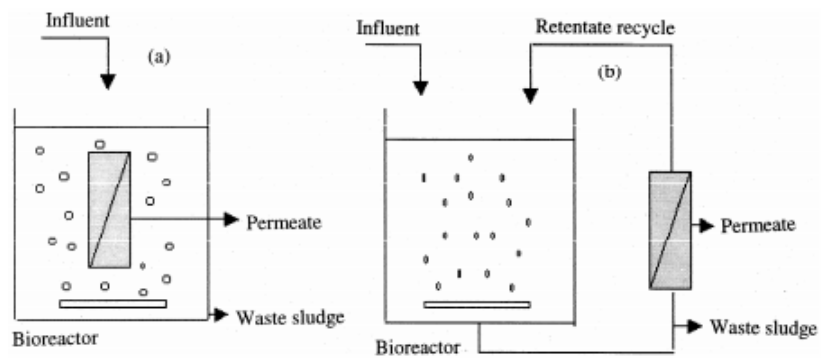


Figure II- 2. MBR configurations (a) Submerged/immersed MBR, (b) Side-stream/ external MBR (Chang et al., 2002b)

Table II- 1. Key facets of the MBR configurations. (Judd, 2004)

Sidestream	Submerged
Longest history (since early 1970s).	Most recent development (since 1990).
Membrane placed external to bioreactor.	Membrane placed in bioreactor.
Pumped system with permeation rate determined by transmembrane pressure and crossflow.	Permeate removed under hydrostatic head, with or without permeate suction, at rate partly determined by aeration
Higher flux and hydraulic resistance; lower aeration and membrane area requirement.	Lower flux and hydraulic resistance; greater aeration and membrane area requirement.
Stabilized flux with periodic chemical cleaning.	Stabilized flux with periodic chemical cleaning for flat plate membrane configuration; short backwash cycle with periodic chemical cleaning for hollow fiber configuration.
Greater overall energy demand; greater process (hydrodynamic) control.	Lower overall energy demand; reduced process (hydrodynamic) control.

Table II- 2. Summary of commercial MBR membrane module (Santos and Judd, 2010)

<b>Immersed (iMBR)</b>	
Flat sheet	Hollow fiber
A3- <i>MaxFlow</i> <sup>DE</sup>	Asahi Kasei- <i>Microzoa</i> <sup>®JP</sup>
Alfa Laval <sup>SE</sup>	Beijing Origin Water Technology Co. <sup>CN</sup>
Brightwater- <i>Membright</i> <sup>®IRL</sup>	<i>Ecologix-EcoFlon</i> <sup>TM</sup> , <i>EcoFil</i> <sup>CN</sup>
Colloide- <i>Sub snake</i> <sup>NIR</sup>	ENE Co., Ltd.- <i>SuperMAK</i> <sup>KR</sup>
Ecologix- <i>Ecoplate</i> <sup>TM</sup> , <i>EcoSepro</i> <sup>CN</sup>	GE Zenon- <i>Zeeweed</i> <sup>®US</sup>
Huber- <i>VRM</i> <sup>®</sup> ; <i>VUM</i> <sup>®</sup> / <i>GreyUse</i> <sup>DE</sup>	Hangzhou H-Filtration Membrane Technology Engineering Co., Ltd. <sup>MR</sup> <sup>CN</sup>
Jiangsu Lantian Peier Memb. Co. Ltd. <sup>CN</sup>	Koch Membrane System- <i>Puron</i> <sup>®US</sup>
KOReD- <i>Neofil</i> <sup>KR</sup>	Korean Membrane System- <i>KSMBR</i> <sup>®KR</sup>
Kubota-ES/EK <sup>JP</sup>	Litree- <i>LH3</i> <sup>CN</sup>
Microdyn-Nadir- <i>Biocel</i> <sup>®DE</sup>	Memstar-SMM <sup>SG</sup>
Pure Envitech Co., Ltd.- <i>ENVIS</i> <sup>KR</sup>	Mitsubishi Rayon- <i>Sterapore SUR</i> <sup>®</sup> ; <i>Sterapore SADP</i> <sup>®JP</sup>
Shanghai Megavision Memb. Tech. <sup>CN</sup>	Philos <sup>KR</sup>
Toray- <i>TRM</i> <sup>JP</sup>	Porous Fibers S.L.- <i>Micronet</i> <sup>®JP</sup>
Vina Filter- <i>Vinap</i> <sup>CN</sup>	SENUO Filtration Technology Co., Ltd.- <i>SENUOFIL</i> <sup>CN</sup>
Weise- <i>MicroClear</i> <sup>®DE</sup>	Shanghai Dehong Biology Medicine Sie- ce & Tech. Development Co., Ltd. <sup>CN</sup>
	Siemens Water Tech.- <i>Memjet</i> <sup>TM</sup> <sup>DE</sup>
	Sumitomo- <i>PoreFlon</i> <sup>®JP</sup>
	Superstring MBR Tech. Corp.- <i>SuperUF</i> <sup>CN</sup>
	Tianjin Motimo- <i>FP AIV</i> <sup>CN</sup>
	Vina Filter- <i>F08</i> <sup>CN</sup>
	Zena Membranes- <i>P5</i> <sup>CZ</sup>

## **II.1.2. Membrane Modules**

Because MBR consists of a membrane process and a suspended biological activated sludge, membrane is one of key component in MBR system. There are three major forms of membrane commercially available for use in MBRs: Hollow fiber, flat sheet, and tubular membrane. Each of the configurations has tended to be better suited for particular applications, so the choice of configuration is important when considering selecting MBR technology for a particular use. In general terms, it appears that flat sheet membranes are used almost exclusively for immersed MBRs for both industrial and municipal applications, where they are sometimes favored for smaller installations on the basis of their operational simplicity. Hollow fiber membranes are used almost exclusively for immersed MBRs, both for industrial and municipal applications, where they are often favored for larger installations on the basis of their lower membrane aeration energy demand. Also, advantages and disadvantages of hollow fiber, flat sheet and tubular membrane were summarized in Table II- 3

### **(1) Hollow fiber membranes**

Hollow fiber membrane was first developed in the 1960's by Mahon and the group of Dow chemical(Baker, 2004). Hollow fibre membranes continue to attract a considerable interest due to their exceptionally high surface area per volume, enabling membrane units to have a much higher packing density compared to flat-sheet and tubular membranes (Conte et al., 2006). For this reason, 75% of the total MBR installed capacity employs hollow fibers (Cote et al., 2012). Real MBR plants using a hollow fiber membrane uses such a packed and complicated module

as shown in Figure II- 3, a hollow fiber membrane with packed or dense bundles are applied in a real MBR plants to enhance its effective area for filtration. Currently, most of the commercially available hollow fibre membranes are made from polymeric materials such as polypropylene, polyethylene, polyimide and most of which are susceptible to chemical and thermal stresses, leading to membrane swelling and morphological changes (Cote et al., 2012, Wang et al., 2004b). They are constructed of a microporous structure having a dense selective layer on the outside surface. Numerous fibres must be packed into bundles and potted into tubes to form a membrane module. Modules with a surface area of even a few square feet may require many miles of fibers. Because a module must contain no defective or broken fibers, production requires strict quality control. Hollow fiber membranes can withstand very high pressures from the outside, but are limited on pressure exerted from the inside of the fiber, therefore backwash rates are limited to around twice the normal permeate rate. The feed fluid is applied on the outside of the fibers and the permeate is removed down the fiber bore. Hollow fiber membranes are applied in clean water applications and are used in MBR, but are limited to lower concentrations of solids than other membrane types. Major companies for supplying hollow fiber membrane are listed in Table II- 4

## (2) Flat sheet membranes

Flat sheet membranes have been used in membrane bioreactor (MBR) systems for the last 20 years. The membranes are typically built-into a submerged vacuum driven filtration systems which consist of stacks of modules each with a number of sheets. They are constructed of a paper like backing material with a membrane cast



on the surface of the paper. The membrane sheet is ultrasonically welded to both sides of a plastic plate. These sheets are assembled into a submerged membrane unit and spaced about 1/4" apart. The permeate passes through the membrane unit from the outside in. Course bubble air is sparged between the sheets to prevent solids from building up on the plates and dewatering the membranes. Flat sheet membranes used in Membrane Bioreactor (MBR) applications require a biofilm to be attached to the membrane. The membrane is a support structure to the biofilm which actually provides the filtration. Care must be taken to maintain the biofilm on the membranes to prevent failure. Major companies for supplying flat sheet membrane are listed in Table II- 4.

### (3) Tubular membranes

Tubular membranes were available for laboratory use as early as the 1920's and were first used in industrial application in the 1960's. Tubular membrane modules have one or more tubes of varying diameter. The tubes themselves are constructed of a microporous substrate material which provides mechanical strength and the membrane is cast on the inside of the tube as a finely porous surface layer. Wastewater is pumped through the membrane tubes and permeates flows through the engineered pores to produce treated water. Tubular membranes are known for their sturdy construction, long membrane life and high flux rates. Of all membrane types, they are more robust and can be subjected to high pressures in demanding applications. Tubular membranes are backwashed in some applications. With Backwash pressures of up to 15 psi, the large flow in the reverse direction efficiently removes solids from the membrane surface.

a) ZW150



b) ZW500A



c) ZW500C



d) ZW500D



Figure II- 3. Pictures of Zeeweed-hollow fiber modules (manufactured by GE-Zenon) used in real wastewater treatment plants .

Table II- 3 Advantages and disadvantages of three major membrane configurations, hollow fiber membrane, flat sheet membrane, and tubular membrane. (Source: <http://dynatecsystems.com>)

<b>Membrane configuration</b>	<b>Advantages</b>	<b>Disadvantages</b>
<b>Hollow Fiber</b>	<ul style="list-style-type: none"> <li>- Low Energy</li> <li>- Membrane Space efficient for large installations &gt;5 MGD</li> <li>- Cost effective for large installations</li> </ul>	<ul style="list-style-type: none"> <li>- Not Cost Effective for small plants</li> <li>- Membranes damaged easily</li> <li>- System is somewhat complicated</li> <li>- Can not operate with high MLSS</li> </ul>
<b>Flat Sheet</b>	<ul style="list-style-type: none"> <li>- Can be Low Energy</li> <li>- Cost effective for medium installations 0.5-5 MGD</li> </ul>	<ul style="list-style-type: none"> <li>- Not Cost Effective for small plants</li> <li>- Membranes damaged easily</li> <li>- Membrane can not be backwashed</li> <li>- Can not operate with low MLSS</li> </ul>
<b>Tubular</b>	<ul style="list-style-type: none"> <li>- Low Cost</li> <li>- Simple Operation</li> <li>- No special building or tank requirements</li> <li>- Entire system may be placed indoors</li> <li>- Membrane tank not required</li> </ul>	High Energy

Table II- 4. Major manufacturing company for flat sheet and hollow fiber membrane (Santos et al., 2011)

Flat sheet (FS)—20 products	Hollow fibre (HF)—25 products
A3— <i>MaxFlow</i> <sup>DE</sup>	Asahi Kasei— <i>Microzoa</i> <sup>JP</sup>
Alfa Laval— <i>Hollow Sheet</i> <sup>SE</sup>	Beijing EDI— <i>Canfil</i> <sup>CN</sup>
Brightwater— <i>MEMBRIGHT</i> <sup>IRL</sup>	Beijing Origin Water Technology— <i>BSY/RF</i> <sup>CN</sup>
Colloide— <i>SubSnake</i> <sup>NIR</sup>	Ecologix— <i>EcoFlon</i> <sup>TM</sup> , <i>EcoFil</i> <sup>CN</sup>
Ecologix— <i>EcoPlate</i> <sup>TM</sup> , <i>EcoSepro</i> <sup>CN</sup>	ENE Co., Ltd.— <i>SuperMAK</i> <sup>KR</sup>
Huber— <i>VRM</i> <sup>®</sup> ; <i>VUM</i> <sup>®</sup> / <i>GreyUse</i> <sup>DE</sup>	GE Zenon— <i>ZeeWeed</i> <sup>®</sup> <sup>US</sup>
Hyflux— <i>Petaflex</i> <sup>SG</sup>	Hangzhou H-Filtration— <i>MR</i> <sup>CN</sup>
Jiangsu Lantian Peier Memb. Co., Ltd <sup>CN</sup>	Koch Membrane Systems— <i>Puron</i> <sup>®</sup> <sup>US</sup>
LG/KOReD— <i>Green Membrane</i> <sup>KR</sup>	Korean Membrane Systems— <i>KSMBR</i> <sup>®</sup> <sup>KR</sup>
Kubota— <i>ES/EK</i> <sup>JP</sup>	Litree— <i>LH3</i> <sup>CN</sup>
Microdyn-Nadir— <i>BioCel</i> <sup>®</sup> <sup>DE</sup>	Memos— <i>MEMSUB</i> <sup>DE</sup>
Pure Envitech Co., Ltd.— <i>ENVIS</i> <sup>KR</sup>	Memstar— <i>SMM</i> <sup>SG</sup>
Shanghai Megavision <sup>CN</sup>	Mitsubishi Rayon— <i>Sterapore SUR</i> <sup>®</sup> ; <i>SADF</i> <sup>®</sup> <sup>JP</sup>
Shanghai SINAP <sup>CN</sup>	Philos <sup>KR</sup>
Toray— <i>TRM</i> <sup>JP</sup>	Porous Fibers S.L.— <i>Micronet</i> <sup>®</sup> <sup>SP</sup>
Vina Filter— <i>Vinap</i> <sup>CN</sup>	SENUO Filtration Technology— <i>SENUOHL</i> <sup>CN</sup>
Weise— <i>MicroClear</i> <sup>®</sup> <sup>DE</sup>	Shanghai Dehong <sup>CN</sup>
	Siemens Water Tech.— <i>MemPulse</i> <sup>TM</sup> <sup>DE</sup>
	Sumitomo— <i>PoreFlon</i> <sup>®</sup> <sup>JP</sup>
	Superstring MBR Tech. Corp.— <i>SuperUF</i> <sup>CN</sup>
	Tianjin Motimo— <i>FP AIV</i> <sup>CN</sup>
	Vina Filter— <i>F08</i> <sup>CN</sup>
	Zena Membranes— <i>P5</i> <sup>CZ</sup>

CN: China/Taiwan; CZ: Czech Republic; DE: Germany; DK: Denmark; FR: France; IRL: Southern Ireland; JP: Japan; KR: Korea; NIR: Northern Ireland; NL: Netherlands; SE: Sweden; SG: Singapore; SP: Spain; US: United States.

### **II.1.3. Trend in MBR Market**

MBR has been recognized as innovative technology for industry, sanitary and municipal wastewater treatment. Despite its relatively short history, the application of MBR has been grown rapidly showing its high potential for wastewater treatment and water reuse. As a result, these reasons, the global market for MBR system grew to \$838.2 million in 2011 and forecast to reach up to \$3.44 billion by 2018. It suggests that a compound annual growth rate of 22.4% over this period, which is faster than the total market for wastewater treatment plant of 7.3% CAGR (Hai et al., 2013). Figure II- 4 shows the trends in global MBR market and treatment volume.

In addition to their steady increase in number, MBR installations are also increasing in terms of scale. A number of plants with a treatment capacity of around 5 to 10 ML/d have been in operation for several years now whilst the next generation have design capacities up to 45 ML/d. Table II- 5 show the large-scale MBR plant (over 100 MLD) in the world. Especially, to date, the MBR plant in Stockholm, Sweden is the largest MBR plant in the world.

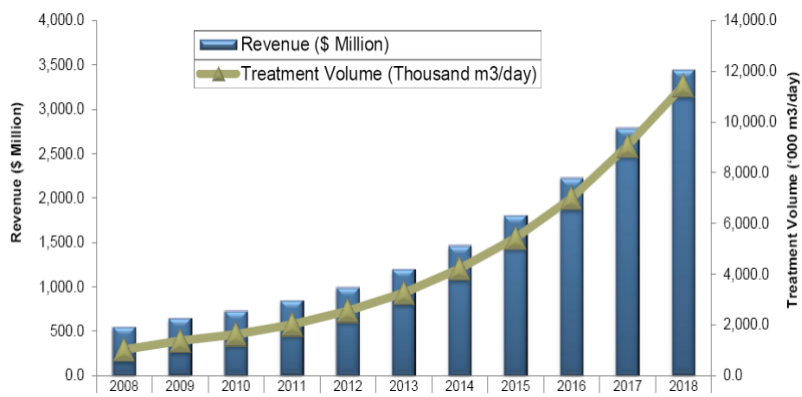


Figure II- 4. Global MBR market revenue and volume for wastewater treatment (Frost&Sullivan, 2013)

Table II- 5. The 16 Largest-scale MBR plants in the world (Judd, S., the MBR site, <http://www.thembrsite.com>)

Installations	Location	Technology Provider	(Expected)Date of Commissioning	PDF (MLD)
Henriksdal, Sweden	nr Stockholm, Sweden	GEWPT	2016-2019	864
Seine Aval	Acheres, France	GEWPT	2016	357
Canton WWTP	Ohio, USA	Ovivo USA/ Kubota	2015-2017	333
Water Affairs Integrative EPC	Xingyi, Guizhou, China	OW		307
Euclid, OH, USA	Ohio, USA	GEWPT	2018	250
9th and 10th WWTP	Kunming, Yunnan, China	OW	2013	250
Shunyi	Beijing, China	GEWPT	2016	234
Macau	Macau Special Administrative Region, China	GEWPT	2017	210
Wuhan Sanjintang WWTP	Hubei Province, China	OW	2015	200
Jilin WWTP (Phase 1, upgrade)	Jilin Province, China	OW	2015	200
Caotan WWTP PPP project	Xian, Shaanxi, China	OW		200
Brussels Sud	Brussels, Belgium	GEWPT	2017	190
Macau	China	GEWPT	2014	189
Riverside	California, USA	GEWPT	2014	186
Brightwater	Washington, USA	GEWPT	2011	175
Visalia	California, USA	GEWPT	2014	171

PDF: Peak daily flow, Megaliters per day (MLD)

GEWPT: GE Water and Process Technologies

OW: (Beijing) Origin Water

#### **II.1.4. Membrane Fouling in MBR**

During MBR operation, permeability performance continuously is reduced due to membrane fouling. As shown in Figure II- 5, the membrane fouling is the phenomenon for the accumulation of soluble materials and microbial flocs onto the filtration membrane, leading to increase in the overall membrane resistance. In practice, this is observed as an increase in the transmembrane pressure (TMP) as an increase in membrane fouling in MBRs operated at constant flux.

Membrane fouling can be divided into reversible fouling and irreversible fouling (Tsuyuhara et al., 2010). Physically reversible fouling can be restored through appropriate physical washing procedures such as backwashing or hydrodynamic scouring (surface washing) and chemical cleaning because the fouling can be easily removed. However, irreversible fouling occurs by pore plugging mechanisms and chemisorption, making it be harder to clean the membrane. In case of irreversible fouling, the loss in transmembrane flux cannot be recovered physically or chemically. Thus, the membranes should be treated by extensive chemical cleaning or be replaced.

MBR systems are operated under constant flux conditions with convection of foulant towards the membrane surface. Since fouling rate increases roughly with flux (Le Clech et al., 2003, McAdam et al., 2010a, McAdam et al., 2010b), sustainable operation dictates that MBRs should be operated at modest fluxed and preferably below the critical flux. Even sub-critical flux operation may lead to fouling according to a two-stage pattern (Pollice et al., 2005, Jefferson et al., 2000): a low TMP increase over an initial period followed by a rapid increase after a



certain critical time period. Prior to these two filtration stages, a conditioning period is generally observed (Zhang et al., 2006a, Jiang and Liu, 2010). The three-stage process (conditioning fouling, slow steady fouling and TMP rise-up) is summarized in Figure II- 6. (Jen et al., 1996, Zhang et al., 2006b, Jiang et al., 2013, Zhang et al., 2006c, Jiang and Liu, 2010)

Various studies on MBR fouling encompassing its mechanism have been presented in the literature (Johir et al., 2011, Judd, 2008, Meng et al., 2009). As shown in Figure II- 7, the numbers of published papers have dramatically increased since 2005.

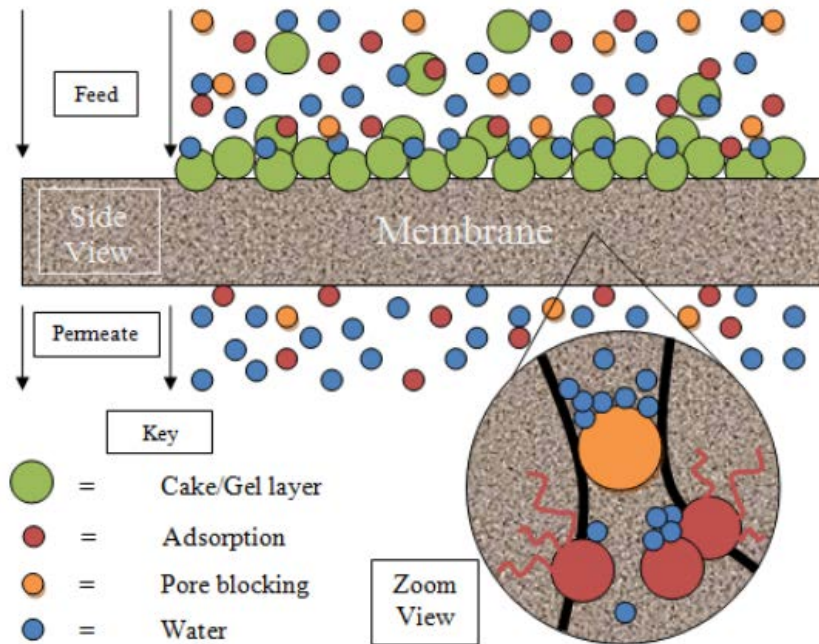


Figure II- 5. Idealised view of fouling on membrane surface (Source: <https://sites.google.com/site/algaeultrafiltration/current-issues/fouling-and-flux-optimisation>)

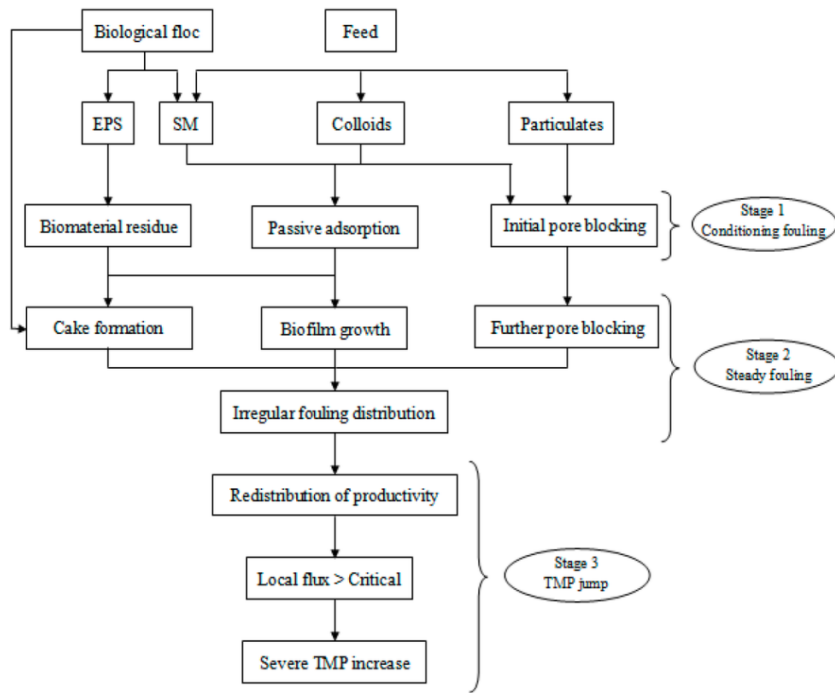


Figure II- 6. MBR fouling mechanism for operating at constant flux (Gkotsis et al., 2014)

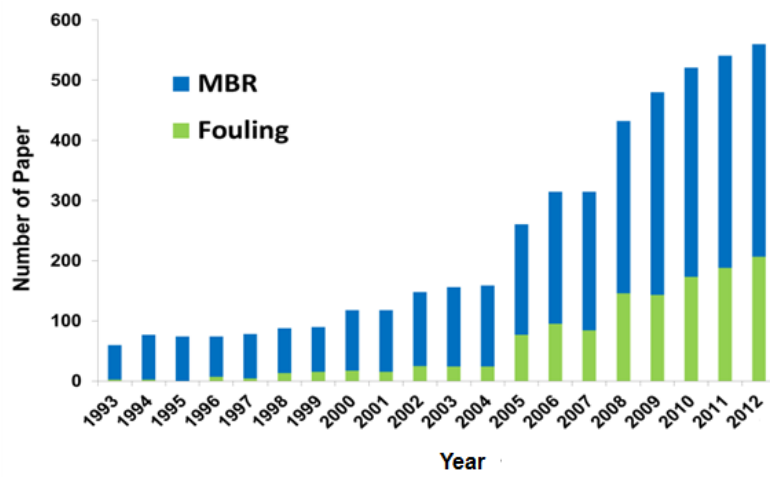


Figure II- 7. The number of published research on MBR and fouling since 1993  
 (Source: Web of science)

## **II.1.5. Fouling Control in MBR**

As mentioned previously, membrane fouling is one of the biggest challenges for MBR technology. Thus, many researchers have endeavored to overcome the fouling problem in MBR over 30 years. Several common and effective strategies for fouling control in MBR will be discussed in this section.

### **II.1.5.1. Physical Approach**

Aeration is an important factor to reduce the membrane biofouling in MBR system due to shear stress and surface tension (Xiong and Liu, 2010). In addition, it provides the oxygen required for the microbial growth. However, an aeration process significantly increases the energy consumption of MBR operation. Intermittent aeration, in which aeration was switched on and off alternatively was used as an alternative to solve the high consuming energy for aeration (Nagaoka et al., 1996, Yeom et al., 1999).

Another physical approach can be achieved either by backflushing (reversing the flow of permeation) or relaxation (pausing the permeation), while continuing to scour the membrane with air bubbles. Relaxation is a common fouling control method for either hollow fiber or flat sheet membranes, whereas backwashing is applicable only for hollow fiber membranes, not in flat sheet membranes (Hentzer et al., 2001, Monclus et al., 2010, Yuniarto et al., 2013). These strategies reduce the membrane fouling efficiently, but frequent application can hinder the production of the permeate.

Granular activated carbon (GAC) and powder activated carbon (PAC) are also commonly used as important physical approach for reduction the membrane

fouling because they remove organic matter by its adsorption ability (Loiselle and Anderson, 2003, Nguyen et al., 2012).

Application of particles has been emerged as one of great options for physical control because they have mechanical washing effect which reduces membrane fouling through the friction between the particles and membrane surface (Serra et al., 2013, Rosenberger et al., 2011).

### **II.1.5.2. Chemical Approach**

There are two chemical approaches for of membrane cleaning. One is the backwashing with chemicals such as chlorine (or bleach). For effective removal of residual and irreversible fouling, physical cleaning is supplemented with chemical cleaning (Judd, 2010). Another is a clean in place (CIP) to stay membrane module in the reactor during cleaning. Chemical cleaning is usually carried out with mineral or organic acids, caustic soda or sodium hypochlorite. These physical approaches are limited to solve the irreversible interactions between soluble compounds or bacteria and membrane material (Serra et al., 2013).

### **II.1.5.3. Biological Approach**

Microbial adhesion to surfaces and the consequent biofilm formation are universal phenomena occurring in both natural and engineering systems. It is responsible for numerous types of biofouling. Therefore, biological based strategies have great potential in mitigating biofouling because they target the essence of biofouling problems. In addition, the biological approaches provide many advantages such as higher efficiency, low toxicity, more sustainability and less bacterial resistance. Common biological approaches for fouling control are quorum quenching (QQ), enzymatic disruption of extracellular polymeric substances (EPS), disruption of biofilm by bacteriophage, application energy uncoupling and application of cell wall hydrolases. Detail description on QQ and enzymatic disruption of EPS will be discussed in next chapter.

#### (1) Control of membrane biofouling by bacteriophage

Bacteriophage or phage can infect the host bacteria by the rapid replication of virions to lyse the host cells or by incorporation into the host cell's genome (McGrath and van Sinderen, 2007). Doolittle et al. successfully used bacteriophages to disrupt *E. coli* and *P. aeruginosa* biofilms, respectively (Wang et al., 2004b, Santos et al., 2011). Also, bacteriophage T4 at a multiplicity of infection of ten was reported to a one-log decrease in biofilm density after a 90-min treatment. Another study also showed that phage F116 could cause a two-log decrease of *P. aeruginosa* biofilm (Le Clech et al., 2003). In addition to the natural phage, an engineered phage with multifunctions was able to enhance biofilms dispersal. Lu and Collins et al., designed an enzymatic phage which can express the Dispersin B,

a polysaccharide-hydrolyzing enzyme.(Lu and Collins, 2007)

Goldman et al., probably for the first time, employed bacteriophage to control ultrafiltration membrane biofouling. As shown in Figure II- 8, the addition of phages resulted in the reduction of microbial attachment to membrane surface by around 40%, and the performance of the membrane bioreactor treating the effluents from the sewage treatment plant was improved significantly in terms of membrane permeability. (Yoon, 2015)



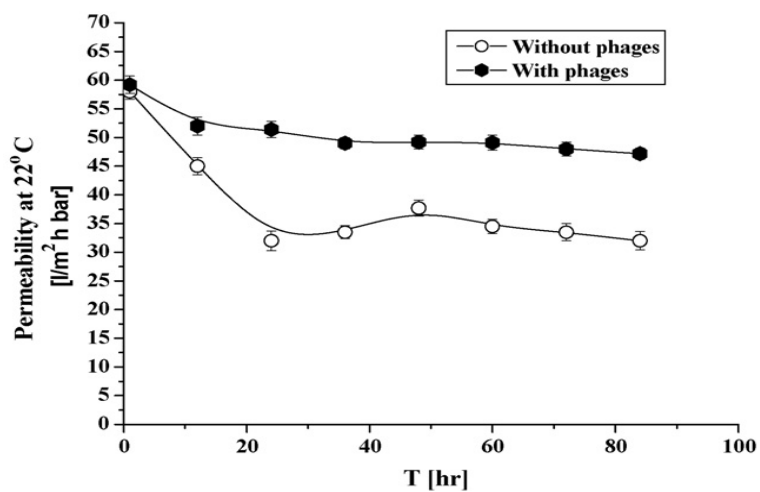


Figure II- 8. UF permeability on application of *P. aeruginosa* and *Acinetobacter johnsonii* simultaneously with/without their lytic phages (Yoon, 2015).

## (2) Control of membrane biofouling by energy uncoupling

Uncoupling of electron transport or oxidative phosphorylation is an effective strategy to inhibit the energy production, which can be achieved by adding various chemical uncouplers. Typically, uncouplers of oxidative phosphorylation are consisting of weak acids with substantial lipid solubility and can carry protons across the cellular membrane. Once inside the membrane matrix, the higher pH causes the uncoupler to deprotonate. As a result, the uncoupler has the effect of transporting hydrogen ion back into the matrix, bypassing the F<sub>0</sub> proton channel, and thereby preventing ATP synthesis. Jiang et al. investigated the effect of energy uncoupling on aerobic granular sludge biofilms and found that, when aerobic granular sludge biofilms were exposed to 3,3',4',5-tetrachlorosalicylanilide (TCS), a typical chemical uncoupler, complete disintegration of aerobic granular sludge biofilms was observed (McAdam et al., 2010a). Recently, the effect of a chemical uncoupler, dinitrophenol (DNP), was studied on microbial attachment to nylon membrane and glass slide surfaces. The attachment of microorganisms exposed to DNP onto the surfaces of nylon membrane and glass slide was reduced substantially as compared to the control free of DNP (Xu and Liu, 2010).

## (3) Control of membrane biofouling by cell wall hydrolase

Lysozyme can damage bacterial cell walls as one of hydrolytic enzymes of cell wall, and consequently it has been employed to prevent microbial attachment and biofilm formation onto solid surfaces. The lysozyme-immobilized polymeric packaging films exhibit bacterial growth-inhibiting properties (Pollice et al., 2005, Zhang et al., 2006a). Caro et al. coated the glycosidase hen egg white lysozyme to

a stainless steel surface and found that microbial attachment on the substrate coated with lysozyme could be completely inhibited as compared to the control without immobilization of lysozyme (Zhang et al., 2006b).

## **II.2. Quorum Sensing (QS)**

### **II.2.1. Definition and Mechanism**

Quorum sensing (QS) is a process of bacterial cell to cell communication where bacteria regulate gene expression in accordance with cell density through the use of signal molecules. Bacteria produce diffusible chemical signals called autoinducer, allowing bacteria population to communicate and coordinate group behavior (Withers et al., 2001, Waters and Bassler, 2005). In Figure II- 9, at low autoinducer concentration, a single cell doesn't include group behavior, however, as they grow, the concentration increases and thus a threshold level of autoinducer leads to an alteration in gene expressions (Federle and Bassler, 2003). Virulence is a phenotype of one such QS activity where pathogens commonly use in disease and infection processes. Bacterial activity involving QS was first observed in the mid-1960s by Hungarian microbiologist, Alexander Tomasz, in his studies of *Streptococcus pneumoniae* to take up DNA from its environment (Tomasz, 1965). Recently, QS process has been reported to regulate a diverse array of physiological activities. These processes include not only virulence but also motility, sporulation, sporulation, and biofilm formation (Akin, 1987b, Waters and Bassler, 2005).

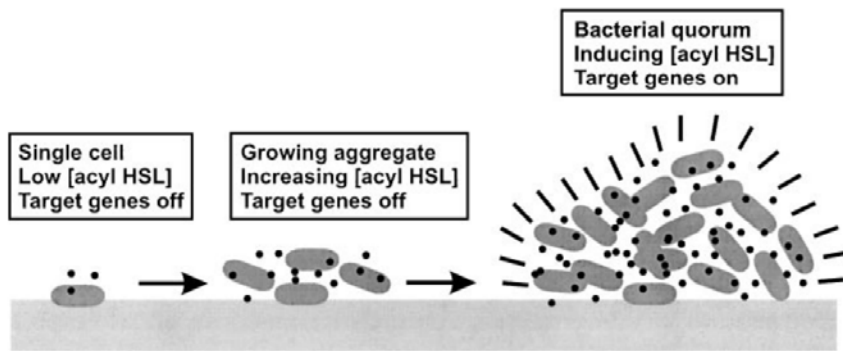


Figure II- 9. Population density-dependent gene regulation. Increasing number of bacterial cells may due to clonal growth. Filled dots indicates the intercellular signal molecule (Federle and Bassler, 2003)

## II.2.2. Mechanism

There are three general classes and some other classes of QS system based on the type of signal molecules and method used for their detection (Figure II- 10).

- (i) Gram-negative bacteria QS with *N*-acyl-homoserine lactone (AHL).
- (ii) Gram-positive bacteria QS with oligopeptide signal molecules.
- (iii) Interspecies QS communication with AI-2 molecules
- (iv) Other QS system

### II.2.2.1. Gram-Negative Bacteria QS

*N*-acyl homoserine lactones (AHLs) QS is commonly found in Gram-negative bacteria that interact with animal and plant hosts. As shown in Figure II- 10, AHLs consist of a homoserine lactone ring which is linked with an amide bond to a fatty acid chain of various length of carbon chains ranging from 4 to 14 carbon atoms that may contain an oxo or hydroxyl group at the third chain position and unsaturated bond (Federle and Bassler, 2003). AHL and its cognate regulatory circuit were first discovered in the bioluminescent marine bacterium *Vibrio fischeri*, which colonizes the light organ symbiosis with Hawaiian Bobtail squid *Euprymna scolopes* (Ruby and Lee, 1998).

General mechanism of LuxI/LuxR signaling circuit of gram-negative bacteria is depicted in Figure II- 11 (Nagaoka et al., 1996). The stages of QS step include the signal synthesis, diffusion, signal binding to receptor binding to promoter and QS gene expression. In detail, the LuxI-like proteins synthesize a specific AHL signaling molecule from the substrates *S*-adenosyl-L methionine

(SAM) and acylated acyl carrier protein (acyl-ACP) in a sequentially ordered reaction. The AHLs freely diffuse through the cell membrane. When there is sufficient population of the AHL-producing bacteria, the LuxR-like proteins are responsible for the specific receptors for AHLs signals and, when bound to AHLs, activate transcription of target gene. Up to date, the LuxI/R systems have been identified in over 25 species of Gram-negative bacteria and these bacteria were summarized in Table II- 6.

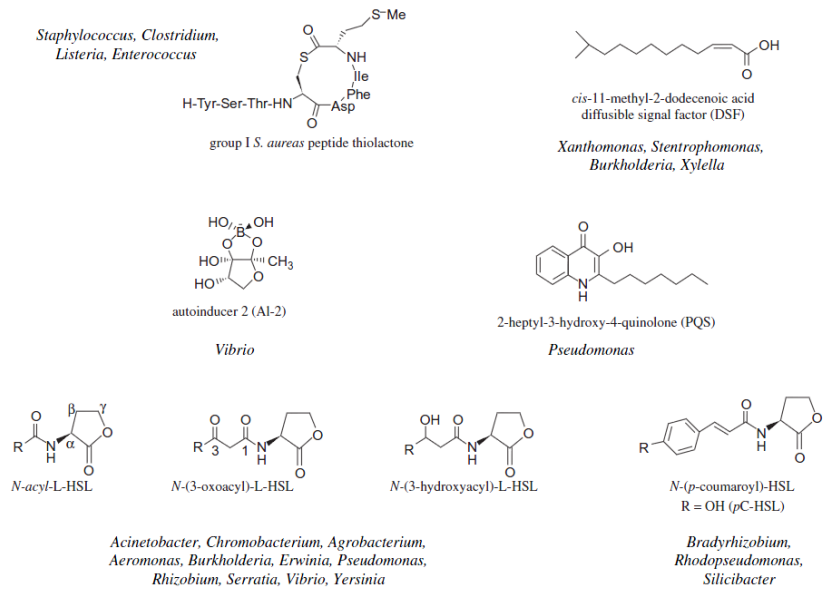


Figure II- 10. Structures of different QS signal molecules. (Saghi et al., 2015).



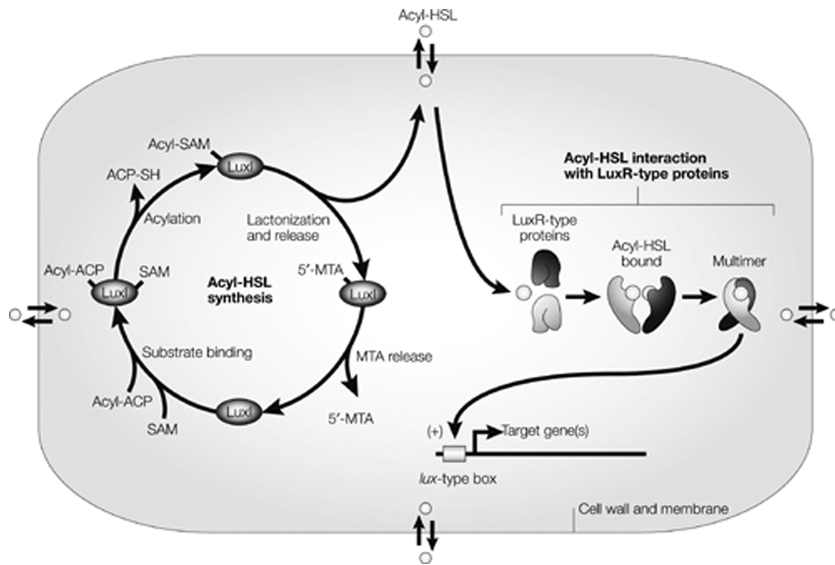


Figure II- 11. General model of AHL QS process in Gram-negative bacteria (Fetzner, 2015).

Table II- 6. General model of AHL QS process in Gram-negative bacteria.

(Matthysse and McMahan, 1998)

<b>Organism</b>	<b>Phenotype</b>	<b>Major AHLs</b>
<i>Aeromonas hydrophila</i>	Biofilms, exoproteases, virulence	C4-HSL, C6-HSL
<i>Aeromonas salmonicida</i>	Exoproteases	C4-HSL, C6-HSL
<i>Agrobacterium tumefaciens</i>	Plasmid conjugation	3-oxo-C8-HSL
<i>Agrobacterium vitiae</i>	Virulence	C14:1-HSL, 3-oxo-C16:1-HSL
<i>Burkholderia cenocepacia</i>	Exoenzymes, biofilm formation, Swarming motility, siderophore, virulence	C6-HSL, C8-HSL
<i>Burkholderia pseudomallei</i>	Virulence, exoproteases	C8-HSL, C10-HSL, 3-hydroxy-C8-HSL, 3-hydroxy-C10-HSL, 3-hydroxy-C14-HSL
<i>Burkholderia mallei</i>	Virulence	C8-HSL, C10-HSL
<i>Chromobacterium violaceum</i>	Exoenzymes, cyanide, pigment	C6-HSL
<i>Erwinia carotovora</i>	Carbapenem, exoenzymes, virulence	3-oxo-C6-HSL
<i>Pantoea (Erwinia) stewartii</i>	Exopolysaccharide	3-oxo-C6-HSL
<i>Pseudomonas aeruginosa</i>	Exoenzymes, exotoxins, protein secretion, biofilm, swarming motility, secondary metabolites, 4-quinolone signalling, virulence	C4-HSL; C6-HSL, 3-oxo-C12-HSL
<i>Pseudomonas aureofaciens</i>	Phenazines, protease, colony morphology, aggregation, root colonization	C6-HSL
<i>Pseudomonas chlororaphis</i>	Phenazine-1-carboxamide	C6-HSL
<i>Pseudomonas putida</i>	Biofilm formation	3-oxo-C10-HSL, 3-oxo-C12-HSL

Table II- 6. (continued)

<b>Organism</b>	<b>Phenotype</b>	<b>Major AHLs</b>
<i>Pseudomonas syringae</i>	Exopolysaccharide, swimming motility, virulence	3-oxo-C6-HSL
<i>Rhizobium leguminosarum</i> bv. <i>Viciae</i>	Root nodulation/symbiosis, plasmid transfer, growth inhibition, stationary phase adaptation	C14:1-HSL, C6-HSL, C7-HSL, C8-HSL, 3-oxo-C8-HSL, 3-hydroxy-C8-HSL
<i>Rhodobacter sphaeroides</i>	Aggregation	7-cis-C14-HSL
<i>Serratia</i> spp. ATCC 39006	Antibiotic, pigment, exoenzymes	C4-HSL, C6-HSL
<i>Serratia liquefaciens</i> MG1	Swarming motility, exoprotease, biofilm development, biosurfactant	C4-HSL, C6-HSL
<i>Serratia marcescens</i> SS-1	Sliding motility, biosurfactant, pigment, nuclease, transposition frequency	C6-HSL, 3-oxo-C6-HSL, C7-HSL, C8-HSL
<i>Serratia proteamaculans</i> B5a	Exoenzymes	3-oxo-C6-HSL
<i>Sinorhizobium meliloti</i>	Nodulation efficiency, symbiosis, exopolysaccharide	C6-HSL, C12-HSL, 3-oxo-C14-HSL, 3-oxo-C16:1-HSL, C16:1-HSL, C18-HSL
<i>Vibrio fischeri</i>	Bioluminescence	3-oxo-C6-HSL
<i>Yersinia enterocolitica</i>	Swimming and swarming motility	C6-HSL, 3-oxo-C6-HSL, 3-oxo-C10-HSL, 3-oxo-C12-HSL, 3-oxo-C14-HSL
<i>Yersinia pseudotuberculosis</i>	Motility, aggregation	C6-HSL, 3-oxo-C6-HSL, C8-HSL

### **II.2.2.2. Gram-Positive Bacteria QS**

The QS phenomenon is well established in Gram-negative bacteria, where N-acyl homoserine lactones are the diffusible signal molecules that regulate cell density dependent phenotypes. Similarly, Gram-positive bacteria regulate a variety of processes in the response to increasing cell density or growth phase dependent manner. However, because the QS circuit of gram-positive bacteria is completely different from that of gram-negative bacteria, they do not employ AHLs as signal molecules nor use LuxI/LuxR signaling circuit. Instead, the peptide (Figure II- 10) as a signal molecule of QS in gram-positive bacteria, secreted via a dedicated ABC (ATP-binding cassette) transporter protein.

As shown in Figure II- 12, the peptide molecules (extracellular pheromones) are recognized by two-component sensor kinase proteins interacting with cytoplasmic response regulator proteins (Kleerebezem et al., 1997, Novick and Muir, 1999). Most Gram-positive bacteria employ a common signaling substructure, a two-component circuit, with variation in the type and complexity of additional regulatory factors. Peptide autoinducers (pheromone) are secreted and recognized by membrane bound two-component sensor kinase proteins. The auto-phosphorylate on a histidine residue (H) and subsequently transfer the phosphoryl group to response regulators, which are phosphorylated on aspartate residues (D). Following phosphorylation, response regulator proteins activate or repress transcription of target gene.

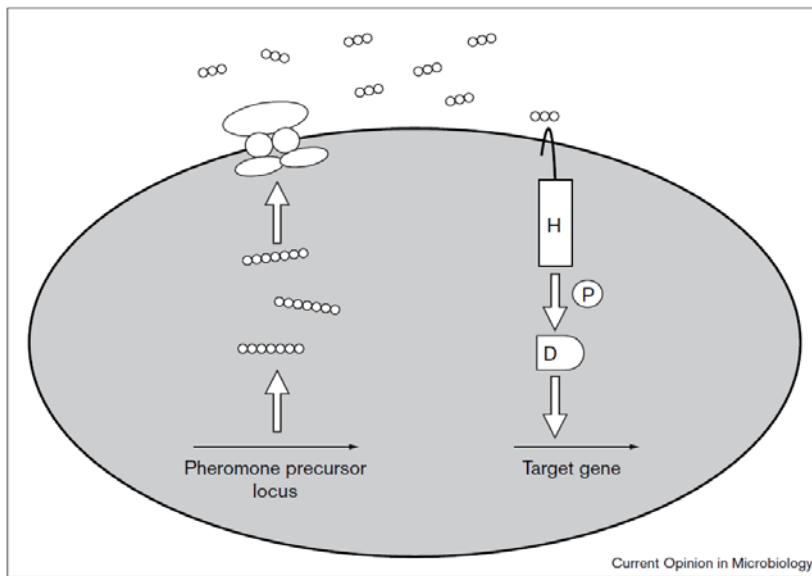


Figure II- 12. General model for peptide QS in Gram-positive bacteria. (Akin, 1987b)

### II.2.2.3. Interspecies QS communication

For intra-species cell to cell communication, AHLs and peptides represent two major classes of QS signal molecules used by Gram-negative bacteria and Gram-positive bacteria, respectively. Recently, a family of molecules called autoinducer-2 (in short, AI-2) has been found in both Gram-negative and Gram-positive bacteria (Figure II- 10) (Chen et al., 2002). It has been proposed that AI-2 is a non-species signal molecules that mediates intra- and interspecies communication among Gram-negative and Gram-positive bacteria (Thiel et al., 2009).

Bassler et al. first founded AI-2-based QS mechanism of *Vibrio harveyi* (Bassler et al., 1993, Bassler et al., 1994). This bacterium possesses two QS circuits to control expression of the luciferase structural gene (*luxCDABE*) (Federle and Bassler, 2003). As shown in Figure II- 13, *V. harveyi* produces and responds to AHLs and AI-2 signal molecules in the first and second circuits, respectively. Synthesis of AHLs and AI-2 molecules is dependent on LuxLM and LuxS, respectively. Also, LuxN and LuxQ is protein responsible for detection of AHLs and AI-2, respectively. Signals from both sensors are channeled to the shared integrator protein LuxU and LuxO. Each step flows phosphor-relay cascade. Finally, LuxO-phosphate controls the expression of the luciferase structural operon *luxCDABE* (Mc Grath and van Sinderen, 2007). Therefore, even though, if one QS circuit was blocked, *V. harveyi* produces luciferase gene using other QS circuit.

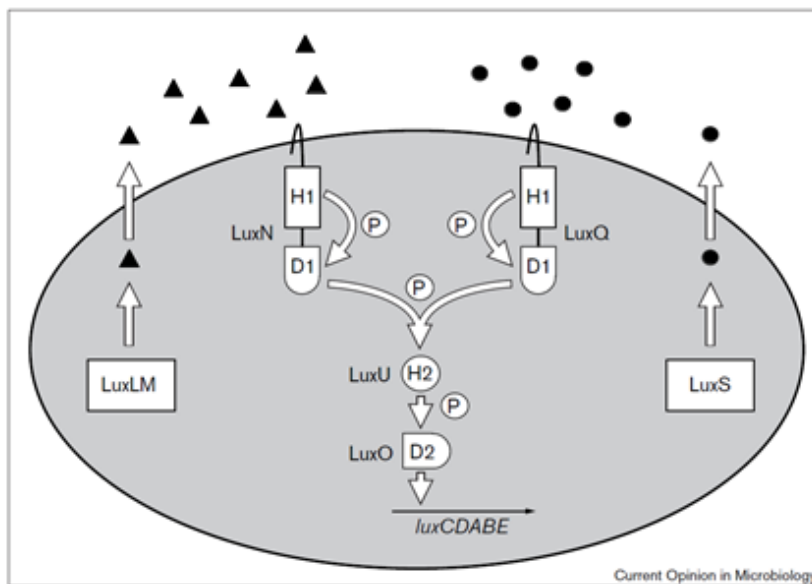


Figure II- 13. QS circuits in *V. harveyi* bacteria (Mc Grath and van Sinderen, 2007)

#### II.2.2.4. Other QS System

Along with AHLs signal molecules, at least two additional QS signal molecules have been identified in Gram-negative bacteria. These signal molecules include autoinducer 3 (AI-3), which is associated with virulence regulation in EHEC O157:H7 and the *Pseudomonas* quinolone signal (PQS), which is associated with *Pseudomonas aeruginosa* (Mashburn and Whiteley, 2005). AI-3 is associated with luxS homologs in EHEC O157:H7, however this signal itself is hydrophobic and the chemical or biological properties of AI-3 are totally different from those of the polar AI-2 signal molecule. Up to date, the molecular structure of AI-3 is unknown as is the gene responsible for AI-3 production (LaSarre and Federle, 2013).

Another novel autoinducer has recently been demonstrated to be involved in QS system of *Pseudomonas aeruginosa*. This chemical signaling molecule is noteworthy because the chemical nomenclature is 2-heptyl-3-hydroxy-4-quinolone (denoted PQS for *Pseudomonas* quinolone signal), totally different from homoserine lactone class (Pesci et al., 1999). PQS partially controls the expression of the elastase gene *lasB* in conjunction with the Las and Rhl QS systems. The expression of PQS requires LasR, and PQS in turn induces transcription of *rhII*. These data indicate that PQS is an additional link between the Las and Rhl circuits. The notion is that PQS initiates the Rhl cascade by allowing the production of the Rhl-directed autoinducer only after establishment of the LasI/LasR signaling cascade. PQS molecules are quite hydrophobic and have been shown to be transported between cells by outer membrane vesicles. There is also strong evidence that the PQS actually induces the formation of these vesicles through

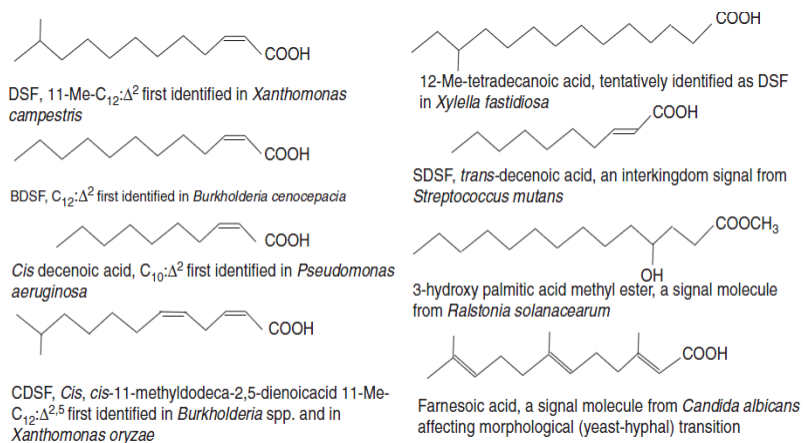


interference with  $Mg^{2+}$  and  $Ca^{2+}$  ions in the outer membrane. In a recent review, it was suggested that membrane vesicles may represent a mechanism for inter-kingdom signaling in the plant rhizosphere.

In addition, an interesting QS signal molecules called diffusible signal factors (DSF) has been found in the plant pathogen *Xanthomonas campestris pv. campestris* (*Xcc*) (Greiner and Wendorff, 2007). As shown in Figure II- 14, DSF has been characterized as the unsaturated fatty acid, cis-11-methyl-2-dodecenoic acid (Wang et al., 2004a) and its chemically related compounds have been considered to the DSF family. Synthesis and perception of the DSF signal require products of the *rpf* gene cluster. The synthesis of DSF is dependent on RpfF, which has some amino acid sequence similarity to enoyl-CoA hydratases, whereas the two-component system comprising the sensor kinase RpfC and regulator RpfG is implicated in DSF perception (Greiner and Wendorff, 2007, Slater et al., 2000, Fuqua and Greenberg, 2002, Ryan et al., 2006) Homologues of Rpf proteins occur widely in xanthomonads, including *Xylella fastidiosa* and other *Xanthomonas* spp. and *Stenotrophomonas maltophilia*, some strains of which are nosocomial pathogens. The *rpf*/DSF system controls diverse functions in these bacteria, including virulence, virulence factor synthesis, aggregative behaviour and biofilm formation (Han et al., 2004, Hanlon et al., 2001).

Although general QS system is known to have a close relationship with a biofilm formation, the addition of DSF triggered dispersion of the *Xcc* aggregates formed by the *rpfF* strain but not those of *rpf* strains defective in DSF signal transduction (Figure II- 15) (Fuqua and Greenberg, 2002). In addition, DSF family signals have been implicated in interspecies and inter-kingdom signaling, where

they can modulate the behavior of other microorganisms that do not produce the signal (Fuqua and Winans, 1996). *Pseudomonas aeruginosa* produces a DSF-like molecule, *cis*-2-decenoic acid, which is capable of inducing the dispersion of established biofilms and of inhibiting biofilm development. This molecule was also shown to induce dispersion of biofilms, formed by *Escherichia coli*, *Klebsiella pneumoniae*, *Proteus mirabilis*, *Streptococcus pyogenes*, *Bacillus subtilis*, *Staphylococcus aureus*, and the yeast *Candida albicans* (Fuqua et al., 2001). *cis*-2-decenoic acid is functionally and structurally related to the class of short-chain fatty acid signaling molecules such as diffusible signal factor, which act as cell-to-cell communication molecules in bacteria and fungi. As prokaryote–eukaryote interactions are ubiquitous, such cross-kingdom conservation in cell–cell communication systems might have significant ecological and economic importance.



TRENDS in Microbiology

Figure II- 14. Structure of DSF family and related signal molecules from a range of bacteria (Ryan and Dow, 2011)

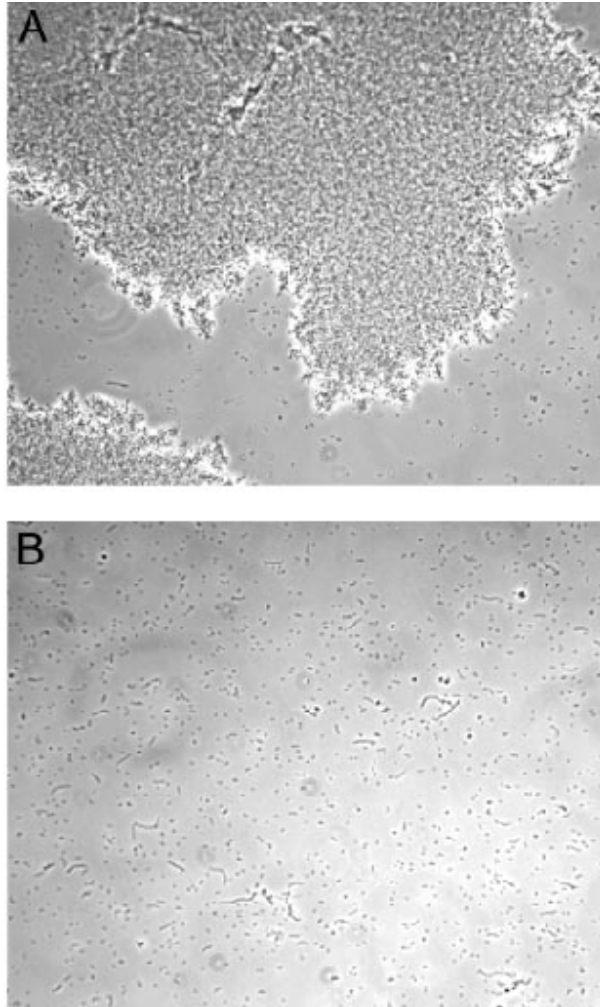


Figure II- 15. An extracellular enzyme from *X. campestris* can disperse the aggregates light microscopy of (a) cultures of an *rpf* mutant after growth and (b) the same culture after treatment of DSF

### II.2.3. Role of QS in Biofilm Formation

Generally, bacterial cells in biofilm encounter much higher cell densities than free-living planktonic cell. An obvious consequence of this is the elevated levels of metabolic by-products, secondary metabolites and other secreted or excreted microbial factors that biofilm cells encounter. Of particular interest is intercellular signaling or QS molecules. Because biofilms generally consist of aggregates of cells, one could argue that they present an environmentally relevant context for QS. This idea that the biofilms are optimum sites for expression of phenotypes regulated by QS has led to numerous studies of QS mechanism in the bacterial biofilms including its various phenotypes. The maturation of a biofilm community occurs downstream of adherence. Several factors have been shown to influence biofilm architecture, including motility, homogeneity of microorganisms, extracellular polymeric substance matrix production and rhamnolipid production (Klausen et al., 2003, Hentzer et al., 2001, Davey et al., 2003).

AHL-based QS has been shown to influence biofilm maturation for the gram-negative bacterium *Serratia liquefaciens* (Labbate et al., 2004). QS Regulates swarming motility in *S. liquefaciens* (Eberl et al., 1996). Wild-type *S. liquefaciens* biofilms are heterogeneous, consisting of cell aggregates and long filaments of cells. A mutation in the AHL synthesis gene, *swrI*, resulted in thin biofilms that lacked aggregates and filaments. Two regulated genes, *bsmA* and *bsmB*, were implicated in biofilm development. The AhyI/R AHL QS system of *Aeromonas hydrophila* has also been shown to be required for biofilm formation (Lynch et al., 2002). A strain harboring an *ahyI* mutation formed biofilms that were structurally less differentiated than the wild-type strain. For all three of the systems mentioned,

the functional consequence of this altered architecture is unclear. According to *Pseudomonas aeruginosa* biofilm inhibition test, it has revealed that QS is crucial for proper biofilm formation. Specifically, *Pseudomonas aeruginosa lasI* mutants do not develop into mature biofilms. Rather, they terminate biofilm formation at the micro-colony stage (Davies et al., 1998). These mutants can be complemented to wild-type biofilm production by the exogenous addition of the LasI-dependent 3-oxo-C12-HSL autoinducer.

There are growing evidences that QS constitutes a global regulatory system in many different parts. Many studies have shown that QS affects the biofilm development for several bacterial species. As shown in Figure II- 16, the biofilm of *Pseudomonas aeruginosa* (Parsek and Greenberg, 2000) was affected by the addition of AHLs. In addition, *Burkholderia cepacia*, and *Aeromonas hydrophila*, are known to require a functional AHL-mediated QS system for formation of biofilms (Davies et al., 1998, Huber et al., 2001, Lynch et al., 2002). The biofilm formation control by inhibiting QS signal molecules will be described in more detail in the next section.

Recently, Yeon et al. revealed that QS plays a key role in biofilm formation on membrane surface in MBRs (Yeon et al., 2008). They showed that blue color indicating the presence of AHL signal molecules was not detected at the early stage but the blue color development gradually became stronger as the membrane fouling proceeded (Figure II- 17).

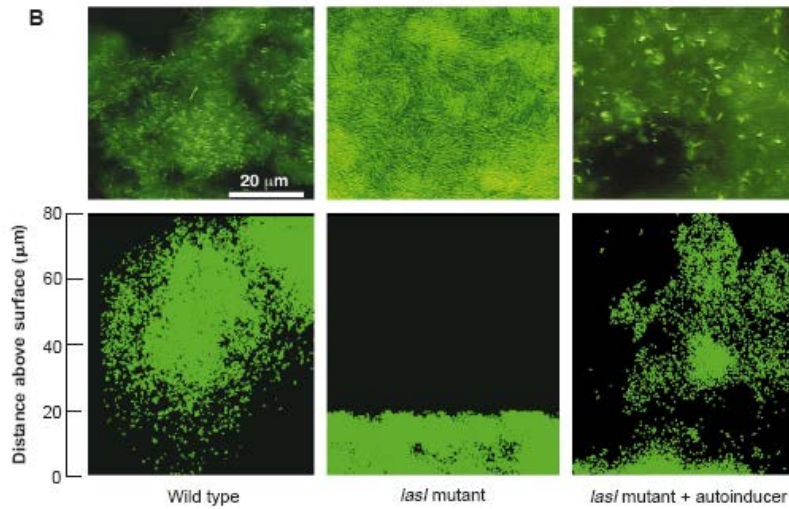


Figure II- 16. (Top) epifluorescence photomicrographs of the wild type (PA01) and the *lasI* mutant (PA0-JP1) grown with or without the autoinducer, 3OC12-HSL added to the medium. (Bottom) views of Z series of wild-type and *lasI* mutant biofilms (with or without 3OC12-HSL) acquired by scanning confocal laser microscopy

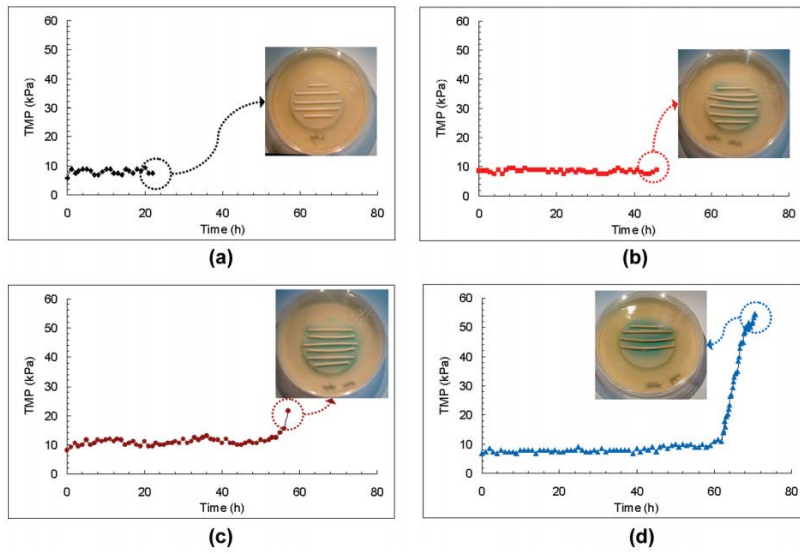


Figure II- 17. Occurrence of AHL signals in biocake during continuous MBR operation: (a) 22 h, (b) 46 h, (c) 58 h, and (d) 72 h (Yeon et al., 2008).



#### **II.2.4. Detection of AHL Signal Molecules**

Detection of AHL signal molecules is one of the most important techniques in the research of QS. In nature, the concentration of the AHLs is usually too low to be detected, and thus special experimental methods are required. There are two common methods for detection of AHL molecules.

##### **(1) Biosensors for detection of AHLs**

Bacterial sensor (reporter strain) has been widely used to detect the presence of AHLs. These reporter strains allow sensitive, quantitative and real time detection of QS signals such as AHLs. They are usually detectable up to nanomolar concentration of AHLs. The biosensors have detectable phenotypes such as light emission, expression of  $\beta$ -galactosidase activity or production of pigments upon the presence of exogenous AHLs (Figure II- 18). In

Table II- 7, bacterial reporter stains used to detect AHL QS signal molecules are listed (Venturi, 2006, Steidle et al., 2001, Winson et al., 1998, Lindum et al., 1998, Wood et al., 1997, Swift et al., 1997, Shaw et al., 1997, McClean et al., 1997, Givskov et al., 1996, Fuqua and Winans, 1996, Bassler et al., 1993). However, it is difficult to measure the accurate AHL concentrations if there are impurities to affect the expression of reporter strains.

## (2) HPLC-MS for detection of AHLs

Although methods can detect the presence of HSLs *in situ*, they cannot provide information for a wide or complete spectrum and of AHLs (i.e., identification). Spectroscopic properties have been widely used to characterization of QS molecules structures. Most procedures have been carried out by using a combination of reversed-phase HPLC and MS for selective detection. The target molecules are usually separated in C18 silica columns by isocratic or gradient elution with water–methanol or water-ACN as mobile phases (Teplitski et al., 2003). In addition, although AHLs can be determined by GC-MS, quantification of AHLs by HPLC-MS is better than that of GC-MS due to the low volatility of AHL molecules (Wang et al., 2011). However, the detection limit for HPLC is much less sensitive than that for the reporter strain extraction process should be required to obtain high concentration and purity of AHL molecules before the detection of AHL molecules.

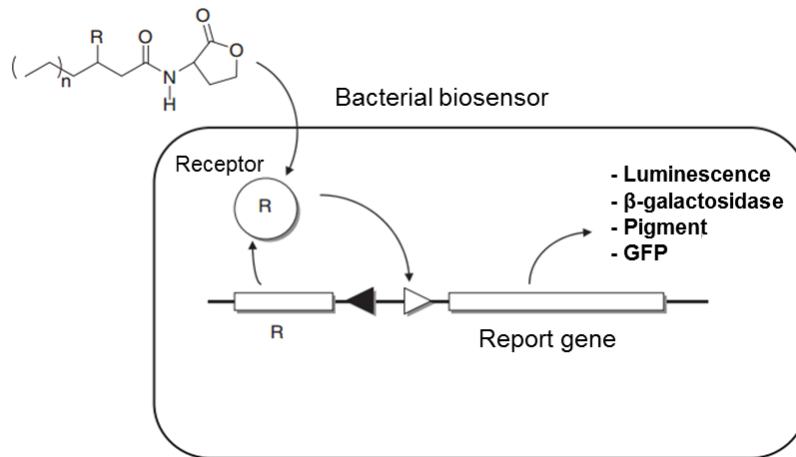


Figure II- 18. Construction and use of a bacterial AHL biosensor. The exogenous AHL interact with a LuxR family protein inside the bacterial biosensor (non-AHL producer), which results in the transcription of a reporter gene from a LuxR family-AHL regulated promoter as shown by the open triangle. The LuxR family gene is usually expressed from a constitutive promoter as shown with a filled triangle. The properties of biosensor can be dependent on report gene (s) (Steindler and Venturi, 2007)

Table II- 7. AHL QS signal reporter strain

Reporter strain	QS signal detected	Phenotype
<i>Agrobacterium tumefaciens</i> A136 [traI-lacZ fusion (pCF218)(pCF372)]	C6-HSL to C14-HSL	$\beta$ -galactosidase activity
<i>A. tumefaciens</i> strain NT1 (pDCI41E33 containing a traG::lacZ fusion)	AHLs with 3-oxo-, 3-hydroxy-, and 3-unsubstituted side chains of all lengths, (C6-HSL to C14- HSL) with the exception of C4- HSL	$\beta$ -galactosidase activity
<i>Chromobacterium violaceum</i> strain CV026–CviR receptor	Wide host range of AHLs	Violacein pigment production
<i>Escherichia coli</i> plasmid carrying a <i>luxCDABE</i> cassette activated by AhyRI' receptor of <i>Aeromonas</i> <i>hydrophila</i> (pSB536)	C4-HSL	Bioluminescent
<i>E. coli</i> plasmid carrying a <i>luxCDABE</i> cassette activated by AhyR receptor of <i>A. hydrophila</i> (pSB403)	Wide host range of AHLs	Bioluminescent

Table II - 7. continued.

<i>E. coli</i> JM109 plasmid carrying a <i>luxCDABE</i> cassette activated by LuxR receptor of <i>Vibrio fischeri</i> (pSB401)	C6-HSL	Bioluminescent
<i>E. coli</i> JM109 plasmid carrying a <i>luxCDABE</i> cassette activated by LasR receptor of <i>Pseudomonas</i> <i>aeruginosa</i> (pSB1075)	C12-HSL	Bioluminescent
<i>E. coli</i> JM109 plasmid carrying a <i>luxCDABE</i> cassette activated by RhIR receptor of <i>P. aeruginosa</i>	C4-HSL	Bioluminescent
<i>Pseudomonas aurofaciens</i> strain 30-84I	C6-HSL	Phenazine antibiotic production
<i>Pseudomonas putida</i> 117(pAS-C8)- CepR receptor	C8-HSL	Green Fluorescent Protein
<i>P. putida</i> IsoF/gfp	3-oxo-C12-HSL	Fluorescence
<i>Serratia liquefaciens</i> strain MG44	C4-HSL	Biosurfactant production

Table II - 7. (continued)

<i>S. liquefaciens</i> strain PL10 - LuxAB reporter	C4-HSL	Bioluminescent
<i>Sinorhizobium meliloti</i> Rm41 sinI::lacZ (pJNSinR)	C16-HSL to C20-HSL	$\beta$ -galactosidase activity
<i>Vibrio harveyi</i> BB170 - LuxP receptor	AI-2	Bioluminescent
<i>V. harveyi</i> BB886 - LuxP receptor	AI-1	Bioluminescent

## **II.3. Quorum Quenching (QQ)**

### **II.3.1. QS Control Strategy**

Bacteria use QS to coordinate their group behaviors such as swarming, sporulation, and biofilm formation (Li et al., 2007, Ng and Bassler, 2009, Lowery et al., 2008). The QS mechanism can be achieved by production, release and detection of a signal chemical compound (i.e., signal molecule or autoinducer). Three major signal molecules, i.e., AHLs, AIP, and AI-2, are responsible for communication of Gram-negative bacteria, Gram-positive bacteria, and inter-species bacteria, respectively. Among the signal molecules, the strategies to control the AHL-type QS system of Gram-negative bacteria are well-known.

Three key factors are generally involved in control of QS system.

- (1) Signal generator (LuxI homologue)
- (2) Signal receptor (LuxR homologue)
- (3) Signal molecule (AHL)

Therefore, there are three major ways for inhibition of AHL QS system (Figure II- 19)

- (1) Blockage of AHL synthesis (Targeting signal generation)
- (2) Interference with signal receptor (Targeting signal receptor)
- (3) Inactivation of AHL signal molecules (Targeting AHL signal dissemination)

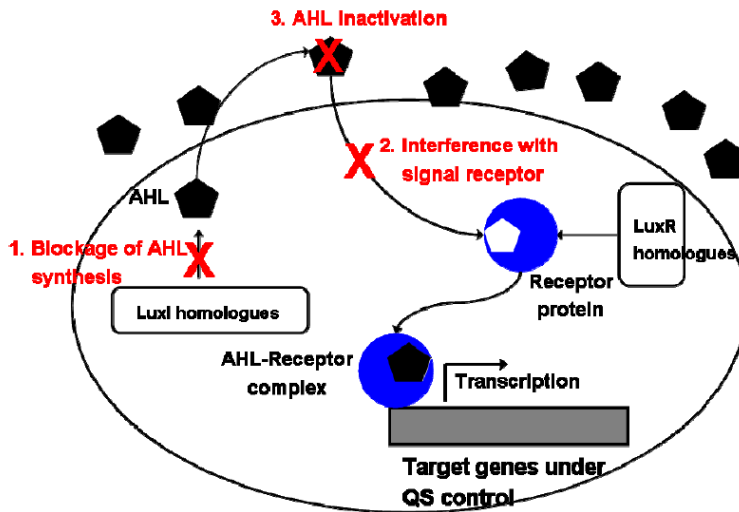


Figure II- 19. Three major AHL QS control strategies: (1) Blockage of AHL synthesis, (2) Interference with signal receptor, and (3) AHL inactivation (Yeon et al., 2008)



### **II.3.1.1. Blockage of AHL Synthesis**

As shown in Figure II- 11, the LuxI family proteins receive *S*-adenosyl-L-methionine (SAM) and specific acyl-acyl carrier proteins (acyl-ACP) to use as substrates for AHL biosynthesis. As shown in Figure II- 20a, the LuxI-type proteins direct the formation of an amide linkage between SAM and the acyl moiety of the acyl-ACP (Figure II- 20b). Subsequently, lactonization of the ligated intermediate with the concomitant release of methylthioadenosine occurs and thus results in the production of AHL (Parsek et al., 1999, Kai et al., 2014).

The blockage of AHL production was achieved by using the analogues of these AHL building blocks such as L/D-*S*-adenosylhomocysteine, sinefungin and butylryl-*S*-adenosylmethionine (butylryl-SAM) (Cheng et al., 2009). However, to date, none of them have been studied on bacteria *in vivo* and how these analogues of AHL building block would affect other cellular functions. In addition, few studies were reported to investigate this strategy to interfere with QS or find the target for specific synthase protein (Cheng et al., 2009, Parveen and Cornell, 2011).

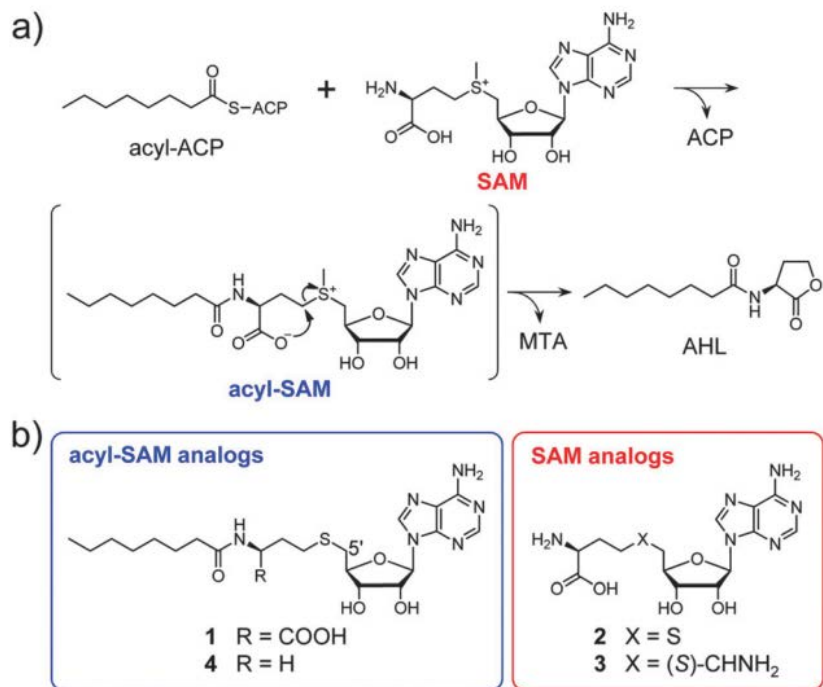


Figure II- 20. (a) Mechanism of AHL production by LuxI-type AHL syntheses. (b) Structure of acyl-SAM analogs and SAM analogs (Cheong et al., 2013).

### II.3.1.2. Interference with Signal Receptors

The most widely used interference method is to block the receptor with an analogue of the AHL. The initial step in QS is to bind specific AHL signal molecules to a LuxR responsible for reception of AHLs. The analogues of signal molecules (i.e., antagonist) bind to the AHL receptor and interfere with QS system. The advantage of this strategy is to regulate unwanted microbial activity without any side effects because the antagonist specifically interferes with expression of specific traits. AHL analogs can be substituted in either ring moiety or the chains.

Many studies have been conducted to identify synthetic analogues of AHLs that function as AHL antagonists. Analogs of the 3-oxo-C<sub>6</sub> HSL molecule with different substituent in the side chain are able to displace the native signal from the LuxR receptor. However, most of these compounds also exhibit agonists effect, which limit their use as QS inhibitor (Schaefer et al., 1996). If the C-2 atom in the side chain is replaced by a sulfur atom, it will produce a potent inhibitor of both the *lux* and *las* systems (Persson et al., 2005).

Furthermore, in nature, algae and plants have been found to produce substances that inhibit AHL-regulated signaling (Matthysse and McMahan, 1998). In addition, it has been reported that several halogenated furanones interfering AHL based QS by specific interaction with LuxR (Manefield et al., 1999, Manefield et al., 2002).

### **II.3.1.3. Degradation of AHL Signal Molecules**

As shown in Figure II- 21a, it is presumable that four potential cleavage sites in *N*-acyl homoserine lactone (AHL) are likely to degrade enzymatically(Chen et al., 2013). Quorum quenching enzymes (QQ enzymes) degrades or inactivated AHL molecules. The QQ enzymes can be classified to two groups: one that leads to the degradation of homoserine lactone ring and another that leads to cleavage of acyl chain from AHLs (Figure II- 21b)

The former group of QQ enzymes is involved in the cleavage of the QS signal molecules. AiiA-like AHL-lactonases ('lactonase') and AiiD-like AHL-acylases ('acylase') hydrolyze cyclic ester and amide linkage of the AHL structure, respectively (Ryan and Dow, 2011, Leadbetter and Greenberg, 2000, Oh et al., 2013). The latter group of QQ enzymes was found to catalyze the oxidation or reduction of acyl side chain, but not destroy AHL (Uroz et al., 2005, Chen et al., 2013)

Although various QQ enzymes have been found, the physiological function of QQ enzymes and whether AHLs are their primary substrates have not been entirely clarified. Some characterized QQ enzymes are shown with their origin and substrate specificity in Table II- 8 (Chen et al., 2013, Chen et al., 2002).

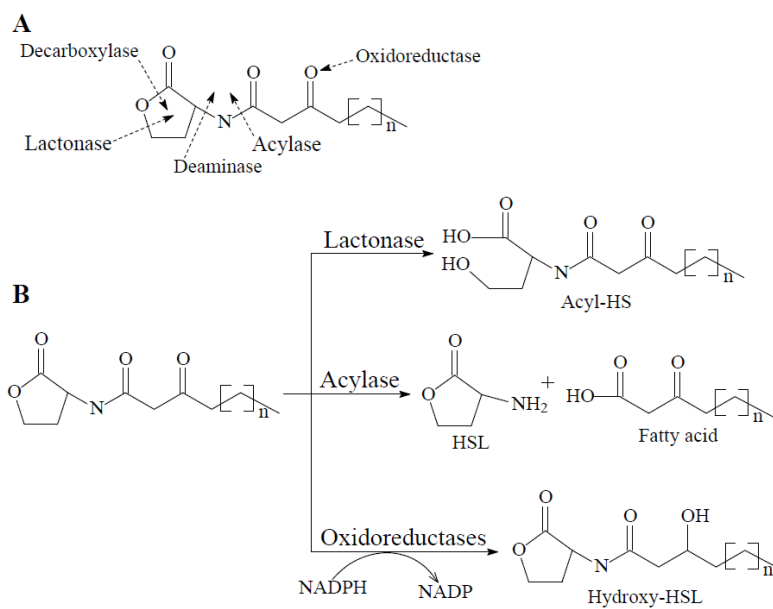


Figure II- 21. (A) Possible linkage degraded by quorum quenching enzymes in quorum sensing molecule *N*-acyl homoserine lactone and (B) corresponding degradation mechanism of quorum quenching enzymes. (Mashburn and Whiteley, 2005)

Table II- 8. List of QQ enzymes involved in the degradation of AHL QS signals  
(Chen et al., 2013, Chen et al., 2002)

<b>Enzyme</b>	<b>Host</b>	<b>Substrate</b>
AHL-lactonase		
AiiA	<i>Bacillus</i> sp. 240B1	C6-10-HSL
	<i>Bacillus cereus</i> A24	AHL
	<i>Bacillus mycoides</i>	AHL
	<i>Bacillus thuringiensis</i>	AHL
	<i>Bacillus anthraeis</i>	C6, C8, C10-HSL
AttM	<i>Agrobacterium tumefaciens</i>	C6-HSL; 3OC8-HSL
AiiB	<i>Agrobacterium tumefaciens</i> C58	Broad
AiiS	<i>Agrobacterium tumefaciens</i> K84	Broad
AhID	<i>Arthrobacter</i> sp. IBN110	Broad
AhIK	<i>Klebsiella pneumoniae</i>	C6-8-HSL
QlcA	<i>Acidobacteria</i>	C6-8-HSL
AiiM	<i>Microbacterium testaceum</i> StLB037	C6-10-HSL
QsdA	<i>Rhodococcus erythropolis</i> W2	C6-14-HSL
AhIS	<i>Solibacillus silvestris</i> StLB046	C6, C10-HSL
QsdH	<i>Pseudoalteromonas byunsanensis</i> 1A01261	C8, C14-HSL; 3OC6-HSL
AidH	<i>Ochrobactrum</i> sp. T63	C4, C6, C8, C10-HSL; 3OC6, C8, C10, C12-HSL
PON2	All mammalian tissues	C7, C12, C14-HSL; 3OC6- 10,12-HSL
MCP	<i>M. avium</i> spp. <i>Paratuberculosis</i> K-10	C6, C7, C8, C10, C12-HSL; 3OC8-HSL
BpiB07	Soil metagenome	3OC8-HSL
DlhR	<i>Rhizobium</i> sp. NGR234	3OC8-HSL

Table II- 8. (Continued)

Enzyme	Host	Substrate
AHL-acylase		
Acylase I	Porcine (Kidney)	C4, C6, C8-HSL; 3OC10, C12-HSL
AibP	<i>Brucella melitensis</i> 16M	C12-HSL; COC12-HSL
AhlM	<i>Streptomyces</i> sp. M664	C6, C8, C10-HSL; 3OC6, C8, C12- HSL
AiiD	<i>Ralstonia</i> sp. Xj12B	3OC6, C8, C10, C12-HSL
PvdQ	<i>P. Aeruginosa</i> PAO1	C7, C8, C10, C11, C12, C14- HSL; 3OC10, C12, C14-HSL;
HacA	<i>P. Syringae</i> B728a	3OH-C14-HSL
HacB	<i>P. Syringae</i> B728a	C8, C10, C12-HSL; 3OC8-HSL C4, C6, C8, C10, C12-HSL; 3OC6, C8-HSL
AiiC	<i>Anabaena</i> sp. PCC7120	C4, C6, C8, C10, C12, C14- HSL; 3OC4, C6, C8, C10, C12, C14-HSL
AiiO	<i>Ochrobactrum</i> sp. A44	C4, C6, C8, C10, C12, C14- HSL; 3OC3, C6, C8, C10, C12, C14-HSL
QsdB	Soil metagenome	C6-HSL; 3OC8-HSL
Aac	<i>Ralstonia solanacearum</i> GM11000	C7, C8, C10-HSL; 3OC8-HSL

Table II- 8. (Continued)

<b>Enzyme</b>	<b>Host</b>	<b>Substrate</b>
Oxidoreductase		
CYP1041	<i>Bacillus megaterium</i>	C12-C16-HSL; 3OC12-HSL
P450BM3	<i>Bacillus megaterium</i>	C12, C14, C16 ,C20-HSL; 3OC12, C14-HSL
Not identified	<i>Rhodococcus erythropolis</i> W2	3OC8, C10, C12, C14-HSL
Not identified	<i>Burkholderia</i> sp. GG4	3OC4, C6, C8-HSL
BpiB09	Soil metagenome	3OC12-HSL



### **II.3.2. Application of QQ to Control Biofouling in Membrane Process**

Motivated by the discovery of quorum sensing (QS) involved in bacterial biofilm formation (Bassler et al., 1993), the concept of bacterial QS was recently introduced to MBR system as a novel biofouling control strategy (Yeon et al., 2008). In detail, it was confirmed that QS is closely related to membrane biofouling (i.e., the formation of biofilm on the membrane surface in MBR). Since 2009, many researcher have started to study on apply QQ in membrane process for wastewater treatment. The QQ-based strategies have been reported to offer many advantages such as higher filtration efficiency, lower toxicity, and more sustainability over other conventional biofouling control approaches.

#### **II.3.2.1. Enzymatic QQ Application**

The addition of Acylase I suppressed biofilm development of *A. hydrophula* and *P. putida* on RO membrane surface of polystyrene through cleavage of amide bonds (Paul et al., 2008). In detail, the biofilm of *A. hydrophula* and *P. putida* on RO membrane was reduced by around 22% at the concentration of Acylase I at 60 µg/ml; however no further biofilm reduction was observed at higher concentration of Acylase I. It suggests that Acylase I would be able to inhibit the formation of *A. hydrophula* and *P. putida* biofilm on the RO membrane surface and have a good potential for the effective control of microbial attachment and membrane fouling.

Yeon et al. reported that membrane biofouling could be efficiently retarded by applying porcine kidney acylase I to continuous laboratory-scale MBR where a diverse microorganism coexists (Yeon et al., 2008). The QQ enzyme

inhibited biofouling in MBR by quenching AHL signal molecules. In detail, the study demonstrated the potential of QQ enzyme for biofouling control in MBR. However, free enzymes can be easily inactivated their activity due to their low stability in various environmental factors such temperature and pH. Therefore, many researchers endeavored to overcome the technical limitations of using free enzymes and thus developed various strategies for immobilization of the free QQ enzymes.

(1) Magnetic enzyme carrier (MEC)

Magnetic enzyme carrier (MEC) was prepared by immobilization the QQ enzyme (Acylase) on magnetic particles to overcome the limitation of free enzyme (Yeon et al., 2009). As shown in Figure II- 22, a magnetic ion-exchange resin (MIEX), which has a net positive surface charge, was adopted as a magnetic core. And then anionic polyelectrolyte (polystyrene sulfonate, PSS) and a cationic polyelectrolyte (chitosan) were deposition by layer-by-layer (LBL). Finally, porcine kidney acylase I was immobilized on MIEX-PSS-chitosan using glutaldehyde (GA) as a cross-linking agent to produce MEC. When MEC was applied to a continuous MBR, it showed the enhanced membrane permeability to a large extent compared with a conventional MBR without any treatment. Furthermore, MEC has an additional advantage for recovery due to easy separation using magnet.

In addition, Kim et al. (Kim et al., 2013a) reported the elucidate the mechanism of befouling inhibition by the application of MEC in MBR. And, they investigated the changes in population dynamics and gene expression in MBR through

pyrosequencing and proteomics.

### (2) Immobilization of QQ enzyme into nanofiltration (NF) membrane

Kim et al. tried to immobilize acylase directly onto nanofiltration (NF) membrane surface (Kim et al., 2011). Aggregations of chitosan and acylase can be achieved through controlling pH and then to be deposited onto membrane surface using N<sub>2</sub> gas. Lastly, deposited aggregates were cross-linked with glutaldehyde (GA) (Figure II- 23). The acylase-NF membrane showed better permeability than raw NF membrane in MBR. Finally, they observed a significant reduction of EPS content on the surface of acylase-NF membrane (Figure II- 24).

### (3) Immobilization of QQ enzyme into Alginate Beads

Porcine kidney acylase I was encapsulated in sodium alginate matrix. The hydrogel mixture of acylase and sodium alginate was dropped in calcium chloride solution to solidify and form spherical alginate beads using ion exchange cross-linking reaction. Finally, the cross-linked beads were reacted with glutaldehyde (GA) to enhance the mechanical strength and stability. The addition of acylase encapsulating beads in MBR resulted in the enhancement of membrane permeability with no apparent effect of effluent quality of MBR. In addition, the beads reduced the amount of EPS such as polysaccharides and proteins and viscosity and relative sludge hydrophobicity (Davey et al., 2003)

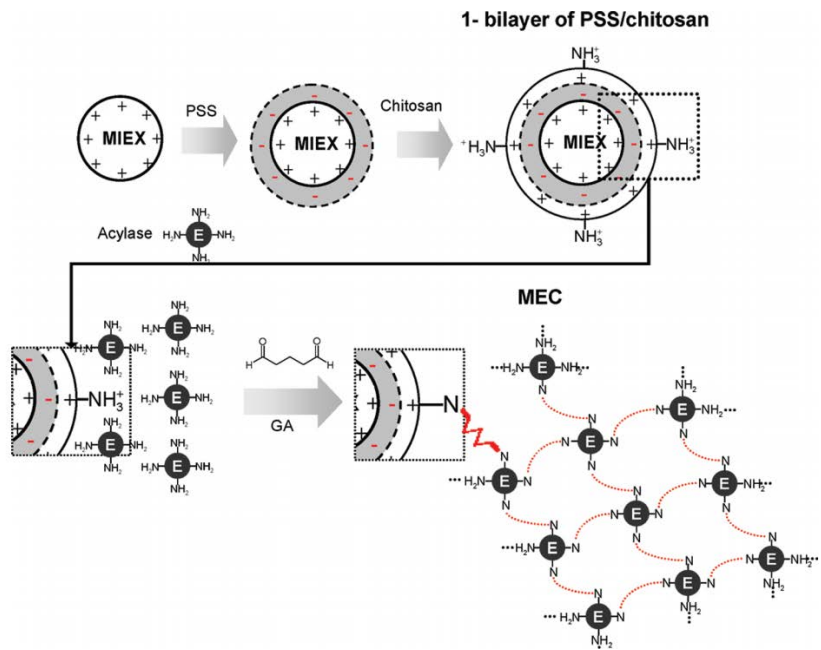


Figure II- 22. Schematic diagram showing the preparation of the MEC through layer-by-layer (LBL) deposition of PSS-chitosan on MIEX resin and enzyme immobilization via glutaraldehyde treatment. (Yeon et al., 2009)

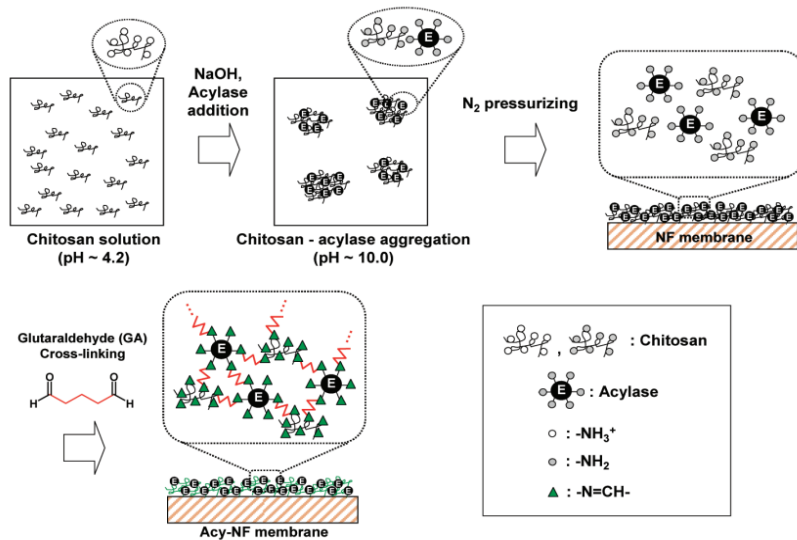


Figure II- 23. Schematic diagram of acylase immobilization onto the nanofiltration membrane surface by forming a chitosan-acylase matrix (Kim et al., 2011)

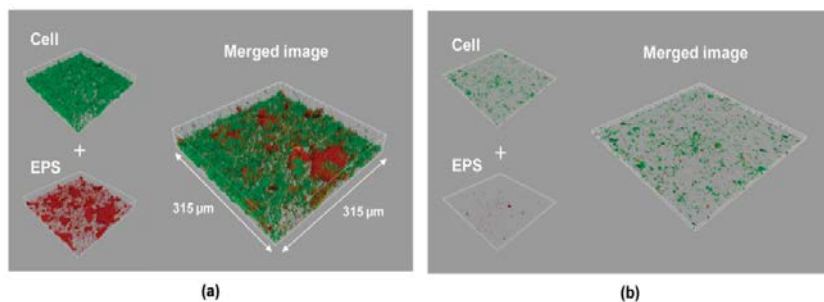


Figure II- 24. Reconstructed CLSM images of biofilm formed on the (a) raw and (b) Acyl-NF membranes after a 38-hour operation of the continuous NF of *P.aeruginosa* and then stained with SYTO 9 and ConA. (Kim et al., 2011).

## **II.3.2.2. Bacterial QQ**

### **II.3.2.2.1. Isolation of QQ enzyme producing Bacteria**

Although various strategies for application free enzyme were developed, direct application is difficult, limiting practical application due to cost and enzymatic instability. Recently, many researchers have attempted to overcome the limitation and subsequently a growing number of QQ enzyme producing bacteria (QQ bacteria) which is capable of degrading AHL signal molecules have been identified. To find the isolate producing QQ enzyme, enrichment culture is commonly used. In detail, samples from different environments are loaded onto minimal medium containing AHLs as the sole carbon source (Christiaen et al., 2011). After repeating enrichment culture for further purification, the cell suspension is spread on LB agar plate, and different types of colony were isolated. Subsequently, AHL degrading activity of the colony is tested and the isolates having QQ activity are identified by DNA sequencing.

From activated sludge in a real wastewater treatment plant, *Rhodococcus* sp. BH4 and *Bacillus methylotrophicus* sp. WY producing lactonase degrading a wide variety of AHL molecules were isolated (Oh et al., 2012, Khan et al., 2016). In addition, Cheong et al. isolated *Pseudomonas* sp. 1A1 which produces three types of acylase enzyme. It was investigated whether their QQ enzymes have intracellular or extracellular activity through LC-MS or bioassay (Slater et al., 2000).

### II.3.2.2.2. Application of Bacterial QQ

To apply bacterial QQ into MBR, carriers or media capable of entrapping QQ bacteria are required. The bacteria entrapping carrier or media enable to protect bacteria from harsh conditions or external stresses such as temperature or pH, or from washing out due to excess sludge discharge. It helps to exhibit steady QQ effect in the MBR and to overcome the limitation of practical issues such as cost and stability of enzymes. Oh et al. proposed that QQ might be more feasible, has a longer life span and does not require enzyme purification (Oh et al., 2012).

#### (1) Microbial-vessel (MV)

A novel QQ bacterium, *Rhodococcus* sp. BH4 was isolated from a real MBR plant for wastewater treatment. The QQ bacterium was identified to produce lactonase enzyme decomposing a wide range of AHL signal molecules. To apply the QQ bacterium into MBR, Oh et al. developed the microbial-vessel (MV) which is porous membrane containing QQ bacteria as shown in Figure II- 25. The MV could successfully control biofouling in continuous MBR system (Oh et al., 2012, Klausen et al., 2003). The QQ performance of the MV could be enhanced by the location close to filtration membrane, and higher recirculation rate between bioreactor and membrane tank in external submerged MBR system (Klausen et al., 2003).

Furthermore, Weerasekara et al. reported that the MV could save the energy consumption in MBR fed with synthetic wastewater by reducing aeration intensity (Weerasekara et al., 2014).

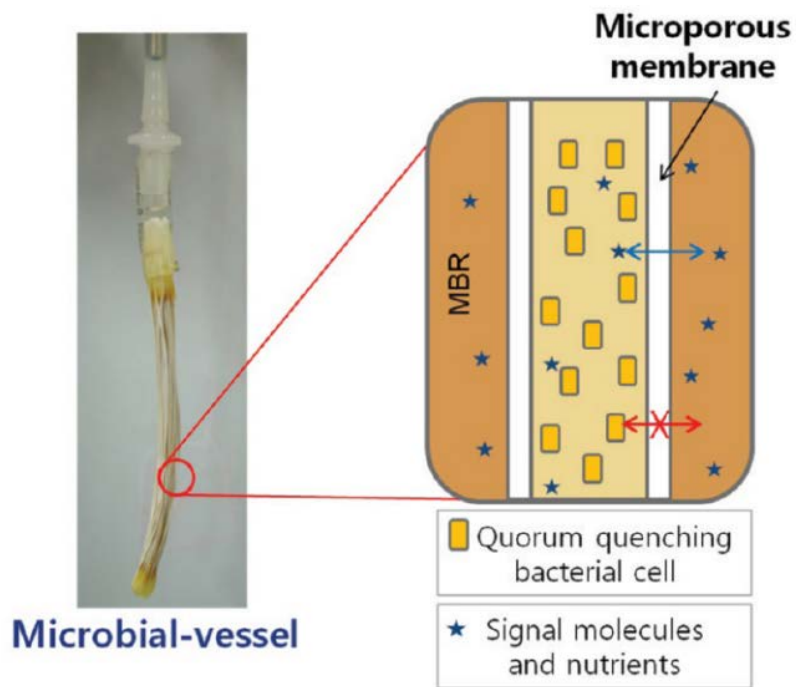


Figure II- 25. Image of a microbial -vessel (MV) (Oh et al., 2012)



## (2) Ceramic microbial-vessel (CMV)

Indigenous QQ bacterium (*Pseudomonas sp.* 1A1) was isolated from real wastewater treatment plants and its QQ activity was demonstrated against AHLs. *Pseudomonas sp.* 1A1 produces extracellular QQ enzyme activity and excretes them out of the cell (Slater et al., 2000). He designed the ceramic microbial-vessel (CMV) to improve activity of encapsulated QQ bacteria inside membranes using intrinsic structure of CMV as shown in Figure II- 26. High concentration of encapsulated QQ bacteria in confined spaces can lead low F/M ratio inside the CMV, which can deteriorate their viability. Therefore, he proposed QQ MBR with ceramic microbial vessel (CMV) which was designed to overcome the extremely low F/M ratio by using inner flow feeding mode which supplies the fresh feed into lumen directly for QQ bacteria inside the CMV (Cheong et al., 2014) (Figure II- 27). As a result, inner flow feeding mode enhanced the viability of QQ bacteria inside the CMV. These result means that the high mass transfer is essential for QQ bacteria's growth and biological stability. Furthermore, Köse-Mutlu et al. developed the rotating microbial-vessel (called rotating microbial carrier frame, RMCF) to effectively increase its mass transfer (Köse-Mutlu et al., 2015)

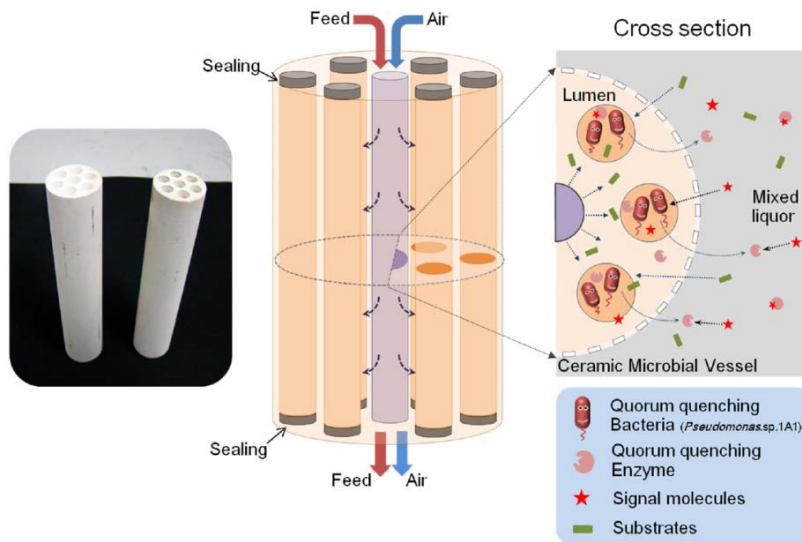


Figure II- 26. Schematic diagram of the ceramic microbial-vessel under the inner flow feeding mode (Cheong et al., 2014).

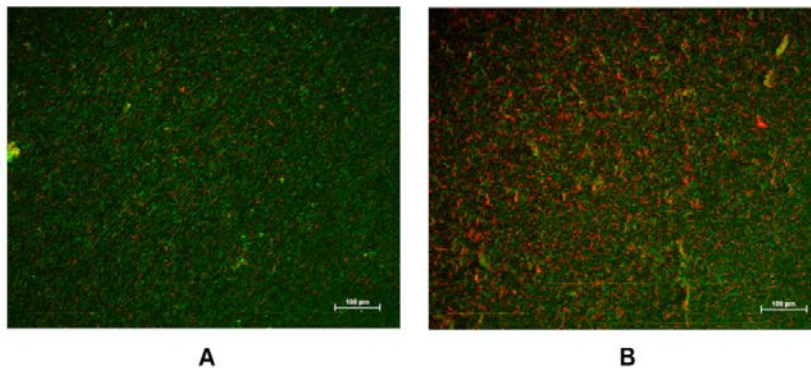


Figure II- 27. Images of live/dead QQ bacteria from the lumens of the used CMVs. (A) MBR-B with the CMV under the inner flow feeding mode, (B) MBR-C with the CMV under the normal feeding mode. Green color: live cell; red color: dead cell (Cheong et al., 2014)

### (3) QQ bacteria entrapping beads (QQ-Beads)

The spherical QQ bacteria entrapping media (QQ-Beads) were developed by entrapping QQ bacteria in alginate matrix. This spherical bead had porous microstructure to give enough inner space for growth of entrapped BH4 bacteria, and the bacteria were well-distributed in the QQ-Beads whereas there was no BH4 in Vacant-Bead as shown in Figure II- 28. The beads can move freely through fluid flow in MBR because the wet density of the beads is approximately 1 g/ml which is similar to that of water. In addition, they are able to collide with the membrane surface, and thus the biofilm on membrane surface can be detached (Figure II- 29). As a result, QQ-Beads significantly mitigated biofouling in MBR due to its combined effect of biological QQ activity and physical washing (detachment of biofilm).

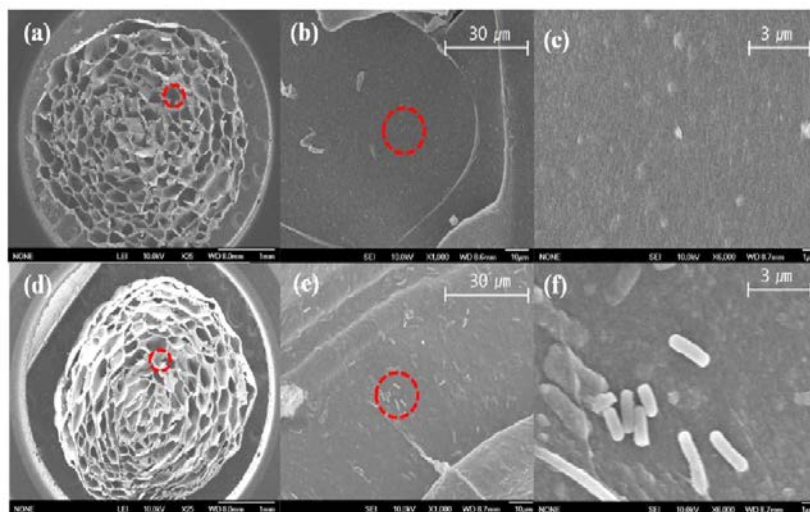


Figure II- 28. Comparison of SEM images of Vacant-Beads and QQ-Beads: cross section of a vacant bead (a)  $\times 25$ , (b)  $\times 1000$ , and (c)  $\times 6000$  and of a CEB (d)  $\times 25$ , (e)  $\times 1000$ , and (f)  $\times 6000$ . (Kim et al., 2013b)

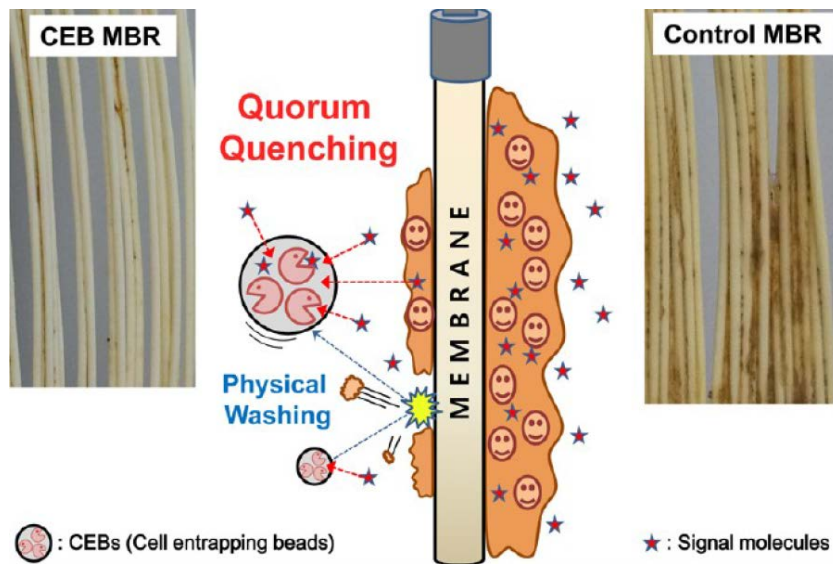


Figure II- 29. Concept of QQ-Beads with combined effect of both biological QQ and physical washing effect (Kim et al., 2013b)

Although the alginate QQ-bead successfully mitigated biofouling in MBR fed with synthetic wastewater, alginate bead was easily decomposed in harsh conditions such as real wastewater containing a wide variety of component including surfactants or salts, which limits practical application. Therefore, Kim et al. reinforced alginate bead by coating synthetic polymer (called macrocapsule). The phase inversion method (Figure II- 30) was used to coat the alginate bead with various synthetic polymers (Figure II- 31). As a result of the coating, the mechanical strength of bead was significantly increased. Even if QQ bacteria was damaged by organic solvent during preparation, QQ activity and cell viability were recovered by restoration culturing in intensive nutrient medium such as LB broth. As a result, macrocapsule inhibited the membrane biofouling in lab-scale MBR fed with real wastewater.

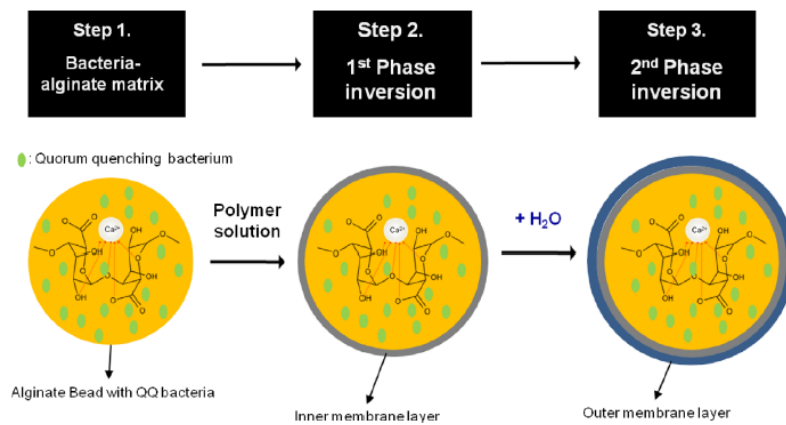
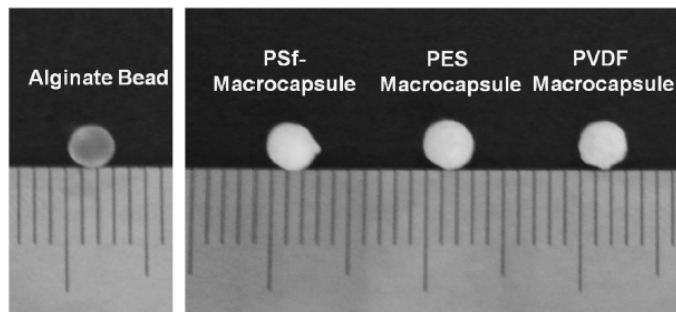


Figure II- 30. Preparation scheme of a macrocapsule coated with a membrane layer through the phase inversion method. (Kim et al., 2015)



b

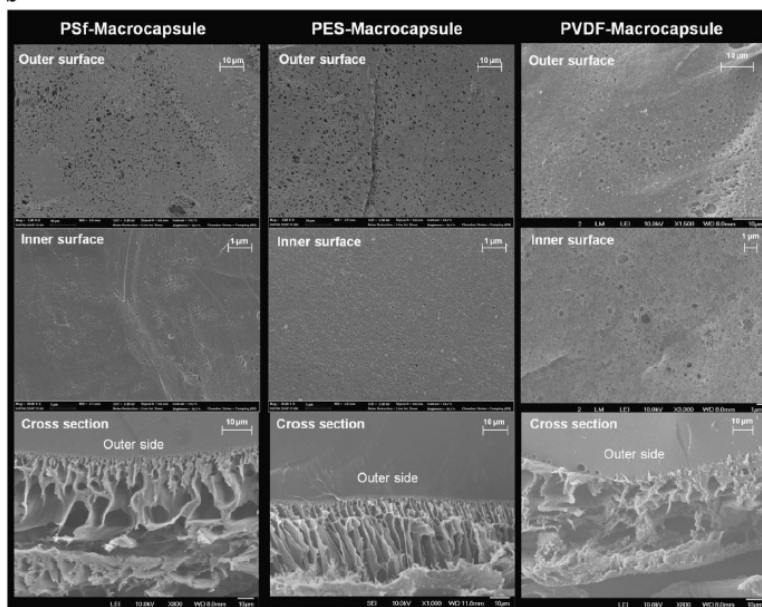


Figure II- 31. (a) Photographs of an alginate bead and PSf, PES, PVDF coated macrocapsules. (b) SEM images of the outer surface, inner surface and cross-section of each macrocapsule coated with PSf, PES, and PVDF, respectively. (Kim et al., 2015)



Recently, a new hydrogel type of spherical beads made of poly(vinyl alcohol) and sodium alginate was developed (Lee et al., 2016b). The use of the hydrogel materials reinforces their stability and prevents a significant damage of bacterial viability. the performance of QQ-Beads for biofouling mitigation was demonstrated not only in lab-scale MBRs (Jo et al., 2016, Kim et al., 2013b, Kim et al., 2015) but in pilot-scale MBRs (Maqbool et al., 2015, Lee et al., 2016b). The biofouling mitigation through QQ-Beads suggests the QQ-MBR is approaching closer and closer to practical application.

#### (4) QQ bacteria entrapping cylinder (QQ-Cylinder & QQ-Hollow Cylinder)

Based on the CLSM cross sectional images of two types of beads, it is concluded that the presence of BH4 limits the diffusion of AHL signal molecules toward the center of the beads because most AHLs were degraded by the BH4 located near the surface of the beads (Figure II- 32). As a result, two kinds of QQ bacteria entrapping cylinder, QQ-cylinder (Lee et al., 2016a) and QQ-hollow cylinder (Lee et al., 2016c), were developed because they are expected to have enhanced QQ activity due to their high total surface area. The greater QQ activity of the media was confirmed in comparison with previously reported QQ-Beads at fixed volume. In addition to the QQ activity, they have greater physical washing effect as a result of the larger contact area of the media with the membrane surface because of their cylindrical geometry. On the basis of the enhanced properties for anti-biofouling, QQ cylinder typed media were more effective in mitigating biofouling compared to QQ-Beads (Figure II- 33)

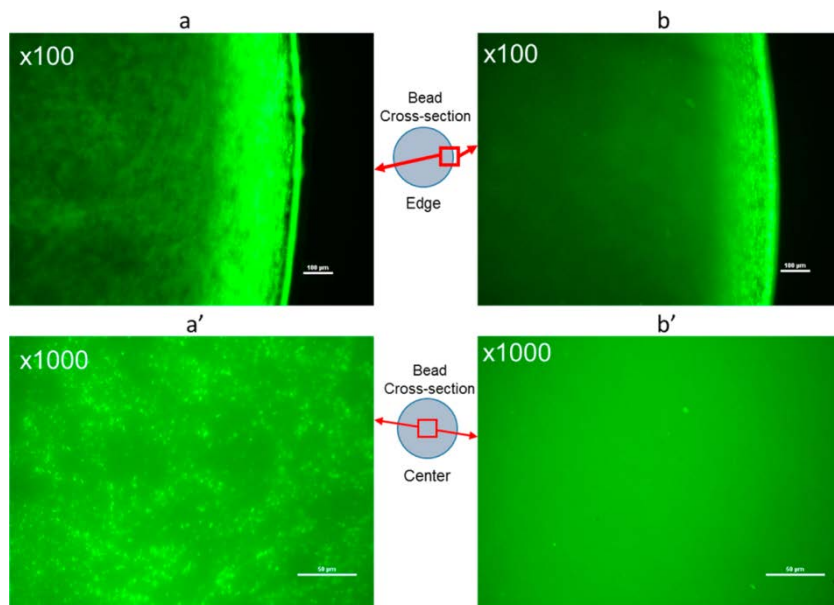


Figure II- 32. Fluorescence images of bead cross-sections entrapped with JB525 (an AHL reporter strain) only (a, near surface; a', center) and with both JB525 and BH4 (b, near surface; b', center). In a bead entrapped only with JB525, green fluorescence was observed across the cylinder, meaning that free diffusion of AHLs occurred within the bead. In contrast, in a bead with both JB525 and BH4, green fluorescence was observed only along the surface of the bead, indicating most AHLs were degraded by the BH4 near the surface.

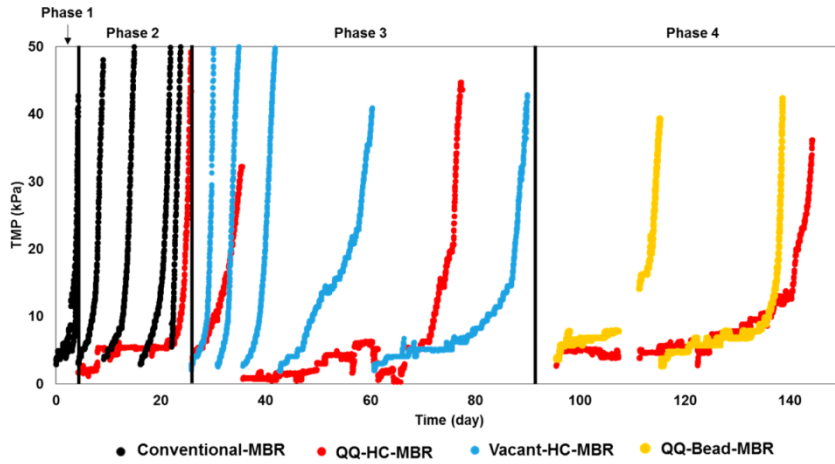


Figure II- 33. TMP profiles of MBRs with no media (Conventional MBR, black line), QQ-hollow cylinder (QQ-HC-MBR, red line), Vacant-hollow cylinder (Vacant-HC-MBR, blue line), and QQ-bead (QQ-bead-MBR, yellow line)

## **II.4. Immobilization Technique for biocatalyst**

Strategies for immobilized microbial enzymes, organelle or cells have been used in various scientific and industrial applications. In addition, the economic importance of immobilization technology has resulted in considerable research for industrial applications such as commercial bioreactor fermentations (Núñez and Lema, 1987)

### **II.4.1. Whole-Cell Immobilization Method**

The immobilized whole-cell technique is an alternative to enzyme immobilization. Unlike enzyme immobilization, where the enzyme is attached to a solid support, in immobilized whole-cell technique, the target cell is immobilized. Whole-cell immobilization methods may be applied when the enzymes required are difficult or expensive to extract, an example being intracellular enzymes. Furthermore, growth of live cells, when immobilized, can be of value in some instances such as MBR process. Therefore, whole cell immobilization may be used for convenience in industrial process. Most of immobilized cells have been used in bioreactors and production of useful compounds such as amino acids, organic acids, antibiotics, steroids (Brodelius, 1987). Various whole cell techniques (Akin, 1987a) and the many applications (Akin, 1987a, Coughlan and Kierstan, 1988) possible have been examined. Whole-cell immobilization describes many different forms of cell attachment or entrapment. These different forms include flocculation, adsorption on surfaces, covalent bonding to carriers, cross-linking of cells, encapsulation in a polymer-gel, and entrapment in a matrix.

In these things, the whole-cell immobilized in a hydrogel matrix can be

protected from harsh environmental conditions such as pH, temperature, organic solvent, and poison. Also, immobilized cells can be handled more easily and recovered from the solution without difficulty. In general few points need to be considered before choosing the materials for the whole cell immobilization as shown in Table II- 9.

Table II- 9. General requirement for whole-cell immobilization

- 
1. The materials should be stable, robust and inert. It must be biocompatible and should not interfere with bioreaction.

---

  2. The materials should be elastic enough to accommodate growing cells.

---

  3. The materials should protect the whole cell containing reactive enzyme against microbial deterioration and render the enzyme accessible to cofactor, metal ions etc.

---

  4. The materials must permit substrate accessibility to immobilized whole cells and thus avoid mass transfer problem.

---

  5. The materials should have high immobilization whole cell loading factor for the efficient transformation reaction, such as large surface and high diffusion coefficient.

---

  6. The immobilization process must be simple, quick, inexpensive and eco-friendly.

---

  7. The materials should have functional groups for cross-linking.

---

  8. The material generally recognized as safe for food and pharmaceutical bioprocess applications.
-

## **II.4.2. Hydrogel**

Hydrogel is networks of hydrophilic polymer chains. Because hydrogel polymers contain over 90% water, they are highly absorbent swell readily without dissolving. Hydrogels are usually being used for cell immobilization in medicine and biotechnology (Shaw et al., 1997). They provide bacterial cells chemical/physical stability, structural support, and immunoisolation. For successful immobilization, the hydrogel must be biocompatible, high permeability and mass transfer. Sufficient supply of oxygen and essential nutrients and substrate through the hydrogel network, plus adequate removal of metabolic waste and phenotypic secretions are essential for sustaining the immobilized cells in the hydrogel complexes (Teplitski et al., 2003).

There are various methods for synthesizing hydrogel polymers as listed in Table II- 10. polyvinyl alcohol (PVA) is one of the most commonly used synthetic hydrogel polymer because it is biocompatible and has excellent physical properties such as elasticity and mechanical strength (Paradossi et al., 2003). In addition, the physical properties of the PVA can be enhanced its properties by compositing or crosslinking to other natural polymers for industrial applications as shown in Figure II- 34

**Table II- 10. Methods for synthesizing physical and chemical hydrogels (Steindler and Venturi, 2007)**

---

***Physical gels***

- Warm a polymer solution to form a gel (e.g., PEO-PPO-PEO block copolymers in H<sub>2</sub>O)
- Cool a polymer solution to form a gel (e.g., agarose or gelatin in H<sub>2</sub>O)
- ‘Crosslink’ a polymer in aqueous solution, using freeze–thaw cycles to form polymer microcrystals (e.g., freeze–thaw PVA in aqueous solution)
- Lower pH to form an H-bonded gel between two different polymers in the same aqueous solution (e.g., PEO and PAAc)
- Mix solutions of a polyanion and a polycation to form a complex coacervate gel (e.g., sodium alginate plus polylysine)
- Gel a polyelectrolyte solution with a multivalent ion of opposite charge (e.g., Na + alginate<sup>-</sup> + Ca<sup>2+</sup> + 2Cl<sup>-</sup>)

---

***Chemical gels***

- Crosslink polymers in the solid state or in solution with:
  - Radiation (e.g., irradiate PEO in H<sub>2</sub>O)
  - Chemical crosslinkers (e.g., collagen with glutaraldehyde or a bis-epoxide)
  - Multi-functional reactive compounds (e.g., PEG+diisocyanate = PU hydrogel)
  - Copolymerize a monomer + crosslinker in solution (e.g., HEMA+EGDMA)
  - Copolymerize a monomer + a multifunctional macromer (e.g., bis-methacrylate terminated PLA-PEO-PLA + photosensitizer + visible light radiation)
- Polymerize a monomer within a different solid polymer to form an IPN gel (e.g., AN + starch)
- Chemically convert a hydrophobic polymer to a hydrogel (e.g., partially hydrolyse PVAc to PVA or PAN to PAN/PAAm/PAAc)

---

Abbreviations: EGDMA, ethylene glycol dimethacrylate; HEMA, hydroxyethyl methacrylate; IPN, inter-penetrating network; PAAc, poly(acrylic acid); PAAm, polyacrylamide; PAN, polyacrylonitrile; PEG, poly(ethylene glycol); PEO, poly(ethylene oxide); PLA, poly(lactic acid); PVA, poly(vinyl alcohol); PVAc, poly(vinyl acetate).



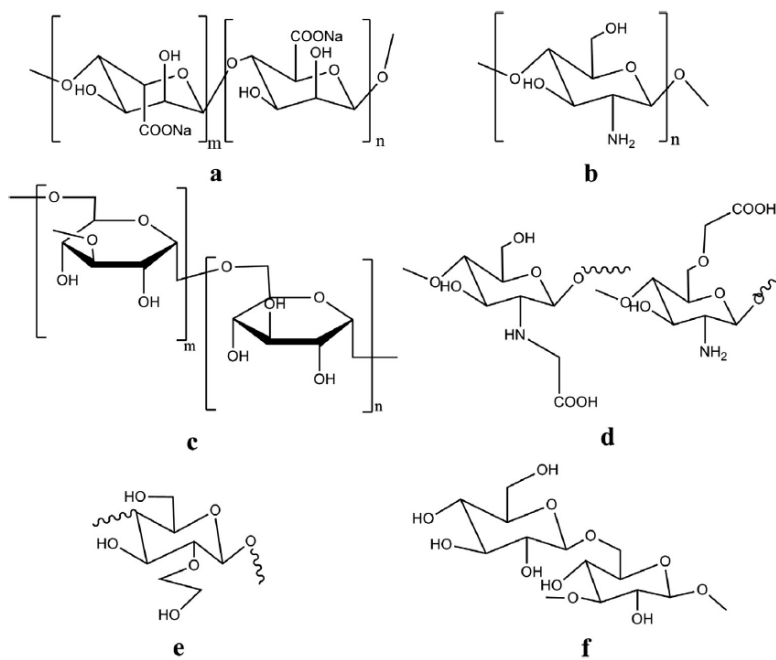


Figure II- 34. Chemical structures of natural polymer and their derivatives which were blended with PVA hydrogel to form wound dressing materials, such as (a) sodium alginate, (b) chitosan, (c) dextran, (d) N-O-carboxymethyl chitosan, (e) hydroxyethyl starch (HES), and (f) (1,3), (1,6)-β-glucan. (Kamoun et al., 2015)

### **II.4.3. Nanofiber (Electrospun)**

Surface area of media is an important parameter because mass transfer is highly dependent on effective area of media as well as permeability related to surface properties (pore size, affinity, etc.). For this reason, nanofiber has attracted considerable attention by immobilizing enzymes onto a high surface area of nanostructured materials.

As shown in Figure II- 35, electrospinning is a common method to produce nanofibres (or electrospun) with a diameter in the range of 100 nm or even less (Salalha et al., 2006). Electrospun possess an extremely high surface-to-volume ratio, tunable porosity, and malleability to conform over a wide variety of sizes and shapes. In addition, its composition can be controlled to achieve desired properties and functionality. Due to these advantages, electrospun nanofibrous scaffolds have been widely investigated in the past several years with materials of different compositions (Yang et al., 2004, Venturi, 2006, Zhang et al., 2005) for applications of varying end-uses, such as filtration (Schreuder-Gibson et al., 2002, Schreuder-Gibson et al., 2005), optical and chemical sensors (Wannatong and Sirivat, 2004, Wang et al., 2004c), electrode materials (Kim et al., 2004a, Kim et al., 2004b), and biological scaffolds (Khil et al., 2005, Ma et al., 2005, Riboldi et al., 2005, Yang et al., 2005).

Functional nanofibrous scaffolds have great potential in many biomedical applications, such as tissue engineering, wound dressing, enzyme immobilization and drug (or gene) delivery. For example, Smith and Reneker describe a processing which a fiber mat is directly electrospun onto the affected skin areas (Smith et al., 2004). Handheld electrospinning devices have been developed for the direct

application of nanofibers onto wounds (Figure II- 36). In such a device, a high voltage is generated with the voltage supplied by standard batteries. The device has a modular construction, so that different polymer carriers and drugs can be applied, depending on the type of wound, by exchanging the vials of spinning solution. From a technical point of view, the device has proven itself in continuous use over several months.

For water treatment, Yoon et al. developed ultrafiltration (UF) / nanofiltration (NF) polyacrylonitrile (PAN) membrane based on electrospun nanofibrous scaffold (Yoon et al., 2006). Such nanofibrous composite membrane exhibit a much higher flux rate for water filtration compared to conventional UF/NF porous membrane.

Recently, electrospun polymer-composite fibers can also be prepared using biological objects, such as living bacteria or active viruses. As shown in Figure II- 37, bacteria (*Escherichia coli*, *Staphylococcus albus*) and bacterial viruses (T7, T4,  $\lambda$ ) were successfully encapsulated by electrospinning and managed to survive in spite of the pressure buildup and the electrostatic field (Eberl et al., 1996). This technique provides an excellent alternative to lyophilization for the preservation of organisms for strain collection and for applications such as biosensing.

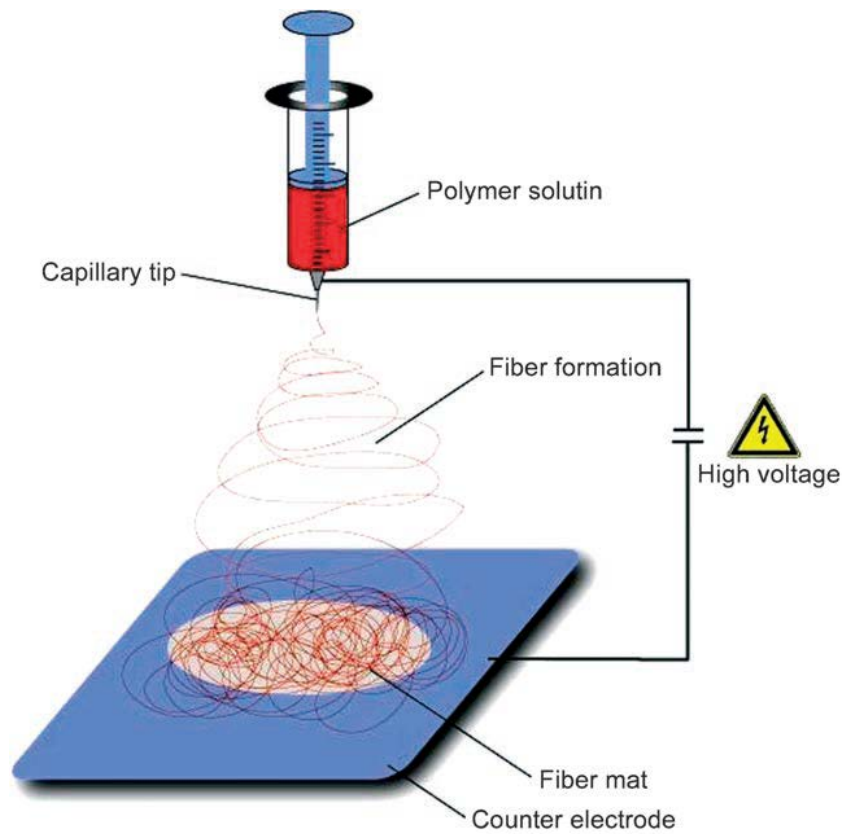


Figure II- 35. Schematic diagram for an electrospinning experiment with a perpendicular arrange (Manefield et al., 1999)



Figure II- 36. Handheld device for the electrospinning of wound dressings. Inset: PEO fibers electrospun from aqueous solution onto a hand (Manefield et al., 1999)

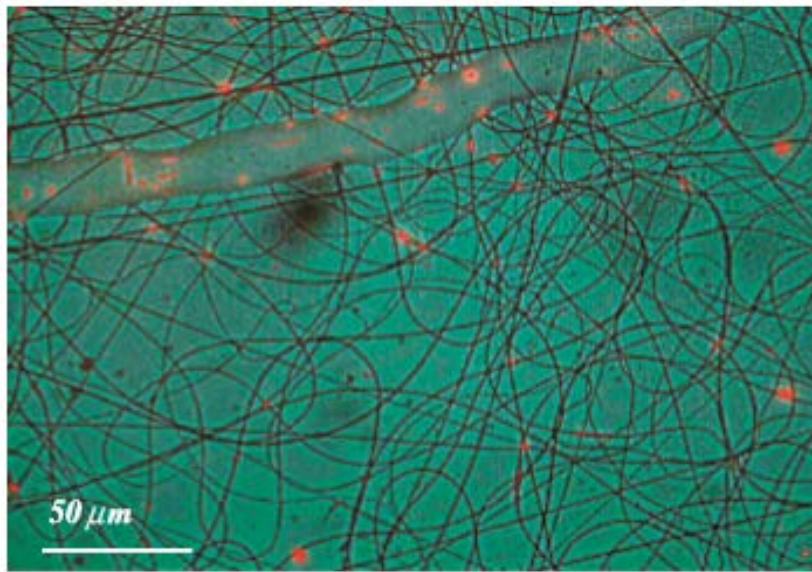


Figure II- 37. An image of fluorescent *E. coli* cells (the red spots) embedded in electrospun PVA-polymer nanofibres. Both a large fibre and individual nanofibres with embedded fluorescent cells are shown (Eberl et al., 1996)

## **II.5. Extracellular Polymeric Substances (EPS)**

### **II.5.1. Role of EPS in Biofilm Matrix: House of Biofilm Cells**

Extracellular polymeric substances (EPS) are defined as natural polymeric components of biological origin that participate in the formation of microbial aggregates (i.e., biofilm). These adherent cells are frequently embedded within matrix of EPS (Figure II- 38) EPS provide structural and the functional integrity of biofilms, and are considered the fundamental component determining the physiochemical properties of a biofilm.

The EPS as the building blocks of biofilms can be described as gel-like and is commonly identified as slime. As shown in Figure II- 39, EPS are mostly composed of polysaccharides and proteins include other macromolecules such DNA, lipids, and humic substances (decaying organic matter) (McDougald et al., 2012). The proportion of these components within EPS depends on the environments, in which the biofilm grows, such as the prevalence of water, pH, temperature, and so on.

The EPS matrix acts as a barrier where diffusive transport prevails over convective transport (Sutherland, 2001), having protective effect on microorganism in biofilm against adverse condition such as antibiotics, defense substances, or other important compounds from the host. As an example, it has frequently observed that microorganisms embedded in EPS matrix can tolerate environmental stress factors, such as UV radiation, pH changes, osmotic stress, and desiccation (Simoes et al., 2010).

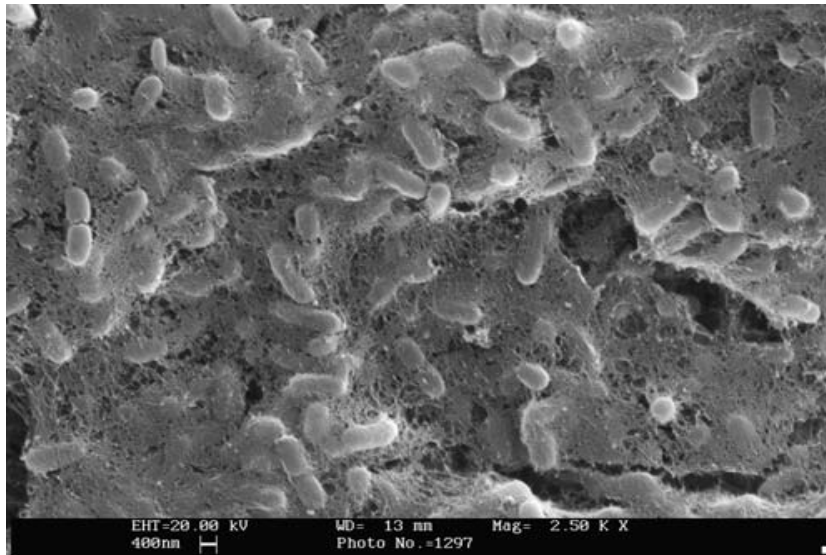


Figure II- 38. Bacterial cells embedded in the matrix of biofilm (Xiong and Liu, 2010)

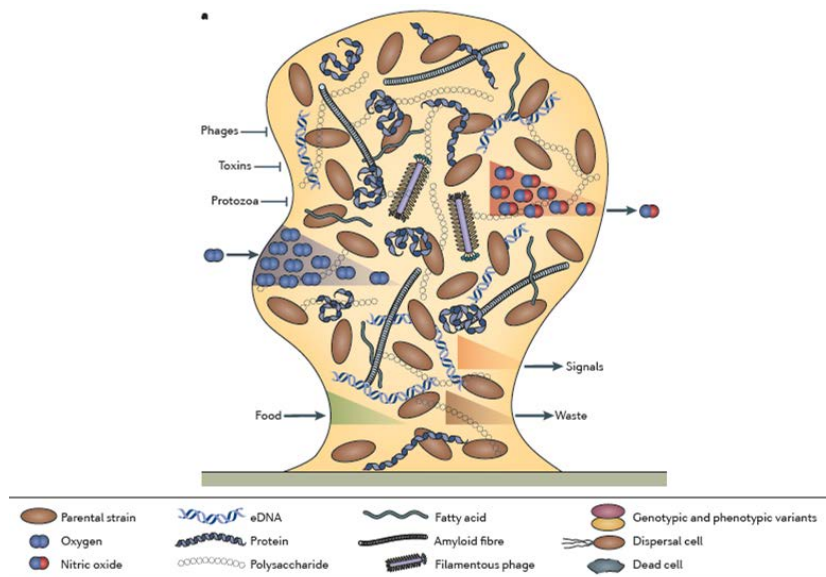


Figure II- 39. Microcolonies in the mature biofilm are characterized by an extracellular polymeric substances (EPS) matrix, composed of extracellular DNA (eDNA), polysaccharides, proteins, amyloid fibres and bacteriophages (McDougald et al., 2012)



## **II.5.2. Polysaccharides: Key Elements of EPS for Biofilm Formation**

Secreted polysaccharides have been recognized as key elements that determines shape and provide structural support for biofilm formation (Sutherland, 2001). These natural polymers are very diverse and are often observed in establishment of cell-cell contacts contributing to the formation of biofilms. Evidence for a structural role of several polysaccharides is accumulating, and the regulation of production of these polysaccharides has been actively investigated in different bacteria (Vu et al., 2009, Branda et al., 2005). Up to date, three polysaccharides have been observed in the bacterial biofilm matrix and have been shown to be important for biofilm formation.

Up to date, the reason why bacteria generate cellulose has been a quest of biologists. However, one considered that cellulose can be produced to provide protection for the cells from damage by ultraviolet (Williams and Cannon, 1989) or entrance of competitor (Iguchi et al., 2000). Iguchi and his coworkers proposed that bacteria construct a 'cellulose' cage and confine themselves in it whereas nutrients can be supplied easily by diffusion. Another assumed that the cellulose fimbriae may also aid in moisture retention to prevent drying of the natural substrates (White et al., 2006). The results raised the possibility that the reason for cellulose production is closely associated with survival and adaptation to diverse environment.

### (1) Cellulose

The cellulose is the most abundant polysaccharide in nature and is produced by both plants and bacteria. Bacterial cellulose production and the role of cellulose

in biofilm formation has described for a number of bacterial species including *Sarcina ventriculi*, *Agrobacterium tumefaciens*, *Rhizobium leguminosarum*, *Escherichia coli*, *Salmonella* spp., and *Pseudomonas fluorescence* (Deinema and Zevenhuizen, 1971, Matthyse et al., 1995, Napoli et al., 1975, Ross et al., 1991, Zogaj et al., 2001, Spiers et al., 2013). In addition, a growing number of bacteria have been reported to produce cellulose in biofilm formation (Trivedi et al., 2016). In the initial stages of biofilm development, cellulose is reported to act as an attachment factor for the developing film due to its micro-fibril structure (Matthyse and McMahan, 1998, Spiers and Rainey, 2005). As shown in Figure II-40, in mature biofilms, cellulose provides structural integrity, as cellulose is anchored and connected to the micro-colonies in the biofilm (Trivedi et al., 2016)

(2) Poly- $\beta$ -1,6,-N-acetyl-glucosamine.

Poly- $\beta$ -1,6,-N-acetyl-glucosamine (in short,  $\beta$ -1,6,-GlcNAc) is a polysaccharide polymer know to be involved in biofilm formation in *Staphylococcus aureus* and *Staphylococcus epidermidis*, where it contributes to their virulence (Maira-Litrán et al., 2002, Götz, 2002). *S. aureus* and *S. epidermidis* are frequently found as harmless inhabitants of the mucosal nasal passages or the normal skin flora of humans. However, these organisms are opportunistic pathogens an they are increasingly found to be the cause of invasive and chronic, medical device associated infections. These infections are difficult to eradicate and it is believed that the biofilm mode of growth is responsible for the inherent tolerance towards host immune responses.

$\beta$ -1,6,-GlcNAc was recently identified in *E. coli* K12 where the expression of

$\beta$ -1,6,-GlcNAc is involved in both cell to cell adhesion and attachment to surfaces (Beloin et al., 2008). Moreover, degradation of  $\beta$ -1,6,-GlcNAc by treatment with Dispersin B which degrade the  $\beta$ -1,6,-GlcNAc leads to nearly complete disruption and dispersion of the biofilm.

$\beta$ -1,6,-GlcNAc serves as an adhesion that stabilizes biofilms of *E.coli* and other species of bacteria such as *A. acinomyetemcomitans* and *Actinobacillus pleuropneumoniae* (Kaplan, 2010)

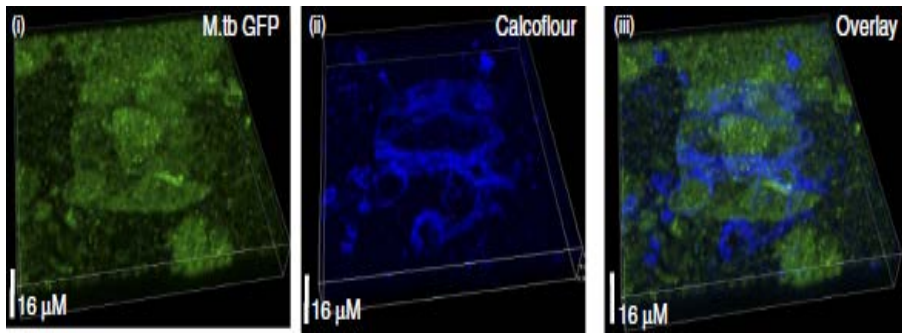


Figure II- 40. Biofilm of *M. tuberculosis* overexpressing GFP were developed in standing culture by exposure to TRS and then stained with specific fluorophores: PYPRO Ruby for staining the proteins (Trivedi et al., 2016).

### (3) PEL and PSL

*P. aeruginosa* can produce at least three different polysaccharides, alginate, PEL, and PSL. While PEL and PSL both seem to be branched heteropolysaccharides, the main component of PEL is glucose, whereas PSL has a high content of mannose (Friedman and Kolter, 2004). High expression of PEL and PSL in *P. aeruginosa* was shown to lead to the formation of wrinkly colonies and synthesis of PEL was shown to enable *P. aeruginosa* to form pellicle-biofilm at the air-liquid interface of broth culture (Friedman and Kolter, 2004). Proteinaceous fimbriae appear to participate together with PEL in *P. aeruginosa* biofilm formation under some conditions, similar to the cellulose and curli fimbriae-containing matrix of *Salmonella* sp. in biofilms. PSL is important in the early stages of *P. aeruginosa* biofilm development, whereas the synthesis of PEL seems to be important in latter stages of biofilm development (Vasseur et al., 2005). It was confirmed that a *P. aeruginosa* strain deficient in PSL production was found to be impaired in biofilm formation, supporting a role of PSL in the early stages of biofilm development (Matsukawa and Greenberg, 2004).

### **II.5.3. Control of Membrane Biofouling by Disruption of EPS**

Bacteria naturally secrete extracellular polymeric substances (EPS) which facilitate bacterial attachment to a solid surface such as membranes. EPS have been believed to be irreversible foulants of membrane fouling (Flemming et al., 1992, Herzberg et al., 2009), which cannot be efficiently removed by traditional physical or chemical cleaning methods. However, EPS can be hydrolyzed by several EPS-degrading enzymes, implying a novel means to control EPS-mediated membrane biofouling. Because polysaccharides and proteins are two main components of the EPS, thus polysaccharides-degrading enzymes and proteins-degrading enzymes (protease) have been applied to membrane process for alleviating membrane fouling (Wang et al., 2004c).

#### (1) Proteolytic enzymes (Protease)

Protease such as the proteinase K and subtilisin have been employed to remove established biofilms. Proteinase K, a widespectrum protease, has been commonly applied to disperse the established biofilm as well as to inhibit biofilm formation as it could effectively cleave the peptides bonds of aromatic, aliphatic, and hydrophobic compounds. Inoculation of bacteria in media with 1 mg/ml proteinase K would inhibit the formation of *Haemophilus influenza* biofilm in polystyrene tube, while no influence on bacterial growth was found in terms of the total CFU at such concentration of proteinase K (Izano et al., 2009).

Subtilisin was also tested for its antifouling activity in polystyrene microplates for the natural seawater. It was found that 99.5% of inhibition of bacterial adhesion was achieved when subtilisin was added to the culture media, whereas 87% of

detachment was observed in the detachment assay (Leroy et al., 2008b). More importantly, subtilisin was found to be much lower for prevention of microbial attachment than for detachment of adhered bacteria. It seems to suggest that subtilisin should be more effective in preventing initial microbial attachment than disrupting established biofilm. In comparison with other commercial protease such as Amano Protease A, papain, and umamizyme, subtilisin was shown to be the most efficient protease for alleviating the fouling by *Pseudoalteromonas* sp. D41. In detail, it had the ability to inhibit microbial attachment as well as detach adhered bacteria (Leroy et al., 2008a)

Protease was also used to remove biofouling on ultrafiltration (UF) membrane for wastewater treatment. Compared to the traditional cleaning method by alkaline, enzymatic cleaning by protease exhibited a much higher efficiency in removing biofouling, leading to a high-efficiency recovery of the permeate flux (Te Poele and Van der Graaf, 2005). Moreover, enzymatic cleaning of the fouled inorganic UF membranes by whey proteins was also tested, and results showed that high removal efficiency would be achievable (Figure II- 41) (Argüello et al., 2002, Argüello et al., 2003).

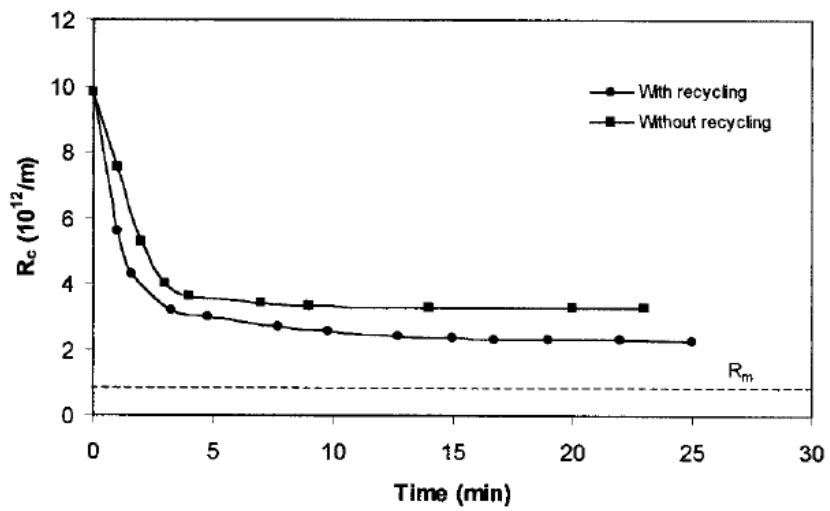


Figure II- 41. Evolution of the hydraulic resistance during the cleaning of Carbosep M5 membranes with Alcalase (1.40 units/L, 8.7 initial pH) (Argüello et al., 2002)



## (2) Polysaccharases

Several polysaccharases are currently available for inhibition of microbial attachment and membrane biofouling by disrupting the matrix structure of extracellular polysaccharides. Dispersin B, which hydrolyzes poly-*N*-acetylglucosamine, could efficiently cleave the biofilm matrix of *S. epidermidis* on the plastic surfaces (Kaplan et al., 2004). When Dispersin B was added to the *S. epidermidis* biofilm developed in the PDMS microfluidic devices, most of the biofilm would be detached from the solid surfaces (Figure II- 42) (Lee et al., 2008).

Mutanase and dextranase, two specific polysaccharide-degrading enzymes, were reported to have the ability of inhibiting the development of dental *Streptococcus* stain biofilms. Consequently, the combined use of polysaccharases and proteases is recommended for a more efficient control of microbial attachment and membrane biofouling (Wiater et al., 2004). In addition to the traditional prevention and cleaning technologies for membrane biofouling, enzymatic disruption of EPS appears to be a promising alternative for high-efficiency control of microbial attachment and membrane biofouling.

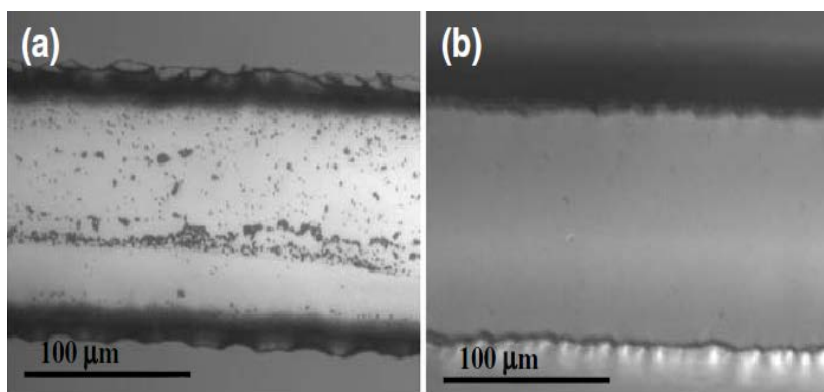


Figure II- 42. Optical images images: (a) device (PBS treated), (b) device treated with dispersin B

Lastly, it should be realized that enzymatic disruption of EPS would have some inherent drawbacks that, to some extent, may limit its large-scale application. Enzyme is unstable in the environment, e.g., the activity of enzyme would be reduced or even totally lost when the optimal pH value is altered. Moreover, enzymes are highly temperature sensitive. High temperature may make enzymes denatured, while low temperature could decrease the enzymatic activity substantially. In addition, enzymes are also sensitive to the elevated salt concentration. As EPS secreted by microorganisms represents a mixture of macromolecules, its removal efficiency by enzymatic disruption would depend on the presence or availability of multiple enzymes, and some successful applications have been reported (Maartens et al., 1996, Allie et al., 2003, Lee et al., 2008). Compared to the chemical methods for EPS removal, the enzymatic method is nontoxic and environmentally friendly, while the problem associated with the bacterial resistance to the antibouling agents would be minimized.

# **Chapter III**

**Application of Quorum Quenching  
Bacteria Entrapping Sheets to Enhance  
Biofouling Control in a Membrane  
Bioreactor with a Hollow Fiber module**



### III.1. Introduction

Recently, quorum sensing (QS), bacterial cell-to-cell communication via signal molecules, was reported to play a key role in biofilm formation (Miller and Bassler, 2001, Nadell et al., 2008), and the concept of quorum quenching (QQ), the inhibition of QS, was introduced to MBRs as a novel molecular biological approach to control biofouling (Yeon et al., 2008).

Previously, the enzymatic decomposition of QS signal molecules called *N*-acyl homoserine lactones (AHLs) (i.e., enzymatic QQ) was used to inhibit membrane biofouling in an MBR (Yeon et al., 2009, Kim et al., 2011, Paul et al., 2009, Chen et al., 2013). In a follow-up study conducted to overcome the limitations of enzymatic QQ such as high costs and enzyme instability, *Rhodococcus* sp. BH4, which produces AHL-degrading enzyme, was isolated from a wastewater treatment plant and applied as a novel QQ bacterium (Oh et al., 2012). Mitigation of biofouling in an MBR was achieved by bacterial QQ through microbial vessels encapsulating BH4 bacteria (QQ-vessels) (Oh et al., 2013, Weerasekara et al., 2014). The success of bacterial QQ shifted toward the development of more efficient QQ-media. Spherical BH4 entrapping beads (QQ-beads) were first reported as moving QQ-media because they have not only a biological (QQ) effect, but also a physical washing effect through frequent collisions between the media and the biofilm on the membrane surface (Kim et al., 2013b). In particular, the performance of QQ-beads in biofouling mitigation has been demonstrated not only in lab-scale (Kim et al., 2013b, Jo et al., 2016, Kim et al., 2015) but also pilot-scale MBRs (Maqbool et al., 2015, Lee et al., 2016b). Most recently, cylinder-shaped moving QQ-media (QQ-Cylinder (Lee et al., 2016a) and

QQ-Hollow Cylinder (Lee et al., 2016c)) were developed for enhanced biological (QQ) and physical washing effects over those with QQ-Beads.

However, all previous studies on QQ-media have focused on improving anti-biofouling capabilities without full consideration of membrane module types. In particular, because commercial hollow fiber (HF) modules, deployed in about 75% of total MBR plants (Cote et al., 2012), are usually composed of HF bundles, the reported media have yet to be identified as their physical washing effect can reach the inner part of HF modules. Moreover, deposition of microbial flocs on the surface of HFs and subsequent clogging problems could attenuate the QQ effect of the reported media due to reduced convection at the inner part of HF modules (Böhm et al., 2012). Taking into account the structure of a HF module, it is required to design new QQ-media suitable for a HF module.

In this study, we developed QQ bacteria entrapping sheets (QQ-sheets) as new moving QQ-media to enhance the anti-biofouling performance in a QQ-MBR with a HF module. Upon the application of two types of HF membrane modules, i.e., a single-layer HF module (S-HF) and a multi-layer HF module (M-HF), both biological (i.e., QQ) and physical washing effects of QQ-sheets were assessed and compared with those of the previously reported QQ-media (QQ-beads). Finally, the anti-biofouling performance of QQ-sheets was evaluated in continuous MBRs.

## III.2. Materials and Methods

### III.2.1. Preparation of QQ-media

The overall preparation scheme of QQ-media is depicted in Figure III- 1. Two different shapes of QQ-media (i.e., QQ-sheets and QQ-beads) were prepared using *Rhodococcus* sp. BH4 as a QQ bacterium, as it has been reported to degrade AHL signal molecules and control biofouling in MBRs (Oh et al., 2012). BH4 grown in Luria-Bertani (LB) broth was collected by centrifugation at 6000 rpm for 10 min. The pellet was re-suspended in deionized (DI) water. At the same time, we prepared a mixed solution of polyvinyl alcohol (Wako, Japan) and sodium alginate (Junsei, Japan) with the mass ratio of 10 to 1, and then the polymer solution was mixed with the re-suspension of BH4 (Step 1 in Figure III- 1). For the preparation of QQ-sheets, the BH4-polymer mixture was cast on a glass board using a micrometer film applicator (Sheen, UK). The cast BH4-polymer mixture was cross-linked via submersion in a boric acid and CaCl<sub>2</sub> solution with the mass ratio of 7 to 4, and subsequently in 0.5 M sulfate solution. The cross-linked sheet was cut into small pieces using 10 mm X 10 mm sized cutting press for finalizing the preparation of QQ-sheets (Step 2a in Figure III- 1). On the other hand, QQ-beads were prepared using the dripping method (Lee et al., 2016b), as shown in Step 2b in Figure III- 1. The concentration of entrapped BH4 in both QQ-sheets and QQ-beads was 5 mg of BH4 (in dry weight) per g of QQ-media (in dry weight). The non-cell entrapping media (i.e., Vacant-beads and Vacant-sheets) were prepared as controls using the same methods as described above, except with an equivalent volume of DI water instead of the BH4 re-suspension. The density of all media



prepared in this study was approximately 1.0 g/mL. The procedure for measuring thickness of QQ-sheets is as follows: after measuring the mass of each piece of QQ-sheet, the mass was converted to the volume considering the density of media (approximately 1.0 g/ml). The resulting value of volume was divided by width (10 mm) and height (10 mm), and thus the thickness of each QQ-sheet was yielded. The thickness of thin QQ-sheets, medium QQ-sheets, and thick QQ-sheets was approximately 0.48 ( $\pm 0.02$ ), 0.73 ( $\pm 0.02$ ), and 1.06 ( $\pm 0.07$ ) mm.

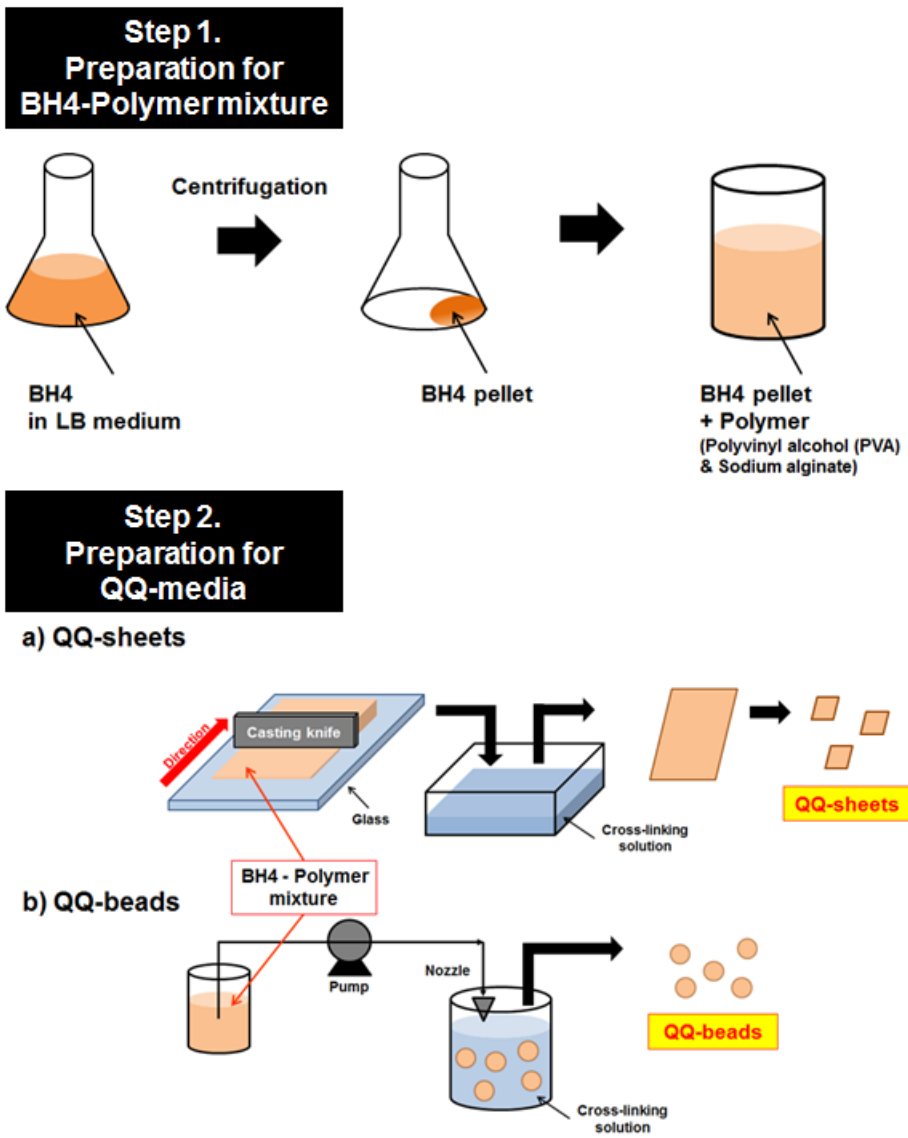


Figure III- 1. Preparation scheme of QQ-media, (a) QQ-beads and (b) QQ-sheets

### **III.2.2. Fabrication of Hollow Fiber Modules**

To fabricate two different HF modules (i.e., S-HF and M-HF) for MBR operation, a polyvinylidene fluoride (PVDF) HF with outer diameter of 1.9 mm (Zeeweed 500, GE-Zenon, USA) was used. Parts for module assembly were prepared using a 3-D printer (Stratasys Object 30, USA). The S-HF (Figure III- 2a) had 13 hollow fibers with a total effective filtration area of 0.0152 m<sup>2</sup>, while the M-HF (Figure III- 2b) consisted of 25 (five by five) hollow fibers with a total effective filtration area of 0.0208 m<sup>2</sup> and spacing of 1 mm. The packing density of the M-HF was around 39%, which is close to that of commercial HF modules from other companies (usually above 45%) (Li et al., 2004)

### **III.2.3. Fabrication of Polyacrylic Stick Modules**

For the assessment of the physical washing effect of the prepared media for HF modules, two polyacrylic stick modules, i.e., single-layer (Figure III- 2c) and multi-layer (Figure III- 2d), were prepared from polyacrylic sticks with the same physical dimensions as the HFs for the actual HF module used in MBR operation. They were fabricated using the same methods as those described in Chapter III. 2.2 for the HF modules.

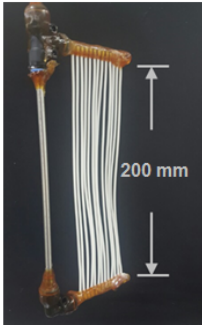
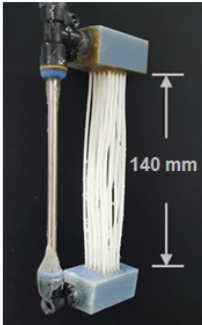
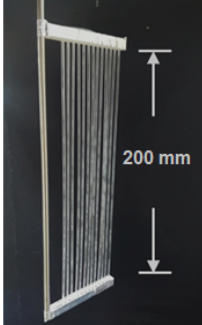
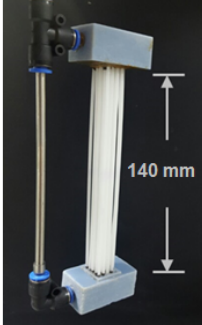
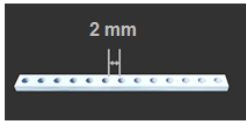
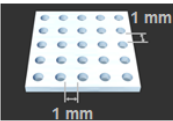
<b>Hollow fiber module</b>		
	<b>(a) Single-layer hollow fiber module (S-HF)</b>	<b>(b) Multi-layer hollow fiber module (M-HF)</b>
<b>Polyacrylic stick module</b>		
	<b>(c) Single-layer Polyacrylic stick module</b>	<b>(d) Single-layer Polyacrylic stick module</b>
<b>Distance between fibers (or sticks)</b>		

Figure III- 2. Schematic diagrams of (a) single-layer hollow fiber module (S-HF), (b) multi-layer hollow fiber module (M-HF), (c) single-layer polyacrylic stick module, and (d) multi-layer polyacrylic stick module. Hollow fiber modules and polyacrylic stick modules were used for MBR operation and batch experiment for assessment of physical washing effect, respectively.

### **III.2.4. Assessment of Physical Washing Effect**

The physical washing effects of Vacant-sheets and Vacant-beads were examined in three batch reactors (working volume of each: 2.5 L) with 10-fold concentrated synthetic wastewater and 3 mL of activated sludge inoculum. The single-layer (Figure III- 2c) or the multi-layer (Figure III- 2d) polyacrylic modules were inserted into each of three batch reactors: control reactor without any medium, reactor with Vacant-beads, and reactor with Vacant-sheets. The loading volume of each medium was fixed at 0.5% (volume of media per volume of reactor). All three batch reactors were operated in parallel at an aeration rate of 1.5 L/min, which is the same as the operating condition of continuous MBRs. After operation for 20 h, the bio-fouled modules were taken out of each reactor and were stained with 0.2% crystal violet (CV) for 10 min, followed by a gentle wash with DI water. The CV-stained sticks in single-layer module (200 mm) were individually dissolved in 25 ml of 95% ethanol for 1 h. In case of the CV-stained stick in multi-layer module, individual CV-stained stick (140 mm) was dissolved 10 ml of 95% ethanol for 1 h. Finally, the absorbance at 570 nm ( $OD_{570}$ ) of the CV-dissolved solution was measured using a spectrophotometer (Epoch, Biotek, USA). The optical densities of the polyacrylic sticks from the module were averaged, representing the amount of biofilm formed. Since CV was slightly adsorbed on fresh polyacrylic stick, the value of CV concentration of the fresh stick, which was immersed in CV solution for 10 min, was used as a blank for the physical washing test. The physical washing effects of Vacant-sheets and Vacant-beads were represented as the percentage of biofilm reduced relative to the control reactor without media.

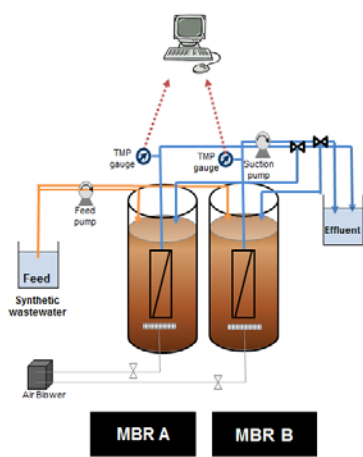
### III.2.5. Assessment of QQ Activity

The QQ activities of the prepared QQ-media were evaluated in terms of the degradation rate of standard *N*-Octanoyl-DL-homoserine lactone or C8-HSL (Sigma-Aldrich, USA), one of the major QS signal molecules of AHLs in MBRs (Yeon et al., 2008). The concentration of this signal molecule was measured via a bioluminescence assay using the reporter strain *A. tumefaciens* A136. In detail, the prepared QQ-media with a fixed volume of 1.0 mL were individually added to 20 mL of 1  $\mu$ M C8-HSL dissolved in 20 mM phosphate buffer, and the mixture was incubated at 30 °C with shaking at 200 rpm. After 30 min, the solution was sampled for measurement of the concentration of residual C8-HSL through an A136 bioassay. The reporter strain A136 and the C8-HSL samples were mixed and loaded onto a microwell plate. The microwell plate was placed in an incubator at 30 °C for 90 min, after which the Beta-Glo Assay System (Promega, USA) was added to the solution for a luminescent reaction with  $\beta$ -galactosidase produced by the reporter strain. After 40 min of reaction, luminescence was measured by a luminometer (Synergy 2, Biotek, USA). The amounts of C8-HSL were calculated using relationship equations based on the calibration curve derived from standard samples of C8-HSL. The QQ activity was presented as the nanomolar concentration of degraded C8-HSL for 30 min in the presence of QQ-media.

### III.2.6. MBR Operation

Two submerged MBRs (MBR A and MBR B), each with a working volume of 2.5 L, were continuously operated in parallel using synthetic wastewater (Figure III- 3). The composition of the synthetic wastewater was as follows in (mg/L): glucose, 200; yeast extract, 7; Bacto Peptone, 57.5;  $(\text{NH}_4)_2\text{SO}_4$ , 52.4;  $\text{KH}_2\text{PO}_4$ , 10.88;  $\text{MgSO}_4$ , 7.82;  $\text{FeCl}_3$ , 0.038;  $\text{CaCl}_2$ , 1.23;  $\text{MnSO}_4$ , 0.9; and  $\text{NaHCO}_3$ , 127.8. MBRs were operated in a total of six different phases (three phases with S-HF and three with M-HF), as shown in Figure III- 3. Except for module and media types, the MBRs were operated under the same operating conditions as listed in Table III- 1.

The concentration of the media applied to each reactor was 0.5% (volume of media per volume of reactor). During MBR operation, transmembrane pressure (TMP) was continuously monitored for evaluation of the extent of biofouling in each MBR. When TMP reached 25 kPa, the used membrane was taken out of each reactor and washed with 1000 ppm NaOCl for 4 h for reuse. The average number of days required for one TMP jump to 25 kPa ( $T_{\text{TMP}}$ ) was calculated for the evaluation of the anti-biofouling performance of the prepared media.



Phase	Hollow fiber membrane module	MBR A	MBR B
S1	Single-layer (S-HF)	Vacant-Beads	QQ-Beads
M1	Multi-layer (M-HF)	Vacant-Beads	QQ-Beads
S2	Single-layer (S-HF)	Vacant-Sheets	QQ-Sheets
M2	Multi-layer (M-HF)	Vacant-Sheets	QQ-Sheets
S3	Single-layer (S-HF)	QQ-Beads	QQ-Sheets
M3	Multi-layer (M-HF)	QQ-Beads	QQ-Sheets

Figure III- 3. Schematic diagram of the two MBRs (MBR A and MBR B) operated in parallel in six phases.



Table III- 1. MBR operating conditions (for all of the operation phases)

<b>Working volume (L)</b>	<b>2.5</b>
<b>SRT (Day)</b>	<b>30</b>
<b>HRT (Hour)</b>	<b>8</b>
<b>Membrane type (Membrane area)</b>	<b>Hollow fiber (HF), PVDF (Single-layer HF membrane: 152cm<sup>2</sup>, Multi-layer HF Module: 208 cm<sup>2</sup>)</b>
<b>Flux (L/m<sup>2</sup>/hr)</b>	<b>23</b>
<b>Aeration (L/min)</b>	<b>1.5 Disk-type</b>
<b>Feed COD (mg/L)</b>	<b>150 ~ 250</b>
<b>COD removal efficiency (%)</b>	<b>Broth: 94 ~ 96 Permeate: 96 ~ 98</b>
<b>MLSS (mg/L)</b>	<b>4500 ~5000</b>
<b>Concentration of Media (%, v (media) / v (reactor))</b>	<b>0.5</b>
<b>QQ media (mg BH4 / g media)</b>	<b>5</b>

### **III.2.7. Analytical Methods**

For the analysis of extracellular polymeric substances (EPS) in the biofilm formed on the membrane surface, the biofilm was extracted using the heat extraction method (ZHANG et al., 2009). The amounts of total polysaccharides and proteins were determined by the phenol-sulfuric acid method (Masuko et al., 2005) and the Bradford assay (Manual), respectively. The morphologies of Vacant- and QQ-sheets were analyzed using scanning electron microscope (SEM) (JEOL JSM-7600F, Japan). Prior to SEM examination, the media were dehydrated through freeze-drying, then coated with platinum.

### **III.3. Results and Discussion**

#### **III.3.1. Comparison of QQ Efficiency using QQ-beads between Single- and Multi-layer HF Modules**

To investigate the potential of QQ-beads for biofouling control in a HF module, Vacant-Beads and QQ-Beads were inserted in MBR A (Vacant-bead-MBR) and MBR B (QQ-bead-MBR), respectively. Two different types of HF modules were installed in both MBRs according to the phase, i.e., S-HF for phase S1 and M-HF for phase M1, respectively (Figure III- 3). For each phase, the Vacant-bead-MBR was run as a control for the evaluation of the net biological QQ effect of the QQ-bead-MBR.

In phase S1, after the application of S-HF, the  $T_{TMP}$  in the Vacant-bead-MBR was 10.2 days, whereas that in the QQ-bead-MBR was 20.9 days (Figure III- 4a), producing a  $T_{TMP}$  ratio of 2.0 between the two reactors (Table III- 2). In other words, in the MBR with the S-HF, the fouling rate could be lowered approximately 2.0-fold through the net QQ effect of QQ-beads. In phase M1, the two MBRs were operated under the same operating conditions as in phase S1, except that the S-HF was replaced by the M-HF in both. As shown in Figure III- 4b and Table III- 2, the  $T_{TMP}$  values in the Vacant-bead- and QQ-bead-MBRs were 8.9 and 10.2 days, respectively, resulting in a  $T_{TMP}$  ratio of approximately 1.1. Thus, the  $T_{TMP}$  ratio between the Vacant-bead- and QQ-bead-MBRs was significantly decreased from 2.0 to 1.1 with the shift from the S-HF to the M-HF, indicating a diminished QQ effect of the QQ-beads with the M-HF.

Such a discrepancy in the QQ effect for biofouling mitigation between the S-HF and M-HF may be attributable to the structural differences in HF modules i.e., the absence (S-HF) or presence (M-HF) of the inner part. According to Böhm et al., (Böhm et al., 2012), flocs are more likely to deposit in the inner part of a HF module in MBRs due to reduced hydrodynamic forces in the inner part compared with the outer part. For a comparison of the amount of biofilm formed between the S-HF and M-HF modules, the used HF modules were taken out from QQ-bead-MBR operated in phase S1 and M1 when TMP reached 25 kPa and the total attached biomass (TAB) was measured. The amount of TAB per unit membrane surface area was 2.6 g/m<sup>2</sup> in the S-HF module and 13.5 g/m<sup>2</sup> in the M-HF module, indicating that more biofilm was deposited on the M-HF than on the S-HF. There was little difference in the amount of the TAB between Vacant-bead- and QQ-bead-MBRs when the same type of HF module was used (data not shown).

QQ-beads are well-known to play an important role in the mitigation of biofouling in MBRs via the QQ effect (Kim et al., 2013b) and physical washing effect involving the collisions of beads with biofilm accumulated on the membrane surface (Lee et al., 2016a, Lee et al., 2016c). Unlike in QQ-bead-MBR with a S-HF (phase S1), QQ-beads would not remove the deposited biofilms through collisions in an MBR with a M-HF (Phase M1) because the diameter of QQ-beads (around 3.5 mm) is comparatively greater than the spacing between HFs (1.0 mm). Thus, QQ-beads cannot significantly affect the inner part of the M-HF. In addition, in the MBR with the M-HF, diffusion of AHLs toward the QQ-beads where AHLs are decomposed by QQ bacteria (*Rhodococcus* sp. BH4) would be retarded (Hoek and Elimelech, 2003) so that QQ-beads could not efficiently degrade AHLs in the

biofilm accumulated in the inner part of the M-HF. This could explain why the  $T_{TMP}$  ratio between Vacant-bead- and QQ-bead-MBRs significantly decreased from 2.0 to 1.1 with the shift from the S-HF to the M-HF. Considering that a commercial HF module resembles a M-HF rather than a S-HF, these limitations of QQ-beads in MBR with a M-HF should be overcome if we bring the bacterial QQ more of a practical solution to the biofouling problem. Consequently, we designed new QQ-media capable of exerting both significant physical washing and biological QQ effects in the inner part of the M-HF.

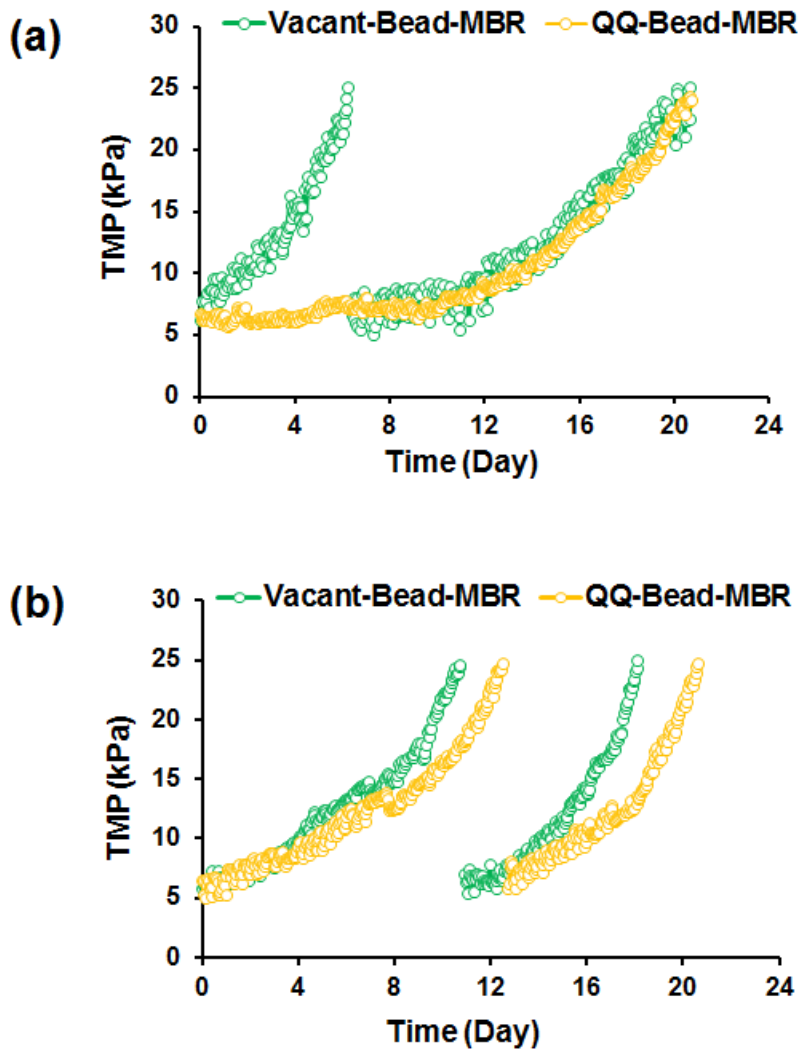


Figure III- 4. TMP profiles of Vacant-Bead-MBR and QQ-Bead-MBR equipped with a) S-HF (phase S1) and b) M-HF (phase M1). Vacant-Beads ( $D = \sim 3.5$  mm,  $N = 568$ ) and QQ-Beads ( $D = \sim 3.5$  mm,  $N = 550$ ) were used in the corresponding MBRs.

Table III- 2. Average number of days required for on TMP jump,  $T_{TMP}$ , to occur in MBR A and B in each of the six phases

<b>Phase</b>	<b>MBR A</b>	<b>MBR B</b>	<b>Ratio (B/A)</b>
<b>S1</b>	<b>10.2 days</b> (Vacant-Beads)	<b>20.9 days</b> (QQ-Beads)	<b>2.0</b>
<b>M1</b>	<b>8.9 days</b> (Vacant-Beads)	<b>10.2 days</b> (QQ-Beads)	<b>1.1</b>
<b>S2</b>	<b>6.6 days</b> (Vacant-Sheets)	<b>14.9 days</b> (QQ-Sheets)	<b>2.3</b>
<b>M2</b>	<b>6.8 days</b> (Vacant-Sheets)	<b>15.0 days</b> (QQ-Sheets)	<b>2.2</b>
<b>S3</b>	<b>10.0 days</b> (QQ-Beads)	<b>14.2 days</b> (QQ-Sheets)	<b>1.4</b>
<b>M3</b>	<b>6.9 days</b> (QQ-Beads)	<b>12.3 days</b> (QQ-Sheets)	<b>1.8</b>

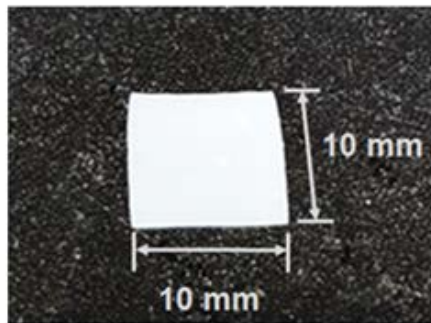
### **III.3.2. Development of Sheet-shaped Media**

#### **III.3.2.1. Characterization of Sheet-shaped Media**

As for a new shape of QQ-media, we developed sheet-shaped media because they can move freely even into the inner part of the M-HF module and have greater surface area, resulting in better decomposition of signal molecules. As shown in Figure III- 5a, both the width and height of QQ-sheet were fixed at 10 mm. In addition, the thickness of the sheet media was fixed at 0.5 mm so that QQ-sheets could easily access the inner part of the module. Cross-sectional SEM images show that both Vacant-and QQ-sheets had numerous pores and that in QQ-sheets, rod-shaped BH4 bacteria were entrapped (Figure III- 5b).



**(a)**



**(b)**

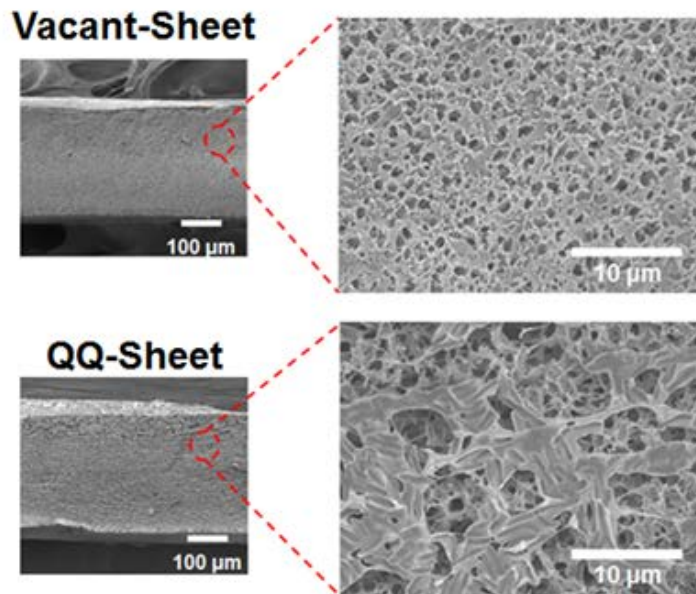


Figure III- 5. (a) Images of a  $10 \times 10$  mm QQ-sheet with a thickness of 0.5 mm, and (b) cross-sectional SEM images of a Vacant-sheet and a QQ-sheet (Magnifications are  $150\times$  and  $2000\times$  for the images on the left and right sides, respectively.)

### **III.3.2.2. Comparison of Physical Washing Effect between Sheets and Beads on a Single-layer module**

To investigate whether the newly developed QQ-sheets were capable of physically detaching biofilms formed on a HF module, we compared the physical washing effect between Vacant-beads and Vacant-sheets. Because the actual porous HF membranes absorbed crystal violet used as a staining agent, hindering accurate quantification of biofilm, imitations of HF modules consisting of polyacrylic sticks were used instead for the assessment of the physical washing effect. A single-layer polyacrylic stick module (Figure III- 2c) was inserted into each of three batch reactors with synthetic wastewater and activated sludge. The reactors were inoculated with no media (control), Vacant-beads, or Vacant-sheets.

As shown in Figure III- 6a, the most biofilm formed on the polyacrylic sticks in the control reactor without any media, while 36% and 60% less formed in the reactors with Vacant-beads and Vacant-sheets, respectively. Thus, the Vacant-sheets were the most effective at removing biofilms formed on the polyacrylic module, despite fewer media ( $N = 260$ ) than that with Vacant-beads ( $N = 550$ ). This is because Vacant-sheets exerted a physical washing effect, even on the hard-to-reach region between the sticks by passing between them, as shown in Figure III- 6b. Based on these results with the single-layer module, we suspected that Vacant-sheets penetrated into the module and thus investigated if they would also work in a multi-layer module.

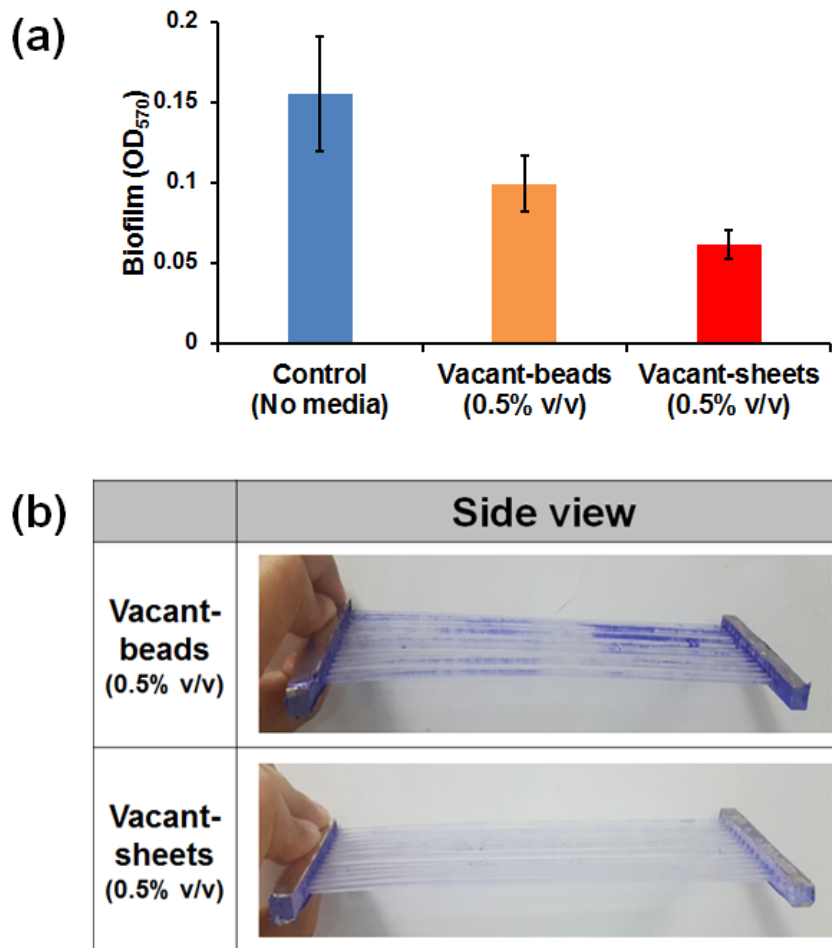


Figure III- 6. (a) Comparison of physical washing effect of Vacant-beads ( $D = 3.5$  mm,  $N = 550$ ) and Vacant-sheets ( $T = 0.5$  mm,  $N = 260$ ) in a single layer polyacrylic fiber module and (b) visual comparison of the crystal violet stained region in the acrylic fibers. Error bar: standard deviation ( $n = 3$ ). Physical washing effect of Vacant-sheets and Vacant-beads was presented in the percentage of biofilm reduced relative to the control reactor.

### **III.3.2.3. Comparison of Physical Washing Effect between Sheets and Beads on a Multi-layer module**

The multi-layer polyacrylic stick module (Figure III- 2d) was substituted for the single module to in each batch reactors for the investigation of the physical washing effect of the media on the multi-layer module, which is similar to a real commercial HF module. In the measurement of biofilm formed on each multi-layer module in the three batch reactors, the inner part (9 fibers) of one multi-layer module was differentiated from the outer part (16 fibers), as shown in Fig. 6a. In the outer part of the multi-layer module, Vacant-beads and Vacant-sheets exerted a physical washing effect amounting to 24% and 54% reductions in biofilm, respectively, as shown in Fig. 6b. This difference may have resulted from the same phenomenon as in the single-layer module. However, in the inner part (Fig. 6c), the Vacant-beads exerted little physical washing effect (less than 6% reduction), while that of the Vacant-sheets was around 46%, similar to the result for the outer part and much greater than that of the Vacant-beads. The statistical analysis revealed that the physical washing effect of Vacant-beads was differed significantly according to the location of membranes ( $p < 0.05$ , one-tailed  $t$ -test), whereas there was no difference in that of Vacant-sheet, regardless of membrane location ( $p > 0.05$ , one-tailed  $t$  test). In sum, Vacant-beads effectively removed biofilm only in the outer part, whereas Vacant-sheets removed biofilm in both the inner and outer parts because of their relatively free passage through spacing between sticks. These findings suggest that thin sheet media have promise for use with the M-HF, which is much more like a real commercial HF than the S-HF.

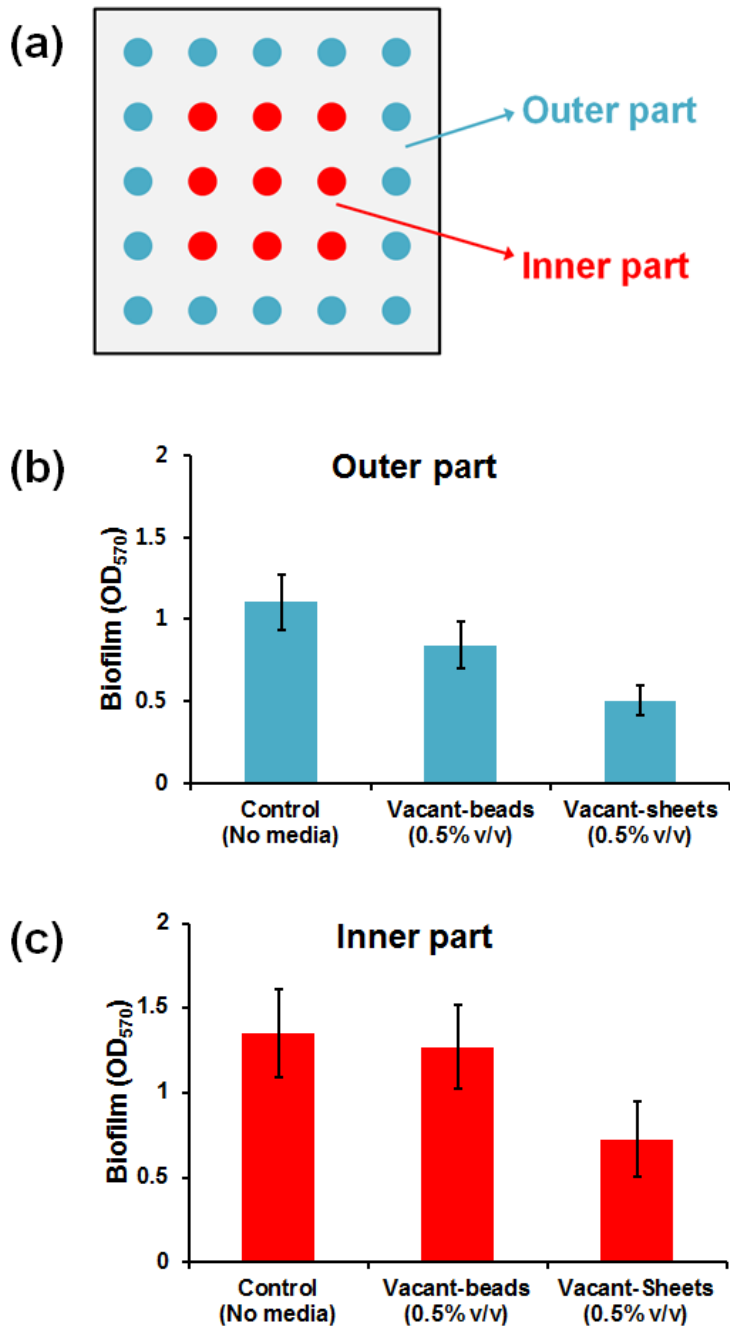


Figure III- 7. Comparison of the physical washing effect between Vacant-beads ( $D = 3.5$  mm,  $N = 545$ ) and Vacant-sheets ( $T = 0.5$  mm,  $N = 267$ ) in a multi-layer polyacrylic fiber module. (a) Differentiation of inner part (9 fibers) from outer part (16 fibers) in M-HF. Comparison of biofilm formed in control reactor with no

media, reactor with Vacant-beads and reactor with Vacant-sheets at (b) the inner and (c) outer part of the multi-layer module. Physical washing effect of Vacant-sheets and Vacant-beads was evaluated in terms of percentage of biofilm reduction in comparison with control reactor. The physical washing effect of Vacant-beads between the inner part and the outer part was significantly different ( $p$ -value  $< 0.05$ ), whereas that of Vacant-sheets was not different between the inner part and the outer part ( $p$ -value  $> 0.05$ ).

### III.3.2.4. Comparison of QQ activity between QQ-sheets and QQ-beads

Following the physical washing effects of QQ-media, the biological effects of various QQ-media were also compared between QQ-bead and QQ-sheets with various thicknesses: thin QQ-sheet (0.5 mm), medium QQ-sheets (0.7 mm), and thick QQ-sheets (1.0 mm). For the comparison of biological QQ effect, the volume of each medium was fixed at 1.0 mL to make the amount of entrapped QQ bacteria (*Rhodococcus* sp. BH4) in each medium become identical (5.0 mg of BH4 per g of medium) for each media. QQ activity, defined as the average number of nanomoles of C8-HSL degraded per min over 30 min in the presence of each QQ-media, was plotted as a function of the total surface area of each medium (Figure III- 8).

At the given fixed media volume (1 mL) and BH4 loading amount (5 mg), the number of QQ-Beads ( $N = 45$ ) was the greatest, but the total surface area of QQ-Beads was the smallest. In contrast, the thin QQ-sheets ( $N = 21$ ) had the largest total surface area due to their geometric structure. The thin QQ-sheets degraded C8-HSLs 2.5 times more efficiently than the QQ-Beads. It is worth noting that the QQ activity was almost linearly proportional to the total surface area of QQ-media. In other words, the order of QQ activity from the lowest to the highest was QQ-bead, thick QQ-sheet, medium QQ-sheet and thin QQ-sheet QQ activity (Figure III- 8). This result was in line with previous studies that found that the QQ activity of media was proportional to their total surface area under identical concentrations of QQ microorganisms (Lee et al., 2016a, Lee et al., 2016c). Consequently, the thin QQ-sheets (with a thickness of 0.5 mm), which exhibited the greatest QQ activity, were selected for a comparison with the QQ-beads in

terms of both physical and biological effects.

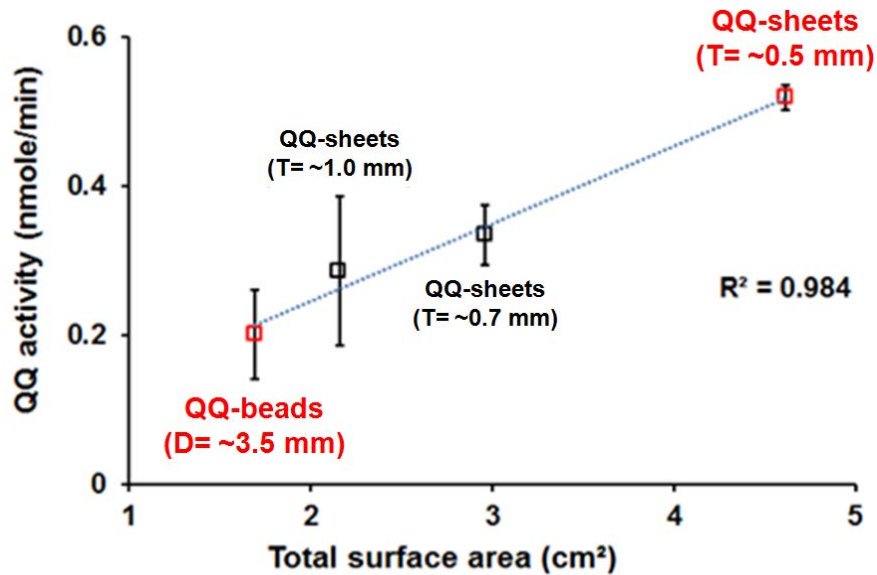


Figure III- 8. QQ activity as a function of total surface area of QQ-sheets and QQ-beads. The QQ activity was defined as the number of nanomoles of degraded C8-HSL per min, which was measured after 30 min in the presence of QQ-media. The prepared QQ-media were as follows: QQ-beads (D = 3.5 mm, N = 45), thick QQ-sheets (W= 10mm, L = 10 mm, T = 1.0 mm, N = 9), medium QQ-sheets (W= 10mm, L = 10 mm, T = 0.7 mm, N = 13), and thin QQ-sheets (W= 10mm, L = 10 mm, T = 0.5 mm, N = 21). D, L, N, W, and T represent diameter, length, number, width, and thickness of the media, respectively. Two QQ-media shown in red points were used in MBR operation. Error bar: standard deviation ( $n = 3$ ).



### **III.3.3. Evaluation of Biofouling Control by QQ-sheets in MBRs with Single- and Multi-layer HF Modules**

For evaluation of the biofouling control capacity of QQ-sheets in MBRs with HF modules, MBR A with Vacant-sheets (Vacant-sheet-MBR) and MBR B with QQ-sheets (QQ-sheet-MBR) were continuously run in parallel as shown in Figure III- 9 (phases S2 and M2). When the S-HF was equipped in each MBR (phase S2), the  $T_{TMP}$  values of Vacant-sheet-MBR and QQ-sheet-MBR were 6.6 and 14.9 days, respectively, and the  $T_{TMP}$  ratio between them was, therefore, 2.3 (Table III- 2). When the M-HF was substituted for the S-HF in each MBR, the  $T_{TMP}$  values in Vacant-sheet-MBR and QQ-sheet-MBR were 6.8 and 15.0 days, respectively, yielding a  $T_{TMP}$  ratio of approximately 2.2 (Table III- 2). In general, QQ-media have two effects, physical washing and biological QQ effects for the biofouling control in MBR for wastewater treatment [12, 17]. Moreover, the ratio of  $T_{TMP}$  is more likely to represent the net biological QQ effect. In this context, we can conclude that QQ-sheets are able to maintain their biological QQ capability in MBR with a S-HF as well as with a M-HF because the two  $T_{TMP}$  ratios in phase S2 (2.3) and M2 (2.2) approach each other. In case of QQ-beads, however, the  $T_{TMP}$  ratio in MBR with a M-HF became much smaller than that with a S-HF (Figure III- 4, Table III- 2), indicating that QQ-beads have some limitations to be used in MBR with a dense and compact commercial HF module.

Because QS is closely related to EPS production (Dobretsov et al., 2009), after 22 days of phase M2, the biofilm formed on used membranes was collected from Vacant-Sheet-MBR and QQ-sheet-MBR for EPS content analysis. Each biofilm was also analyzed in terms of total attached biomass (TAB) and EPS. As

expected from the rate of TMP increase, the TAB in the Vacant-sheet-MBR (0.268 g) was much greater than that in the QQ-sheet-MBR (0.097g). As shown in Figure III- 10, the concentration of polysaccharide and protein from QQ-sheet-MBR were lower than Vacant-sheet-MBR by approximately 38% and 72%, respectively.

There are two possible reasons for the net QQ effect of QQ-sheets upon the application of the M-HF. First, QQ-sheets showed greater QQ activity than QQ-beads due to their large surface area, which is directly related to the net QQ effect. Second, QQ-sheets had a physical washing effect of the inner part as well as the outer part for M-HF. Although we could not determine quantitatively AHL concentration in MBRs, we expected that detachment of the biofilm from the inner part of the M-HF could be helpful in allowing AHLs to diffuse out of the biofilm and toward the QQ-sheets. This physical washing effect of QQ-sheet could indirectly help the degradation of AHLs (i.e., QQ) more efficient for the M-HF. This combined direct and indirect effect of QQ-sheet showed promise in the application of QQ technology to commercial multi-layer hollow fiber modules.

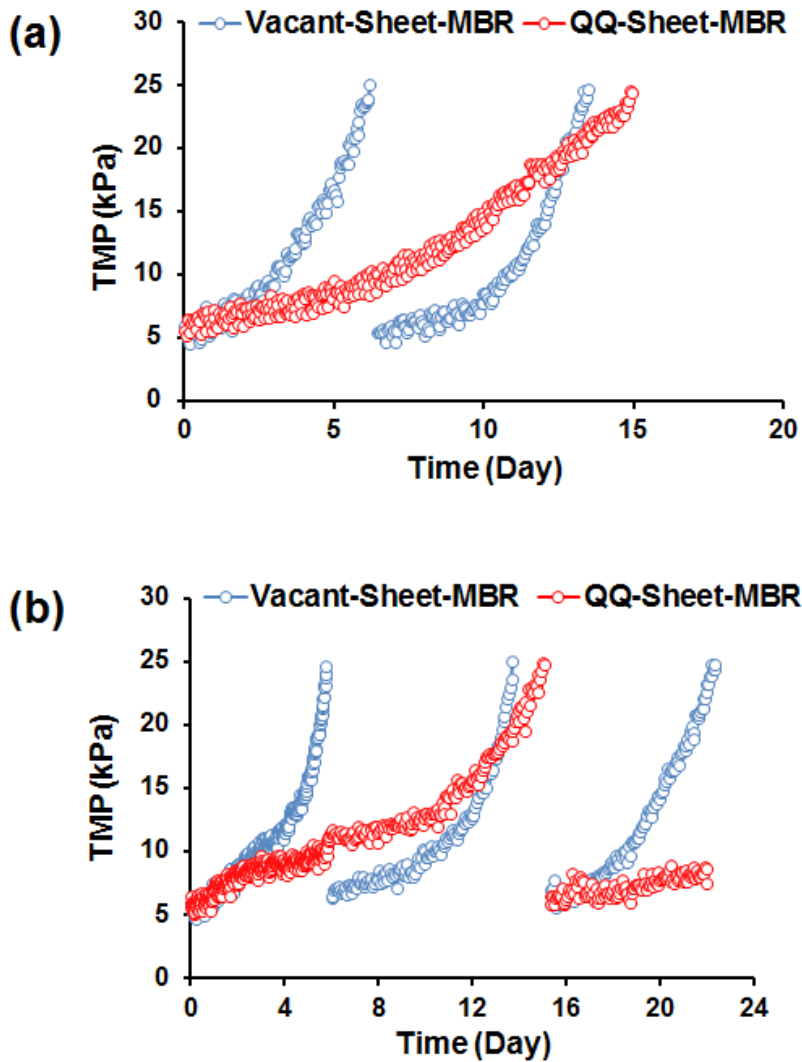


Figure III- 9. TMP profile of Vacant-sheet-MBR and QQ-sheet-MBR equipped (a) with S-HF (phase S2) and (b) with M-HF (phase M2). Vacant-sheets ( $T = 0.5$  mm,  $N = 260$ ) and QQ-sheets ( $T = 0.5$  mm,  $N = 265$ ) were inserted in each corresponding MBR.

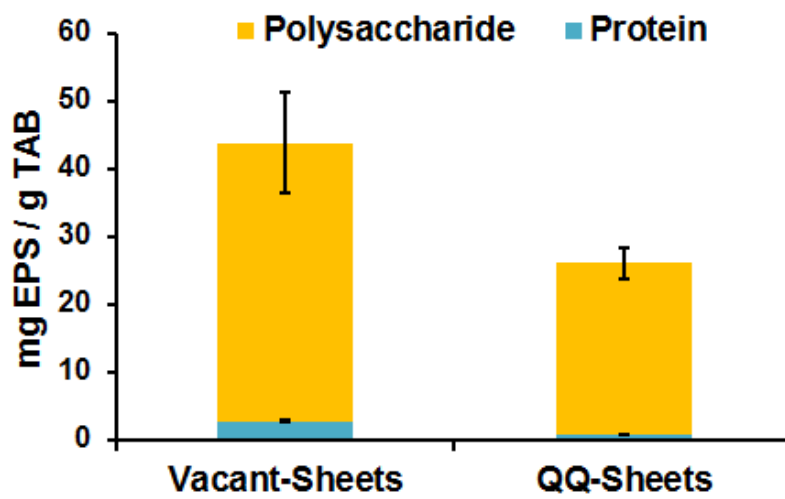


Figure III- 10. Comparison of EPS content in the biofilm formed on the membrane surface in Vacant-sheet-MBR and QQ-sheet-MBR. Error bar: standard deviation ( $n=3$ )

### **III.3.4. Direct Comparison of Biofouling Mitigation between QQ-sheets and QQ-beads in MBR with HF Module**

For confirmation of the aforementioned advantages of QQ-sheets over QQ-beads, QQ-beads were inserted into MBR A (QQ-bead-MBR) and QQ-sheets into MBR B (Figure III- 11). After the application of the S-HF in phase S3 (Figure III- 11a), the  $T_{TMP}$  values of QQ-bead-MBR and QQ-sheet-MBR were 10.0 and 14.2 days respectively, with a  $T_{TMP}$  of 1.4 (Table III- 2). As in phase S3, the MBRs were also continuously operated in parallel using the M-HF in phase M3 (Figure III- 11b). The  $T_{TMP}$  values of the QQ-bead-MBR and QQ-sheet-MBR were 6.9 and 12.3 days, respectively, with a  $T_{TMP}$  ratio of 1.8 (Table III- 2). The increase in the  $T_{TMP}$  ratio with the shift from the S-HF (1.4) to the M-HF modules (1.8) was attributed to the following: in the QQ-sheet-MBR, the physical washing and biological QQ effects of the QQ-sheets on the biofilm formed on the M-HF were similar to those on the S-HF. However, for the QQ-bead-MBR, the effects of QQ-beads on the M-HF were smaller than those on the S-HF. Thus, the superiority of QQ-sheets over QQ-beads was more prominent in the MBR with the M-HF than with the S-HF.

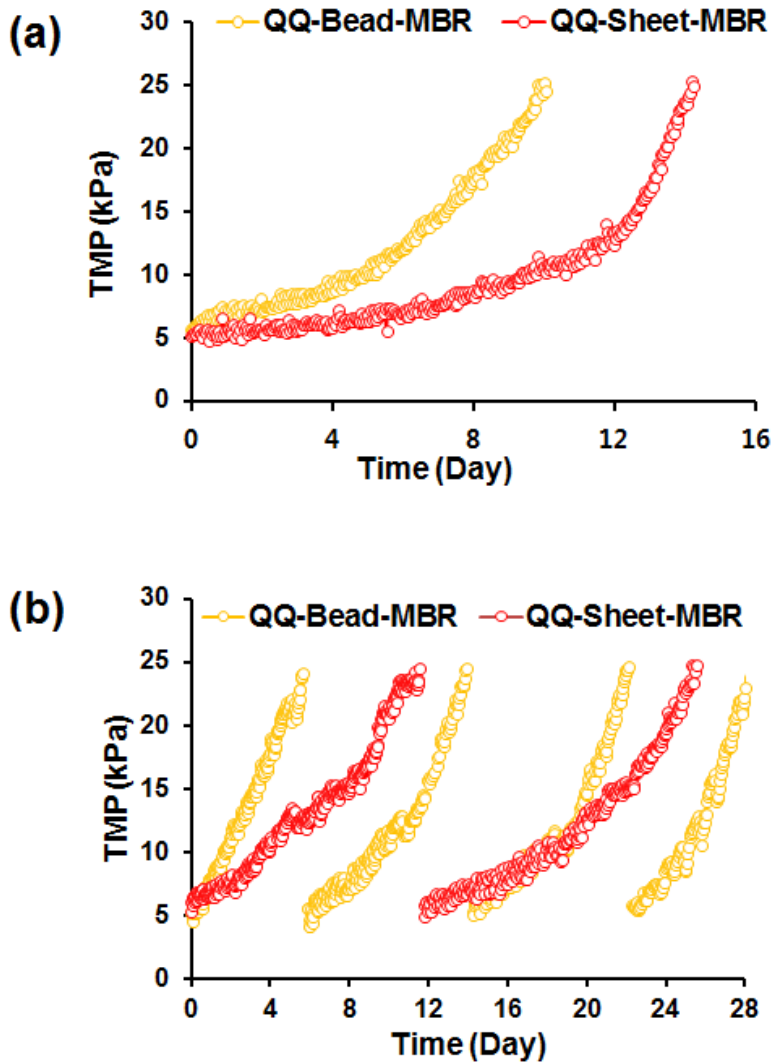


Figure III- 11. TMP profile of QQ-Bead-MBR and QQ-Sheet-MBR equipped (a) with S-HF (phase S3) and (b) with M-HF (phase M3). QQ-Beads ( $D = 3.5$  mm,  $N = 540$ ) and QQ-Sheets ( $T = 0.5$  mm,  $N = 255$ ) were used in each corresponding MBR.

### **III.4. Conclusions**

In this study, we developed QQ bacteria entrapping sheets (QQ-sheets) as new moving QQ-media to overcome limitations of previously used QQ-beads, particularly in MBRs with a HF module. The physical washing effect of QQ-sheets was significant in the inner part as well as the outer part of a multi-layer HF module, whereas QQ-beads only affected the outer part. In addition, QQ-sheets exerted a greater biological QQ effect than did QQ-beads due to their greater surface area. When QQ-sheets were applied to lab-scale continuous MBRs, they, unlike QQ-beads, mitigated biofouling substantially with both the S-HF and M-HF. The enhanced QQ effect of QQ-sheets may have been directly related to this improved biofouling mitigation. The physical washing effect of QQ-sheets may also help in detaching the biofilm at the inner part as well as the outer part of the M-HF, in turn indirectly facilitating AHL degradation. These combined merits of QQ-sheets suggest their potential for practical application in MBRs with commercial HF modules.

# **Chapter IV**

**Mitigation of membrane biofouling in  
MBR using a cellulolytic bacterium,  
*Undibacterium* sp. DM-1, isolated from  
activated sludge**





## IV.1. Introduction

Membrane biofouling is known to be associated with extracellular polymeric substances (EPS) produced by bacteria. Polysaccharides and proteins are two major components of EPS, but polysaccharides contribute more to membrane fouling than proteins because increased polysaccharide content confers stronger adherence to the EPS (Yigit et al., 2008, Sweity et al., 2011). Especially, the production of cellulose, as one of the most abundant polysaccharides (Kjelleberg and Givskov, 2007), has been reported to be closely involved in biofilm formation by *Pseudomonas* sp. (Ude et al., 2006) and *Enterobacteriaceae* family such as *E.coli* (Serra et al., 2013) and *Salmonella* sp. (Solano et al., 2002).

In the initial stage of biofilm development, cellulose is reported to act as an attachment factor for the developing biofilm due to its micro-fibril structure (Khil et al., 2005, Spiers and Rainey, 2005). In mature biofilms, cellulose provides structural integrity as it is anchored and connected to the micro-colonies in the biofilm (Trivedi et al., 2016).

A number of studies have exploited commercial cellulase to inhibit the biofilm formation of single culture bacteria such as *Pseudomonas* sp. (Wang et al., 2004c) and *Burkholderia* sp. (Yang et al., 2005). To date, no information, however, is available on the application of cellulase for mitigation of membrane biofouling in MBR where diverse microbial communities coexist. Moreover, due to cost and enzymatic instability, direct treatment of MBR with cellulase is difficult, limiting practical applications.

In this study, we isolated a cellulolytic (i.e., cellulase-producing) bacterium, *Undibacterium* sp. DM-1, from a lab-scale MBR and verified its ability

to reduce biofilms in activated sludge and in two different cellulose-producing bacteria: *Enterobacter* sp. CPB-1, and *Rhodococcus* sp. CPB-2. Finally, we entrapped DM-1 in beads and applied them to lab-scale MBRs for a more economical and stable approach to biofouling mitigation.

## **IV.2. Material and Methods**

### **IV.2.1. Bacterial Strains and Culture Conditions**

Luria-Bertani (LB) broth (Difco, USA.) was used as growth medium for activated sludge and cellulose-producing bacteria. Cellulolytic microorganisms were cultured in modified NYG broth (Fuqua and Greenberg, 2002) containing Bacto peptone (5.75 g/L) and yeast extract (0.7 g/L). All strains used in this study were incubated at 30 °C with 200 rpm shaking or 120 rpm shaking for microbial cultivation or biofilm production, respectively, unless otherwise specified.

### **IV.2.2. Visualization of Cellulose and Biofilms of Activated Sludge**

An overnight culture of activated sludge was diluted to an optical density of 0.2 at 600 nm ( $OD_{600}$ ) with fresh LB broth. Then, 10 ml of the diluted culture, treated with commercial cellulase (Sigma-Aldrich, USA.), was loaded into a conical tube to a final concentration of 6.5 U/ml. An equivalent volume of diluted activated sludge without cellulase was used as a control. An aseptic glass slide was placed vertically into each tube to allow the biofilm to form on the glass for 12 h. After incubation, the glass was taken out from each conical tube, followed by measuring  $OD_{600}$  of the culture treated with and without commercial cellulase in the tube. The grown biofilms on the glass were stained with SYTO 9 (Molecular Probes, USA) for 15 min to detect bacterial biofilm. Cellulose in biofilm was stained with Calcofluor white dye (Sigma-Aldrich, USA), which is widely used as a marker of cellulose (Muñoz et al., 2014), for 30 min. The stained biofilm was washed thrice with DI water and observed using confocal laser scanning

microscopy (CLSM, Leica TCS SP8, Germany). LAS AF software was used to quantitate biofilm and cellulose in terms of their biovolumes as listed in Table IV- 1

Table IV- 1. Biovolumes of microbial biofilm and cellulose formed by activated sludge in the absence and presence of cellulase. LAS AF software was employed to calculate the biovolume. Parenthesis: Standard deviation ( $n = 4$ ).

	Biovolume ( $\times 10^6 \mu\text{m}^3$ )	
	Without cellulase (Control)	With cellulase (6.5 U/ml of cellulase)
Microbial biofilm	15.0 ( $\pm 2.4$ )	1.5 ( $\pm 0.8$ )
Cellulose	3.1 ( $\pm 0.2$ )	0.2 ( $\pm 0.1$ )

### **IV.2.3. Isolation of Cellulolytic Microorganisms and Cellulose-producing Bacteria from MBR**

To isolate cellulolytic microorganisms, a sample solution taken from the activated sludge in the lab-scale MBR was spread on a minimal medium agar plate containing 0.5% carboxymethyl cellulose (CMC) (Sigma-Aldrich, USA) as a sole carbon source. After incubation at 30 °C for 48 h, the plates were stained with 0.2% Congo red solution for 15 min, followed by destaining with 1 M NaCl for 15 min to observe a cellulose hydrolysis zone as indicated by a light orange color. Single colonies showing the hydrolysis zone (i.e., cellulolytic microorganisms) were individually cultured in a modified NYG broth at 30 °C, and the culture was preserved in a cryotube at -80 °C for further experiments. To examine the cellulolytic activity of the isolated microbes, we obtained cell-free supernatants from the culture of the isolate grown for 48 h. Then, 20 µl of supernatant was loaded onto a new CMC plate and the plate was incubated at 30 °C for 48 h. The isolate with the highest cellulolytic activity was selected on the basis of the diameter of the hydrolysis zone by the Congo red overlay method as described above.

Cellulose-producing bacteria used for the biofilm assay were isolated from activated sludge in the lab-scale MBR using cellulose detection assays (Jo et al., 2016). Briefly, cellulose production was assayed by growing the isolates in LB agar plates containing 20 mg/l of Congo red for 3 days to stain for cellulose, followed by examining Congo red uptake by image analysis.

For identification of the bacterial isolates, 16S rDNA genes were amplified by PCR using two universal primers, 27F and 1492R. The genes of

fungus isolates were amplified with ITS rDNA sequences, e.g., with ITS1 as forward primer and ITS4 as reverse. The resulting PCR products were sequenced by an ABI3700 automatic sequencer (Applied Biosystems, USA) and matched with those in GenBank® database to identify cellulolytic microorganisms (Table IV- 2a) and cellulose-producing bacteria (Table IV- 2b).

Table IV- 2. List of (a) cellulolytic microorganisms and (b) cellulose-producing bacteria isolated from the activated sludge in the lab-scale MBR operated in this study.

(a)			
Bacteria / Fungi	Strain	Colony morphology	Identification (Sequence homology)
Bacteria	<i>Undibacterium</i> sp. DM-1	Yellow	<i>Undibacterium squillarum</i> strain CMJ-15 (99.65%)
Bacteria	<i>Bacillus</i> sp. DM-2	White	<i>Bacillus cereus</i> strain CMCC P0011 (99.60%)
Bacteria	<i>Bacillus</i> sp. DM-3	White	<i>Bacillus thuringiensis</i> strain HS18-1 (99.19%)
Bacteria	<i>Microbacterium</i> sp. DM-4	Yellow	<i>Microbacterium trichothecenolyticum</i> strain A3RC1 (99.64%)
Fungi	<i>Aspergillus</i> sp. DM-5	Black	<i>Aspergillus fumigatus</i> strain PT-B5 (99.83%)
Fungi	<i>Trichosporon</i> sp. DM-6	Ivory	<i>Trichosporon mycotoxinivorans</i> strain R-4272 (99.84%)

(b)			
Bacteria / Fungi	Strain	Colony morphology	Identification (Sequence homology)
Bacteria	<i>Enterobacter</i> sp. CPB-1	Yellow	<i>Enterobacter asburiae</i> strain LF7a (99.16%)
Bacteria	<i>Rhodococcus</i> sp. CPB-2	Yellow	<i>Rhodococcus erythropolis</i> strain zzx26 (99.91%)



#### **IV.2.4. Assay for Biofilm Formation and Detachment**

The inhibition of biofilm at its development stage and detachment of mature biofilm by cellulase secreted from *Undibacterium* sp. DM-1 were tested through biofilm formation assay (O'Toole, 2011, Deng et al., 2014) and biofilm detachment assay (Lequette et al., 2010, Nijland et al., 2010), respectively. Activated sludge and two different cellulose-producing bacteria (*Enterobacter* sp. CPB-1, and *Rhodococcus* sp. CPB-2) isolated from activated sludge were used as test organisms. Three different samples: i) cell-free supernatant of DM-1 grown for 48 h, ii) 6.5 U/ml of commercial cellulase dissolved in a modified NYG broth, and iii) autoclaved supernatant of DM-1 as a control, were treated with biofilms of test organisms, and evaluated for their biofilm removal efficiency. The cell-free supernatant was prepared by centrifugation of the culture for 5 min at 6000 rpm followed by filtration of the supernatant through a 0.45  $\mu\text{m}$  filter.

For the biofilm formation assay, test organisms were individually grown for 24 h and diluted to an  $\text{OD}_{600}$  of 0.4 in fresh LB broth. Next, 75  $\mu\text{l}$  of each bacterial dilution were inoculated into a 96-well plate, and 75  $\mu\text{l}$  of three different samples were individually added. The plate was incubated for 12 h to allow biofilm development. After incubation, the culture was discarded and the plate was gently washed with deionized (DI) water to remove nonattached cells or debris. The biofilm formed on the surface of well was stained with 180  $\mu\text{l}$  of 0.2% crystal violet (CV) for 15 min. The CV stained biofilm was dissolved in 200  $\mu\text{l}$  of 95% ethanol. Finally, the absorbance at 570 nm ( $\text{OD}_{570}$ ) of the CV-dissolved solution was measured using a microplate reader (Epoch, Biotek, USA) to quantitate the biofilm.

For the biofilm detachment assay, the cultures of three test organisms grown for 24 h were individually adjusted to an OD<sub>600</sub> of 0.2 in fresh LB broth. Then, 150 µl of the bacterial dilution was added to a 96-well plate, and the plate was incubated for 48 h to develop mature biofilms. After incubation, non-adherent cells were removed by gentle washing. Then, 200 µl of three different samples were individually added and the plate was further incubated for 1 h at 30 °C, after which the solution was gently washed out. The staining and quantification of biofilm were conducted by CV assay as described above.

#### **IV.2.5. Preparation of Beads for MBR Application**

For the practical application of cellulase to lab-scale MBR systems, *Undibacterium* sp. DM-1 entrapping beads (i.e., cellulolytic-beads) were prepared as described in previous study (Lee et al., 2016b). Briefly, DM-1 was incubated in a modified NYG broth for 24 h and the pellet was collected by centrifugation at 6000 rpm for 10 min. The collected DM-1 cells were re-suspended in DI water and mixed with a solution of alginate (Junsei, Japan) and polyvinyl alcohol (Wako, Japan). The mixture was dripped into solution of boric acid and calcium chloride to form spherical beads. The beads were immersed in sodium sulfate and stored in DI water. The content of DM-1 in the cellulolytic beads was approximately 15 mg cell/g bead. For preparation of non-cell entrapping beads (i.e., vacant-beads) as a control, DI water was used instead of the DM-1 suspension and the same method was followed.

#### **IV.2.6. Biostability of Cellulolytic-beads in MBR**

The biostability of cellulolytic-beads was determined in terms of viability and cellulolytic activity. To measure bead viability, both vacant- and cellulolytic-beads were taken out from the MBR and rinsed thoroughly with DI water. After staining with a live/dead kit (Molecular Probes, USA) for 15 min, DM-1 cells entrapped in the beads were visually observed using CLSM. The viability of the cellulolytic-beads was calculated by taking the ratio of the green and red fluorescent intensity using LAS AF software. In addition, the cellulolytic activity of cellulolytic-beads was quantitatively determined by measuring the reduction in the viscosity of a 0.5% CMC solution (Lee et al., 2007). Briefly, 1 g of cellulolytic beads were added to 100 ml of CMC solution and incubated at 30 °C with 120 rpm shaking. After 2 days incubation, 20 ml of CMC suspension was transferred to the sample adaptor of a viscometer (Brookfield, DV-II, USA). The spindle was immersed in the sample and rotated at a constant speed of 50 rpm. The viscosity was recorded after 30 seconds of rotation. The viscosity of CMC is linearly correlated to concentration (within 0.5%), enabling conversion of the viscosity of residual CMC to concentration data.

#### **IV.2.7. MBR Operation**

Prior to MBR operation, activated sludge from a real wastewater treatment plant (Daejeon, Korea) was acclimated to synthetic wastewater until the MBR operating parameters stabilized. The composition of synthetic wastewater is tabulated in Table S1 in the supplementary information. Two lab-scale submerged MBR reactors, one with vacant-beads containing no DM-1 bacteria (i.e., vacant-MBR)

and another with cellulolytic-beads (i.e., cellulolytic-MBR), were operated continuously in parallel. Because the addition of beads mitigate biofouling in MBR due to physical washing effect by their frequent collisions with membrane surface (Kim et al., 2013b), vacant-MBR was run as a control to evaluate the net biological effect of the cellulolytic-MBR. TMP rise-up, which reflects the extent of membrane biofouling, was continuously monitored during MBR operation and the  $T_{TMP}$  of the two reactors was calculated for quantitative comparison. A hydrophilic polyvinylidene fluoride (PVDF) hollow fiber membrane (Zeeweed 10, GE-Zenon, USA) was used as a filtration membrane with an effective surface area of 150 cm<sup>2</sup>. The schematic and operating conditions are shown in Figure IV- 1. The concentration of beads applied in both reactors was 0.5% (v/v- volume of beads / volume of reactor). Operation of the two MBRs was performed in two phases for two different purpose. In phase 1, to investigate the biofouling mitigation through cellulolytic-beads, both reactors were operated until transmembrane pressure (TMP) reached 20 kPa, and  $T_{TMP}$ , the average number of days for one TMP jump (Lee et al., 2016c), was calculated for comparison of fouling in MBRs. The biofouled membranes from each MBR were cleaned by immersing them in 1000 ppm of NaOCl for 4 h and then reused. In phase 2, both reactors were operated until TMP in either reactor reached 25 kPa and biofilm on membrane surface were analyzed for cellulose and EPS contents without chemical cleaning.

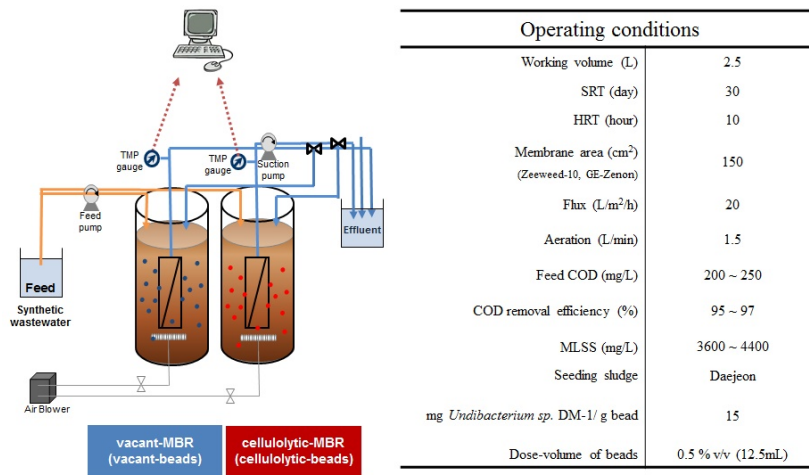


Figure IV- 1. Schematic diagram and operating conditions of vacant- and cellulolytic-MBR

#### **IV.2.8. Analysis of Cellulose and EPS in Biofilm in MBR**

The biofilm was detached from the used membrane by soaking in 450 ml DI water with sonication for 10 min, and harvested by centrifugation at 8000 rpm for 10 min. The harvested biofilm sample was equally divided into two portions to analyze cellulose and EPS content, respectively.

To analyze cellulose content in the biofilm, the first portion of biofilm sample was treated with acetic-nitric reagent (15 ml of 80% acetic acid and 1 ml of concentrated nitric acid) in a water bath for 30 min at 95 °C to dissolve impurities such as lipids, proteins, lignin, and hemicelluloses (Updegraff, 1969). After centrifugation at 12000 rpm for 15 min, the undissolved pellet was obtained and further divided into two portions to perform the cellulose assay and X-ray diffraction (XRD) analysis. For the cellulose assay, the pellet was treated with 67% sulfuric acid to convert cellulose to glucose, and the amount of cellulose was determined using the anthrone method (Scott Jr and Melvin, 1953). The second portion of biofilm sample was extracted using modified thermal extraction method (Maartens et al., 1996) to measure EPS concentration. The amount of total polysaccharides and proteins was determined by the phenol-sulfuric acid method (Masuko et al., 2005) and the Bradford assay (Manual), respectively.

## **IV.3. Results and Discussion**

### **IV.3.1. Effect of Cellulase on Biofilm Formation of Activated Sludge in MBR**

It has been reported that cellulose, a key component comprising the EPS of the biofilm matrix, plays an important role in the attachment of bacterial cells at the surface by connecting micro-colonies and recruiting planktonic bacteria to the biofilm (Khil et al., 2005, Christiaen et al., 2011, Canale-Parola and Wolfe, 1964). It was also reported that treatment of biofilms with cellulase results in a significant decrease in total biomass (Jo et al., 2016). Therefore, it would be interesting to confirm whether cellulose is a key component and whether it can be disrupted by cellulase in the biofilm of activated sludge in MBR for wastewater treatment.

In order to confirm the presence and distribution of cellulose in a biofilm of activated sludge, and to test whether treatment with cellulase would reduce cellulose and microorganisms attached on surface, we tried to visualize cellulose and microorganisms attached on surface, we tried to visualize cellulose and microorganisms using CLSM. Glass slides, on which biofilms were formed, were treated with and without treatment of commercial cellulase. These glass slides were stained with two different dyes, SYTO 9 and Calcofluor white to visualize microbial biofilm and cellulose, respectively. Figure IV- 2a shows a three dimensional image of the biofilm of activated sludge. The blue color, representing cellulose, was clearly enmeshed in the matrix of the biofilm and appears to be significant for the structural integrity of the activated sludge biofilm (in white). This result is in agreement with a previous study (Christiaen et al., 2011) and suggests that cellulose could be a key foulant for membrane biofouling in MBRs.

The effect of cellulase on the inhibition of biofilm formation was determined by staining both biofilms with SYTO 9. Confocal micrographs revealed that numerous microbial cells were attached on the glass surface, forming uniform and aggregated biofilm in the absence of cellulase (Figure IV- 2b, Cellulase-). Smaller aggregates of microbial flocs were observed in the cellulase-treated biofilm (Figure IV- 2b, Cellulase+). Calcofluor white staining for cellulose displayed greater intensity of blue color representing higher cellulose concentration in the biofilm without cellulase (Figure IV- 2c, Cellulase-) than in the biofilm with cellulase (Figure IV- 2c, Cellulase+). This suggests that cellulose degradation in the biofilm predominated in the presence of cellulase. Therefore, since cellulose is known to play an important role in the attachment of bacterial cells, the reduced biofilm by the addition of cellulase would be attributed to the breakage of cellulose linkage between bacterial cells, thereby weakening biofilm attachment on surface.

Biovolumes of biofilm and cellulose formed on both glasses were also determined using LAS-AF software and are shown in Table IV- 1. The addition of cellulase to the activated sludge resulted in an approximately 90% decrease in microbial biovolume, from 15.0 to  $1.5 \times 10^6 \mu\text{m}^3$ . Likewise, the biovolume of cellulose in the activated sludge biofilm was remarkably reduced from 3.1 to  $0.2 \times 10^6 \mu\text{m}^3$  through the addition of cellulase into the activated sludge. On the other hand, there was little effect of commercial cellulase on cell growth ( $\text{OD}_{600}$ ) in the activated sludge culture ( $p > 0.05$ , one-tailed  $t$ -test). Therefore, we concluded that the decrease in the microbial quantity after the addition of cellulase in Figure IV- 2b did not result from the decrease of cell density in suspended activated sludge,



but was caused by the mitigation of microbial biofilm formation on the surface due to the decomposition of cellulose.

In short summary, cellulase was able to effectively hydrolyze cellulose in the activated sludge biofilms to inhibit biofilm formation substantially without affecting the microbial growth. Thus, cellulase could be a promising strategy for the degradation of cellulose and mitigation of biofouling in MBR for wastewater treatment.

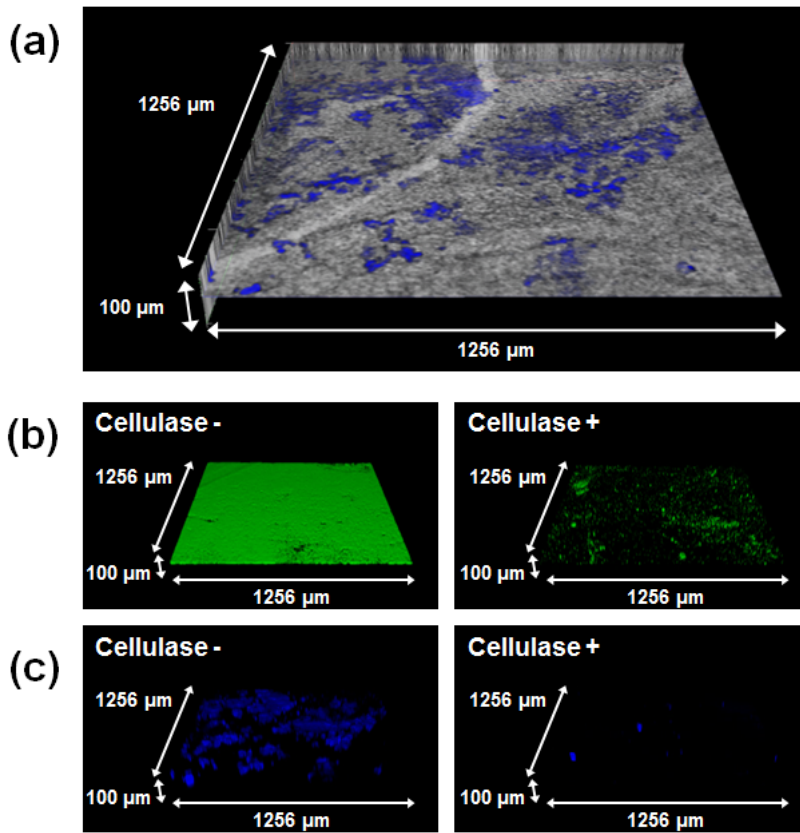


Figure IV- 2. Reconstructed 3D CLSM images: (a) distribution of cellulose enmeshed in the biofilm of activated sludge; (b) distribution of microorganisms in the biofilm before (Cellulase-) and after (Cellulase+) the addition of cellulase in the activated sludge; and (c) distribution of cellulose in the biofilm before (Cellulase-) and after (Cellulase+) the addition of cellulase in the activated sludge. Magnification: 100 X. Image size: 1256 μm (Length) X 1256 μm (Width) X 100 μm (Height).

### IV.3.2. Isolation and Identification of Cellulolytic Microorganism

The preliminary tests demonstrated that cellulase plays an important role in inhibiting microbial biofilm formation of activated sludge in MBR. Because the direct addition of free enzyme to MBR is impractical in terms of cost and stability, however, it might more advantageous to generate enzymes *in situ* using cellulase-producing microorganisms for MBR application. Therefore, we attempted to isolate cellulolytic microorganisms from activated sludge in a lab-scale MBR. Through phylogenetic analysis for potential cellulolytic isolates, six isolates consisting of four bacteria and two fungi were identified as cellulolytic microorganisms which are listed in Table IV- 2a.

Cell-free supernatants of the six isolates were obtained after 48 h incubation and tested for cellulolytic activity using CMC agar plates. As shown in Figure IV- 3, supernatants from all isolates produced cellulase extracellularly. It is worth noting that *Undibacterium* sp. DM-1 showed the largest diameter of the hydrolysis zone on the agar plate among the isolates. As the diameter is correlated to cellulolytic activity (Teather and Wood, 1982), DM-1 had the highest cellulolytic activity and was selected for MBR experiments. Strain DM-1 shared 99.7% sequence identity with 16S rRNA gene sequences of *Undibacterium squillarum* (Table IV- 2a). According to the literature (Sheu et al., 2014), optimum growth for *U. squillarum*, occurs at 25–30 °C and at pH 6.0–7.0, which are comparable to the condition of MBR reactors. It raises the possibility that DM-1 can survive in the reactor without difficulties.

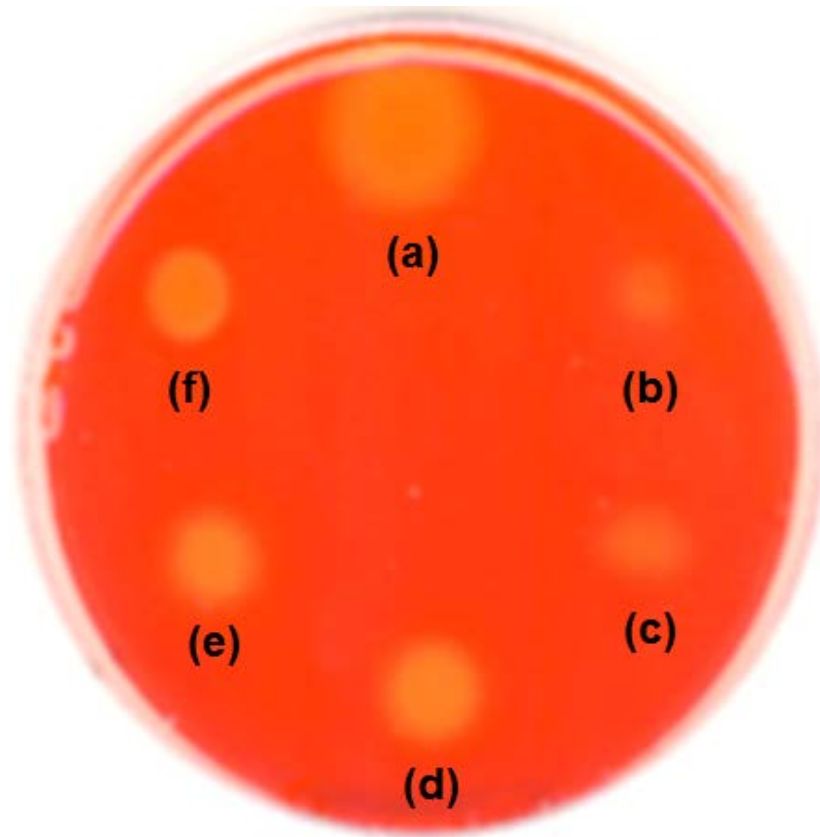


Figure IV- 3. Cellulolytic-activity from cell-free supernatant of six cellulolytic isolates grown for 48 h. Congo red staining (red) indicates presence of CMC and light orange regions are the NaCl-destained zones which indicate hydrolysis of CMC. ((a) *Undibacterium* sp. DM-1; (b) *Bacillus* sp. DM-2; (c) *Bacillus* sp. DM-3; (d) *Microbacterium* sp. DM-4; (e) *Aspergillus* sp. DM-5; and (f) *Trichosporon* sp. DM-6).

### **IV.3.3. Anti-biofouling Activity of *Undibacterium* sp. DM-1**

Biofilm formation is generally initiated by microbial attachment to the surface, followed by growth to establish a mature structure (Kostakioti et al., 2013). Two biofilm assays were performed to investigate whether the supernatant of DM-1, which contains cellulase, can efficiently reduce biofilms at two different stages of biofilm development: attachment (initial stage) and mature biofilm (maturation stage). Along with activated sludge, two different cellulose-producing bacteria (*Enterobacter* sp. CPB-1, *Rhodococcus* sp. CPB-2) isolated from activated sludge were used as test organisms as listed in Table IV- 2b.

For the biofilm formation assay, either a cell-free supernatant of DM-1, 6.5 U/ml of commercial cellulase, or autoclaved supernatant of DM-1 were added to test organisms in a 96-well plate and incubated for 12 h. The CMC agar test showed that cellulolytic activity of the cell-free supernatant of DM-1 was around 2.9 ( $\pm$  0.2) U/ml. The increase in the activity of DM-1 was associated with an increase in cell growth. We determined 12 h to be the optimum period to observe the biofilm inhibitory activity of a cellulolytic treatment. The amount of biofilm was derived by staining with CV as shown in Figure IV- 4a. In comparison with autoclaved supernatant of DM-1, supernatant of DM-1 reduced biofilm of *Enterobacter* sp. CPB-1, *Rhodococcus* sp. CPB-2, and activated sludge by 41, 34, and 21%, respectively, while commercial cellulase decreased each biofilm by 72, 37, and 35%, respectively. Both supernatant of DM-1 and commercial cellulase showed higher inhibitory efficiency in biofilm of cellulose-producing bacteria such as *Enterobacter* sp. CPB-1, and *Rhodococcus* sp. CPB-2 than in activated sludge. This could be attributed to the presence of non-cellulose-producing

microorganisms in activated sludge which could not be controlled through cellulase treatment. Despite the above fact, it is noteworthy that cellulase from DM-1 was workable in suppressing biofilms of activated sludge at a level comparable to commercial cellulase. The reduction in biofilm formation of test organisms suggests that supernatant of DM-1 could effectively prevent microbial attachment occurring in the initial stage of biofilm development from being facilitated by cellulase, thus inhibiting biofilm formation of activated sludge as comparable as possible to commercial cellulase.

For the biofilm detachment assay, a 48-hour grown biofilm was subjected to cellulolytic (supernatant DM-1 and commercial cellulase) treatment and a control sample (autoclaved supernatant of DM-1) for 1 hr. The residual biofilm was quantified through CV staining as shown in Figure IV- 4b. The mature biofilms of *Enterobacter* sp. CPB-1, *Rhodococcus* sp. CPB-2, and activated sludge were removed at 34, 67, and 27%, respectively, when commercial cellulase was used. Similarly, each biofilm was reduced by 20, 41, and 19%, respectively, once supernatant of DM-1 was added. This result suggests that DM-1 is also capable of decomposing mature biofilm by degrading cellulose. In summary, DM-1 was able to inhibit biofilm formation as well as to detach mature biofilms of test organisms, suggesting that it could be a promising bacterium for the mitigation of biofouling in MBRs.

Furthermore, CLSM was performed to confirm the supernatant of DM-1 was able to reduce biofilm and degrade cellulose of activated sludge without affecting cell growth. It suggests that DM-1 supernatant had a similar effect on the biofilm of activated sludge as commercial cellulase.

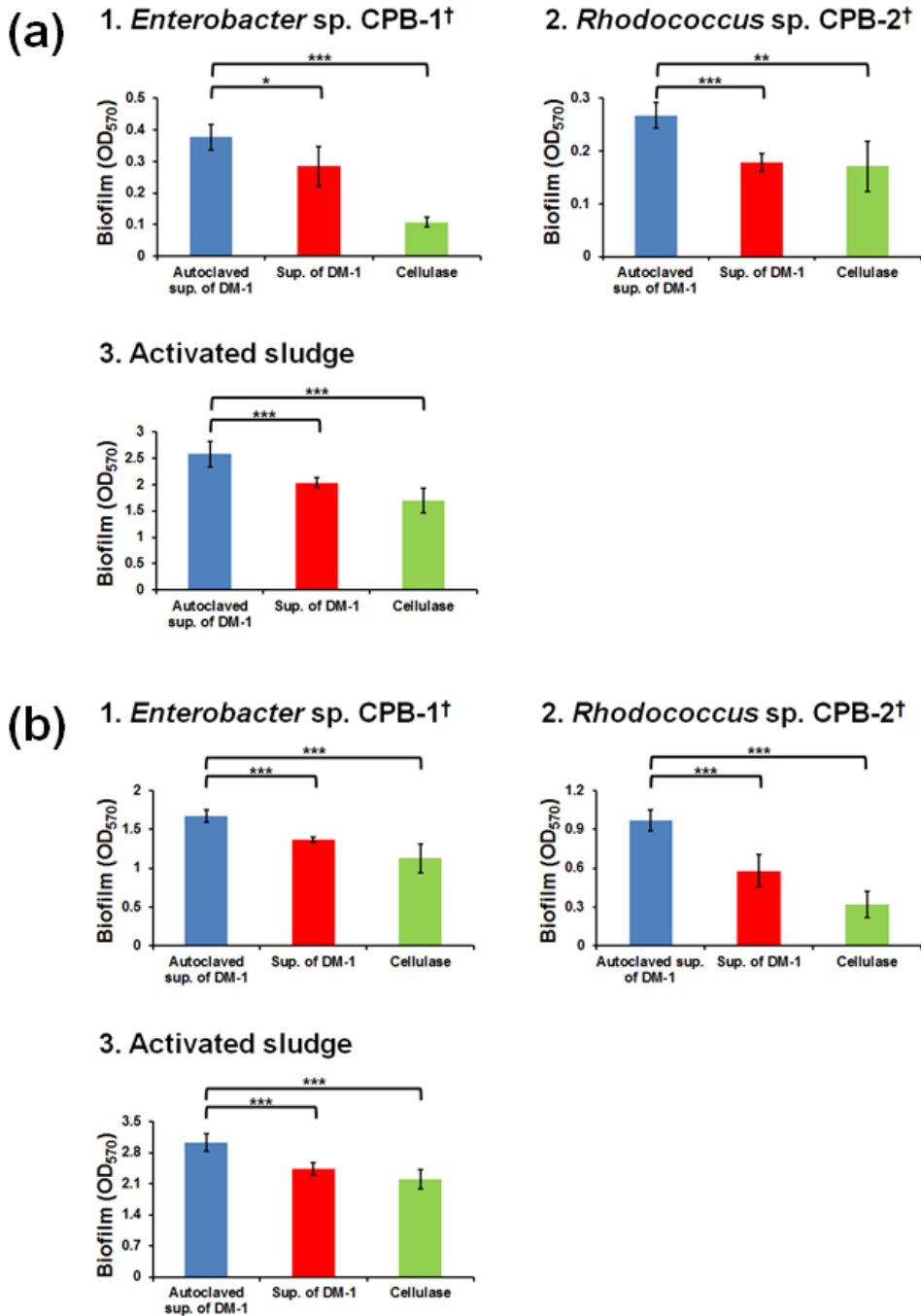


Figure IV- 4. Test of (a) biofilm formation inhibitory and (b) biofilm detachment activity of the supernatant of DM-1 and commercial cellulase on test organisms: 1. *Enterobacter* sp. CPB-1; 2. *Rhodococcus* sp. CPB-2; and 3. Activated sludge. Error

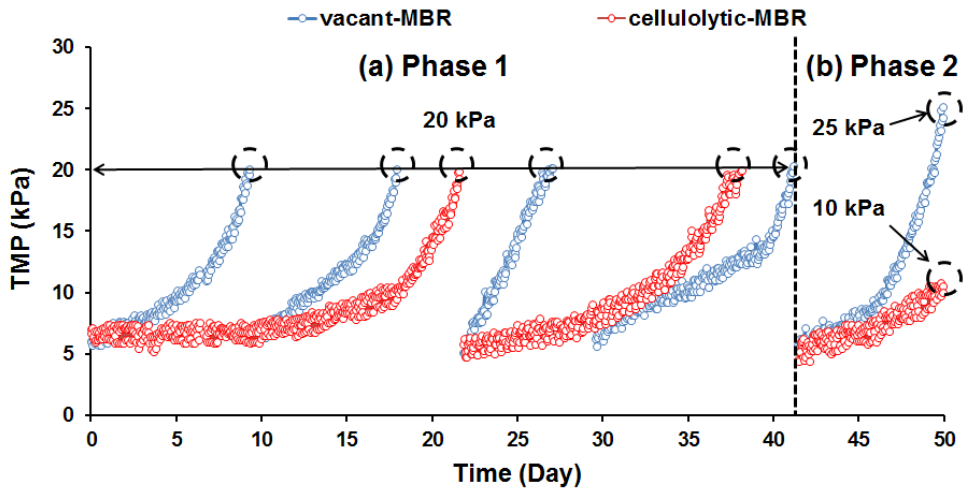
bar: standard deviation ( $n = 6$  as the technical replicates). One-tailed  $t$ -test was performed to compare cellulase treatments (i.e., cell-free supernatant of DM-1 or cellulase) to the control (i.e., autoclaved supernatant of DM-1) where significant differences are indicated as follows: \*  $p < 0.05$ , \*\*  $p < 0.01$ , and \*\*\*  $p < 0.0001$ . † indicates cellulose-producing bacteria isolated from activated sludge in the lab-scale MBR.



#### **IV.3.4. Effect of Cellulolytic-beads on Mitigation of Membrane**

##### **Biofouling**

To investigate effect of DM-1 entrapping beads (i.e., cellulolytic-beads) on biofouling mitigation, two lab-scale MBRs, one with vacant-beads (i.e., vacant-MBR) and the other with cellulolytic-beads (i.e., cellulolytic-MBR) were continuously run in parallel under the identical operating conditions as shown in Figure IV- 1. As shown in Figure IV- 5a, in Phase 1, the  $T_{TMP}$  of vacant- and cellulolytic-MBRs was 8.5 days and 19.0 days, respectively, and the ratio of their  $T_{TMP}$  values was approximately 2.2, indicating that the extent of biofouling in cellulolytic-MBR was mitigated by approximately 2.2 times compared with that in vacant-MBR. Notably, the difference in COD removal efficiency and MLSS (data not shown) between reactors was negligible ( $p > 0.05$ , one-way ANOVA test), suggesting that the addition of cellulolytic-beads has a negligible influence on organic removal efficiencies other than biofouling mitigation.



	<b>vacant-MBR (with vacant-beads)</b>	<b>cellulolytic-MBR (with cellulolytic-beads)</b>
<b>T<sub>TMP</sub> (Day)</b>	<b>8.5 (± 2.7)</b>	<b>19.0 (± 3.8)</b>

Figure IV- 5. TMP profiles of vacant- and cellulolytic-MBRs in (a) Phase 1 and (b) Phase 2, and T<sub>TMP</sub> of the two MBRs in Phase 1. TMP profiles of vacant- and cellulolytic-MBRs in (a) Phase 1 and (b) Phase 2, and T<sub>TMP</sub> of the two MBRs in Phase 1. Parenthesis: standard deviation ( $n = 4$  for vacant-MBR and  $n = 2$  for cellulolytic-MBR). Dotted circle represents the time of replacing used membrane. In phase 1, the biofouled membranes from each MBR were cleaned by immersing them in 1000 ppm of NaOCl for 4 h and then reused. In phase 2, the used membranes from both MBRs were taken out when TMP in vacant-MBR reached to 25 kPa.

### **IV.3.5. The Correlation between Cellulose, EPS and Membrane**

#### **Biofouling in MBR**

Although we observed a biological effect on the mitigation of MBR biofouling (Figure IV- 5a), further experiment was required to demonstrate that mitigation of biofouling results from a reduction in cellulose. Thus, the two MBRs were run in Phase 2 as shown in Figure IV- 5b. Unlike Phase 1, Phase 2 was operated until TMP in either reactor reached 25 kPa instead of 20 kPa because sufficient biofilm samples were required for an accurate analysis of biofilm. As in Phase 1, TMP increased faster in the vacant-MBR than that in the cellulolytic-MBR. At the end of 9 days of Phase 2 operation, the entire biofilm formed on each used membrane surface was collected from the vacant- and cellulolytic MBRs. Each biofilm was analyzed in terms of total attached biomass (TAB), cellulose, and EPS.

As expected from the rate of TMP rise-up, TAB in the vacant-MBR (0.302 g) was much greater than that in the cellulolytic-MBR (0.114 g). Cellulose was successfully extracted from detached biofilms using previously described methods (Kaplan et al., 2004). The cellulose assay using an anthrone reagent showed that the cellulose concentration in the cellulolytic-MBR was 9.2 mg per g TAB, whereas that in the vacant-MBR was 12.8 mg per g TAB. This corresponds to an approximately 30% reduction in cellulose in the cellulolytic-MBR through the application of DM-1 (Figure IV- 6a). In other words, cellulase secreted from the cellulolytic-beads reduced cellulose content in the biofilm, thereby mitigating biofouling in the cellulolytic-MBR.

To further confirm the degradation of cellulose by the cellulolytic-beads,

we conducted X-ray diffraction (XRD) analysis. As shown in Figure IV- 7, diffractograms of cellulose isolated from biofilm revealed a relatively specific structure with a 2 $\theta$  peak at 22° as reported in other studies (Christiaen et al., 2011, Salalha et al., 2006). In addition, taking peak intensities, the cellulose content in the biofilm of the cellulolytic MBR was quantitatively less than that of the vacant-MBR.

The concentration of EPS in the biofilm formed on the membrane was also measured because it is regarded to be closely related to membrane biofouling in MBR (Wang et al., 2009). As shown in Figure IV- 6b, concentrations of both polysaccharide and protein in the cellulolytic-MBR were lower than in the vacant-MBR by approximately 56% and 87%, respectively. In addition, the degradation of cellulose led greater quantitative decrement of polysaccharides (10.3 mg per g TAB) than that of proteins (2.6 mg per g TAB). A possible explanation for the reduction of polysaccharides and proteins other than cellulose may result from cellulose degradation that leads to the disruption overall biofilm architectures because cellulose connects micro-colonies and other components in the biofilm (Canale-Parola and Wolfe, 1964, Wang et al., 2004c).

As mentioned above, the content of cellulose was significantly reduced in biofilm in cellulolytic-MBR compared with vacant-MBR. However, the absolute content of cellulose (9.2 mg per g TAB) was greater than that of polysaccharide (8.1 mg per TAB) although cellulose is just one component of polysaccharides. This discordance may result from different analysis of cellulose (i.e., anthrone method) and EPS (i.e., phenol-sulfuric acid). In order to investigate how cellulose is involved or occupied in EPS matrix, it is required to develop a new and

integrated analysis for measurement of cellulose and polysaccharide.

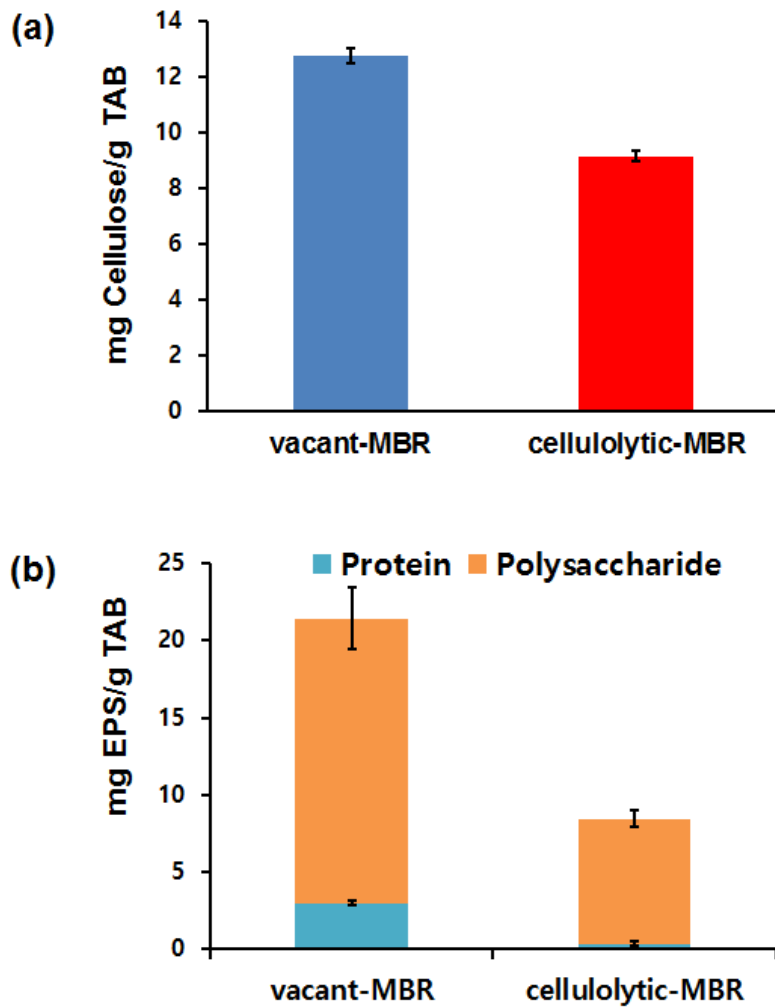


Figure IV- 6. (a) Cellulose and (b) EPS content in the biofilm formed on the membrane surface in vacant- and cellulolytic-MBRs. Error bar: standard deviation ( $n = 3$ ).

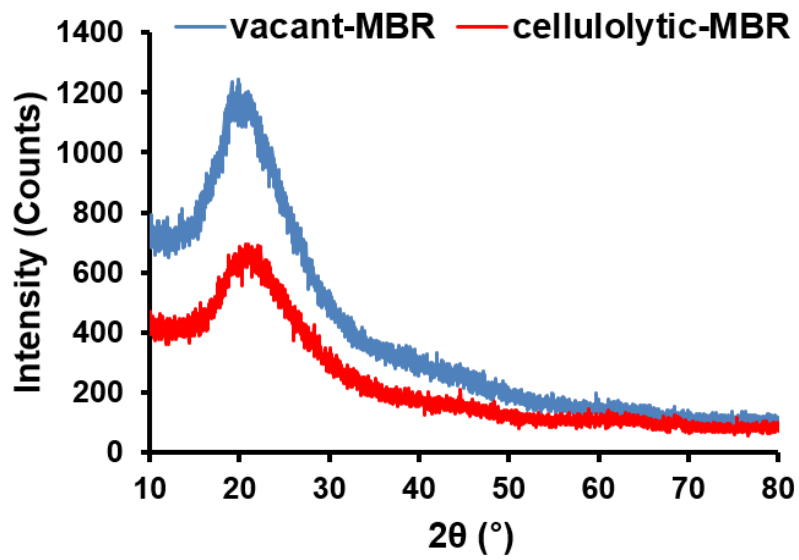


Figure IV- 7. X-ray diffraction (XRD) patterns of extracted biofilm samples from the vacant- and cellulolytic-MBRs

### **IV.3.6. Biostability of Cellulolytic-beads**

The long-term biostability of cellulolytic-beads is an important requirement for their practical application to MBR. We monitored the viability and cellulolytic activity of DM-1 inside the cellulolytic-beads during the cellulolytic-MBR operation. Used beads were taken out from both vacant- and cellulolytic-MBRs and stained using a live/dead kit.

As shown in Figure IV- 8a, green fluorescence was clearly visible in the used cellulolytic-beads for the test period of 50 days, whereas few green spots were observed in the used vacant-beads. During the MBR operation, viability of the cellulolytic-beads was determined by taking the ratio between green and red fluorescence in Figure IV- 8a. Although the green fluorescence from SYTO 9 is not exactly equal to the amount of live cells, the dye have been widely used for an indicator of viable cells in previous studies (Mah et al., 2003, Sachidanandham et al., 2005). Hence we thought that the ratio of green to red fluorescence intensities could serve as an indirect measure of live to dead cell ratio or cell viability. As shown in Figure IV- 8b, the viability of cellulolytic-beads was increased at the beginning and then leveled off, indicating the viability of the cellulolytic-beads were well maintained during the MBR operation. The entrapped DM-1 bacteria could proliferate in the confined environment of the bead by uptake of nutrients in synthetic wastewater (Xie et al., 2016). The relatively low viability of initial cellulolytic-beads might be caused by the acidity of boric acid solution, an agent for cross-linkage of PVA (Takei et al., 2011). However, since DM-1 is an indigenous bacterium isolated from an MBR for wastewater treatment, DM-1 could easily adapt to and survive in the environment of MBR. This illuminates the



possibility of long-term application of cellulolytic-beads to MBR fed with real wastewater. Interestingly, the green spots in cross-section of cellulolytic-beads were well-distributed at the initial period, but gradually moved toward its outer surface with the operation time (Figure IV- 8a). The cellulolytic bacteria seemed to migrate toward the surface of the bead in which more nutrients are available. Another possible reason for greater green fluorescence in the edge of the bead may be that the mass transfer for nutrients at the edge of the bead is superior. Especially, low nutrient concentration of synthetic wastewater (250 mg chemical oxygen demand (COD) per liter) could make a great difference of viability between outer and inner part of the bead.

In addition, the cellulolytic activities of fresh and used cellulolytic-beads were also determined. Cellulolytic activity was defined by the amount of CMC degraded (g/day) per g of cellulolytic-beads in 100 ml of 0.5% CMC solution. As shown in Figure IV- 8c, the cellulolytic activity of fresh and used cellulolytic-beads (i.e., 50 days of operation) was 0.068 g of CMC degraded per day and 0.051 g of CMC degraded per day, respectively, indicating that the cellulolytic activity of DM-1 was decreased by only 25% after 50 days of operation. This suggests the cellulolytic-beads could be applied to real MBRs to control biofouling.

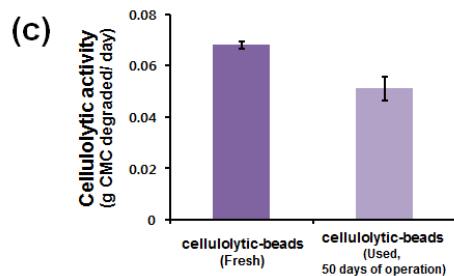
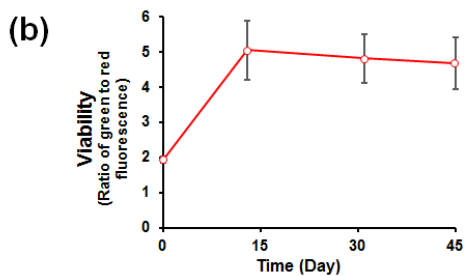
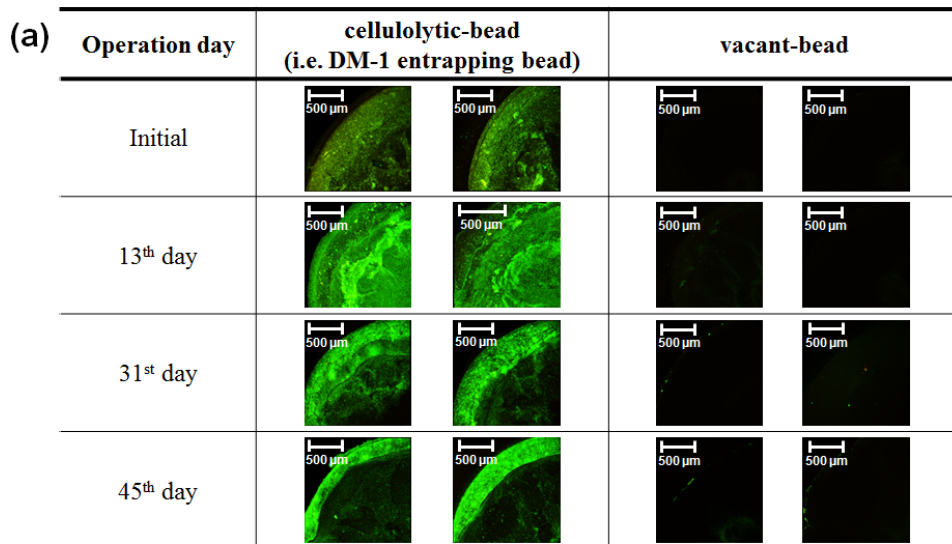


Figure IV- 8. (a) Cross-sectional images of cellulolytic- and vacant-beads; (b) viability of cellulolytic-beads during MBR ( $n = 4$ ); and (c) cellulolytic activity of fresh and used (i.e., 50 days of operation) cellulolytic-bead. Error bar: standard deviation ( $n = 3$ ).

## IV.4. Conclusions

In this study, we found that cellulose was enmeshed in the biofilm of activated sludge, and cellulase can disrupt biofilms substantially through the degradation of cellulose. For practical application of cellulase, a novel cellulolytic bacterium, *Undibacterium* sp. DM-1, was isolated from activated sludge in a lab-scale MBR. DM-1 showed remarkable efficiency in inhibiting biofilm formation as well as detaching mature biofilm of activated sludge and of three cellulose-producing bacteria, *E. coli* K12, *Enterobacter* sp. CPB-1, and *Rhodococcus* sp. CPB-2. When DM-1 entrapping beads (i.e., cellulolytic-beads) were prepared and applied to continuous lab-scale MBR, membrane biofouling was substantially mitigated and long-term biostability was maintained, suggesting that biofouling control through cellulolytic-beads could provide a practical solution to current biofouling problem in MBR.

# **Chapter V**

## **Conclusions**



## V. Conclusions

In this chapter, QQ bacteria entrapping sheets (QQ-sheets) were developed as a new shape of QQ-media to enhance QQ efficiency for biofouling control in MBR with hollow fiber membranes. In addition, cellulolytic bacteria entrapping beads (cellulolytic-bead) were prepared to target biofilm formation pathway besides QQ and to mitigate cellulose-mediated biofouling in MBR. Based on the experimental results, the following conclusions were made:

- QQ bacteria entrapping sheets (QQ-sheets) showed greater biological (QQ) effect as well as physical washing effect than QQ-beads due to their geometric property.
- Physical washing effect of QQ-sheets was significant to the outer part as well as inner part of multi-layer hollow fiber (HF) module whereas QQ-beads had the effect only on the outer part.
- Effectiveness of QQ-sheets for biofouling was identically significant for both single-layer HF module and multi-layer HF.
- It was found that cellulose was enmeshed in the biofilm of activated sludge, and cellulase can disrupt biofilms substantially through the degradation of cellulose.
- *Undibacterium* sp. DM-1 isolated from MBR showed efficiency in inhibiting biofilm formation and detaching biofilms of activated sludge and cellulose-producing bacteria.

- DM-1 entrapping beads (i.e., cellulolytic-beads) substantially mitigated biofouling in MBR and their biostability was well-maintained.

# 국문초록

최근, 분리막 생물반응기(Membrane Bioreactor, MBR) 내 고질적인 문제인 생물막오염(Biofouling)을 근본적으로 해결하고자 미생물 간의 대화(Quorum sensing, QS)를 차단하는 정족수감지 억제(Quorum quenching, QQ) 기술을 적용한 사례가 활발히 보고되고 있다. 하지만 지금까지 개발된 QQ 기술(즉, QQ 미생물 담체 개발)은 평막 또는 실제 분리막모듈과 거리가 먼 일자형의 중공사모듈에서만 적용해왔기 때문에 다발형의 중공사모듈에서 QQ 기술의 생물막오염 제어 성능 확인이 필요하다. 또한, QQ 기술은 생물막이 형성된 이후에는 제어에 효과적이지 않기 때문에 이미 형성된 생물막을 제어할 수 있는 방안도 필요하다. 따라서, 본 연구에서는 분리막 시장에서 가장 많이 사용되고 있는 다발형의 중공사모듈에서 생물막오염 억제가능성을 확인하기 위해 새로운 형태의 QQ 미생물 담체를 개발하였다. 또한, 이미 형성된 생물막을 제어하기 위한 방안으로 생물막 내에 존재하는 셀룰로오스를 분해할 수 있는 미생물을 분리, 동정하고 담체에 고정시켜 MBR에 적용하여 또 다른 생물막오염 제어 방법의 가능성을 확인하였다.

첫째, 새로운 모양인 QQ 미생물 판형담체(QQ-sheets)를 개발하여 기존에 개발된 QQ 미생물 구형담체(QQ-beads)와 생물막오염 제어 성능을 QQ 활성과 물리세정 효과 측면에서 비교하였다. 동일 담체 부피 내에서 QQ 미생물 판형담체는 QQ 미생물 구형담체보다 QQ 활성에서



약 2.5배 뛰어났고 이러한 QQ활성은 담체의 표면적에 비례하는 것이 확인되었다. 또한, 중공사모듈의 바깥쪽에 위치하는 분리막에만 물리세정효과를 보인 구형담체와 달리, 판형담체는 안쪽과 바깥쪽에 위치하는 분리막 모두 고르게 물리세정 효과를 보였는데, 이는 판형담체가 중공사모듈 안쪽까지 자유롭게 침투가 가능하기 때문이다. 다발형의 중공사모듈이 설치된 연속식 MBR의 운전에서 QQ 미생물 판형담체는 기존에 개발된 QQ 미생물 구형담체에 비해 보다 뛰어난 QQ 활성화와 물리세정효과로 인해 약 1.8배가량 생물막오염을 더 지연할 수 있음을 확인하였다.

둘째, MBR에서 생물막오염의 한 요소인 셀룰로오스를 분해하는 셀룰라아제 효소를 MBR에 적용하여 생물막오염 억제 가능성을 확인하였다. 활성슬러지의 생물막 내 셀룰로오스의 존재를 확인하였고 셀룰라아제는 활성슬러지의 생물막 형성을 효과적으로 제어함을 확인하였다. 셀룰라아제 생산 미생물인 *Undibacterium* sp. DM-1을 MBR 내 활성슬러지에서 분리, 동정하였다. 셀룰로오스 분해 미생물인 DM-1 미생물을 고정된 구형담체를 MBR에 적용하였고, 미생물이 고정되어 있지 않은 구형담체가 적용된 MBR에 비해 생물막오염 억제 효과가 약 2.2배 나타남을 확인하였다.

주요어: 분리막 생물반응기, 생물막오염 억제, 미생물 고정화 담체, 정족수감지 억제, 셀룰라아제, 중공사막, 판형, 구형

학번: 2013-20969

# Reference

- AKIN, C. 1987a. Biocatalysis with Immobilized Cells. *Biotechnology and Genetic Engineering Reviews*, 5, 319-367.
- AKIN, C. 1987b. Biocatalysis with immobilized cells. *Biotechnology and Genetic Engineering Reviews*, 5, 319-367.
- ALLIE, Z., JACOBS, E. P., MAARTENS, A. & SWART, P. 2003. Enzymatic cleaning of ultrafiltration membranes fouled by abattoir effluent. *Journal of Membrane Science*, 218, 107-116.
- ARG ELLO, M., ALVAREZ, S., RIERA, F. & ALVAREZ, R. 2003. Enzymatic cleaning of inorganic ultrafiltration membranes used for whey protein fractionation. *Journal of Membrane Science*, 216, 121-134.
- ARG ELLO, M. A., ÁLVAREZ, S., RIERA, F. A. & ÁLVAREZ, R. 2002. Enzymatic cleaning of inorganic ultrafiltration membranes fouled by whey proteins. *Journal of agricultural and food chemistry*, 50, 1951-1958.
- B HM, L., DREWS, A., PRIESKE, H., B RUB , P. R. & KRAUME, M. 2012. The importance of fluid dynamics for MBR fouling mitigation. *Bioresource technology*, 122, 50-61.
- BAKER, R. W. 2004. Pervaporation. *Membrane Technology and Applications, Second Edition*, 355-392.
- BARBER, C., TANG, J., FENG, J., PAN, M., WILSON, T., SLATER, H., DOW, J., WILLIAMS, P. & DANIELS, M. 1997. A novel regulatory system required for pathogenicity of *Xanthomonas campestris* is mediated by a small diffusible signal molecule. *Molecular microbiology*, 24, 555-566.
- BASSLER, B. L., WRIGHT, M., SHOWALTER, R. E. & SILVERMAN, M. R. 1993. Intercellular signalling in *Vibrio harveyi*: sequence and function of genes regulating expression of luminescence. *Molecular microbiology*, 9, 773-786.
- BASSLER, B. L., WRIGHT, M. & SILVERMAN, M. R. 1994. Multiple signalling systems controlling expression of luminescence in *Vibrio harveyi*: sequence and function of genes encoding a second sensory pathway. *Molecular microbiology*, 13, 273-286.
- BELOIN, C., ROUX, A. & GHIGO, J.-M. 2008. *Escherichia coli* biofilms. *Bacterial Biofilms*. Springer.
- BRANDA, S. S., VIK, Å., FRIEDMAN, L. & KOLTER, R. 2005. Biofilms: the matrix revisited. *Trends in microbiology*, 13, 20-26.
- BRODELIUS, P. A. J. V. 1987. *Immobilized cell systems.*, VCH Verlagsgesellschaft mbH.
- CANALE-PAROLA, E. & WOLFE, R. 1964. Synthesis of cellulose by *Sarcina ventriculi*. *Biochimica et Biophysica Acta (BBA)-General Subjects*, 82, 403-405.
- CHANG, I.-S., LE CLECH, P., JEFFERSON, B. & JUDD, S. 2002a. Membrane fouling in membrane bioreactors for wastewater treatment. *Journal of environmental engineering*, 128, 1018-1029.
- CHANG, S., FANE, A. & VIGNESWARAN, S. 2002b. Modeling and optimizing submerged hollow fiber membrane modules. *AIChE journal*, 48, 2203-

2212.

- CHEN, F., GAO, Y., CHEN, X., YU, Z. & LI, X. 2013. Quorum quenching enzymes and their application in degrading signal molecules to block quorum sensing-dependent infection. *International journal of molecular sciences*, 14, 17477-17500.
- CHEN, X., SCHAUDER, S., POTIER, N., VAN DORSSELAER, A., PELCZER, I., BASSLER, B. L. & HUGHSON, F. M. 2002. Structural identification of a bacterial quorum-sensing signal containing boron. *Nature*, 415, 545-549.
- CHENG, K.-C., CATCHMARK, J. M. & DEMIRCI, A. 2009. Enhanced production of bacterial cellulose by using a biofilm reactor and its material property analysis. *Journal of biological engineering*, 3, 1.
- CHEONG, W.-S., LEE, C.-H., MOON, Y.-H., OH, H.-S., KIM, S.-R., LEE, S. H., LEE, C.-H. & LEE, J.-K. 2013. Isolation and identification of indigenous quorum quenching bacteria, *Pseudomonas* sp. 1A1, for biofouling control in MBR. *Industrial & Engineering Chemistry Research*, 52, 10554-10560.
- CHEONG, W. S., KIM, S. R., OH, H. S., LEE, S. H., YEON, K. M., LEE, C. H. & LEE, J. K. 2014. Design of Quorum Quenching Microbial Vessel to Enhance Cell Viability for Biofouling Control in Membrane Bioreactor. *Journal of Microbiology and Biotechnology*, 24, 97-105.
- CHRISTIAEN, S. E. A., BRACKMAN, G., NELIS, H. J. & COENYE, T. 2011. Isolation and identification of quorum quenching bacteria from environmental samples. *Journal of Microbiological Methods*, 87, 213-219.
- CONTE, A., BUONOCORE, G., BEVILACQUA, A., SINIGAGLIA, M. & DEL NOBILE, M. 2006. Immobilization of lysozyme on polyvinylalcohol films for active packaging applications. *Journal of Food Protection*®, 69, 866-870.
- COTE, P., ALAM, Z. & PENNY, J. 2012. Hollow fiber membrane life in membrane bioreactors (MBR). *Desalination*, 288, 145-151.
- COUGHLAN, M. P. & KIERSTAN, M. P. J. 1988. Preparation and Applications of Immobilized Microorganisms - a Survey of Recent Reports. *Journal of Microbiological Methods*, 8, 51-90.
- DAVEY, M. E., CAIAZZA, N. C. & O'TOOLE, G. A. 2003. Rhamnolipid surfactant production affects biofilm architecture in *Pseudomonas aeruginosa* PAO1. *Journal of bacteriology*, 185, 1027-1036.
- DAVIES, D. G., PARSEK, M. R., PEARSON, J. P., IGLEWSKI, B. H., COSTERTON, J. W. & GREENBERG, E. P. 1998. The involvement of cell-to-cell signals in the development of a bacterial biofilm. *Science*, 280, 295-298.
- DEINEMA, M. H. & ZEVENHUIZEN, L. 1971. Formation of cellulose fibrils by gram-negative bacteria and their role in bacterial flocculation. *Archiv für Mikrobiologie*, 78, 42-57.
- DENG, Y., LIM, A., LEE, J., CHEN, S., AN, S., DONG, Y.-H. & ZHANG, L.-H. 2014. Diffusible signal factor (DSF) quorum sensing signal and structurally related molecules enhance the antimicrobial efficacy of antibiotics against some bacterial pathogens. *BMC microbiology*, 14, 1.
- DOBRETSOV, S., TEPLITSKI, M. & PAUL, V. 2009. Mini-review: quorum sensing in the marine environment and its relationship to biofouling. *Biofouling*, 25, 413-427.

- DREWS, A. 2010. Membrane fouling in membrane bioreactors—characterisation, contradictions, cause and cures. *Journal of membrane science*, 363, 1-28.
- EBERL, L., WINSON, M. K., STERNBERG, C., STEWART, G. S. A. B., CHRISTIANSEN, G., CHHABRA, S. R., BYCROFT, B., WILLIAMS, P., MOLIN, S. & GIVSKOV, M. 1996. Involvement of N-acyl-L-homoserine lactone autoinducers in controlling the multicellular behaviour of *Serratia liquefaciens*. *Molecular Microbiology*, 20, 127-136.
- FEDERLE, M. J. & BASSLER, B. L. 2003. Interspecies communication in bacteria. *The Journal of clinical investigation*, 112, 1291-1299.
- FETZNER, S. 2015. Quorum quenching enzymes. *Journal of biotechnology*, 201, 2-14.
- FLEMMING, H.-C., SCHAULE, G. & MCDONOGH, R. 1992. Biofouling on membranes—a short review. *Biofilms—Science and Technology*. Springer.
- FRIEDMAN, L. & KOLTER, R. 2004. Two genetic loci produce distinct carbohydrate-rich structural components of the *Pseudomonas aeruginosa* biofilm matrix. *Journal of bacteriology*, 186, 4457-4465.
- FUQUA, C. & GREENBERG, E. P. 2002. Listening in on bacteria: acyl-homoserine lactone signalling. *Nature Reviews Molecular Cell Biology*, 3, 685-695.
- FUQUA, C., PARSEK, M. R. & GREENBERG, E. P. 2001. Regulation of gene expression by cell-to-cell communication: acyl-homoserine lactone quorum sensing. *Annual review of genetics*, 35, 439-468.
- FUQUA, C. & WINANS, S. C. 1996. Conserved cis-acting promoter elements are required for density-dependent transcription of *Agrobacterium tumefaciens* conjugal transfer genes. *Journal of Bacteriology*, 178, 435-440.
- G TZ, F. 2002. Staphylococcus and biofilms. *Molecular microbiology*, 43, 1367-1378.
- GIVSKOV, M., DE NYS, R., MANEFIELD, M., GRAM, L., MAXIMILIEN, R., EBERL, L., MOLIN, S., STEINBERG, P. D. & KJELLEBERG, S. 1996. Eukaryotic interference with homoserine lactone-mediated prokaryotic signalling. *Journal of bacteriology*, 178, 6618-6622.
- GKOTSIS, P. K., BANTI, D. C., PELEKA, E. N., ZOUBOULIS, A. I. & SAMARAS, P. E. 2014. Fouling issues in membrane bioreactors (MBRs) for wastewater treatment: major mechanisms, prevention and control strategies. *Processes*, 2, 795-866.
- GREINER, A. & WENDORFF, J. H. 2007. Electrospinning: a fascinating method for the preparation of ultrathin fibers. *Angewandte Chemie International Edition*, 46, 5670-5703.
- HAI, F. I., YAMAMOTO, K. & LEE, C.-H. 2013. *Membrane Biological Reactors: Theory, Modeling, Design, Management and Applications to Wastewater Reuse*, IWA Publishing.
- HAN, S. O., SON, W. K., CHO, D., YOUK, J. H. & PARK, W. H. 2004. Preparation of porous ultra-fine fibres via selective thermal degradation of electrospun polyetherimide/poly (3-hydroxybutyrate-co-3-hydroxyvalerate) fibres. *Polymer degradation and stability*, 86, 257-262.
- HANLON, G. W., DENYER, S. P., OLLIFF, C. J. & IBRAHIM, L. J. 2001. Reduction in exopolysaccharide viscosity as an aid to bacteriophage penetration through *Pseudomonas aeruginosa* biofilms. *Applied and*

- environmental microbiology*, 67, 2746-2753.
- HENTZER, M., TEITZEL, G. M., BALZER, G. J., HEYDORN, A., MOLIN, S., GIVSKOV, M. & PARSEK, M. R. 2001. Alginate overproduction affects *Pseudomonas aeruginosa* biofilm structure and function. *Journal of bacteriology*, 183, 5395-5401.
- HERZBERG, M., KANG, S. & ELIMELECH, M. 2009. Role of extracellular polymeric substances (EPS) in biofouling of reverse osmosis membranes. *Environmental science & technology*, 43, 4393-4398.
- HOEK, E. M. & ELIMELECH, M. 2003. Cake-enhanced concentration polarization: a new fouling mechanism for salt-rejecting membranes. *Environmental science & technology*, 37, 5581-5588.
- HUBER, B., RIEDEL, K., HENTZER, M., HEYDORN, A., GOTSCHLICH, A., GIVSKOV, M., MOLIN, S. & EBERL, L. 2001. The cep quorum-sensing system of *Burkholderia cepacia* H111 controls biofilm formation and swarming motility. *Microbiology-Sgm*, 147, 2517-2528.
- IGUCHI, M., YAMANAKA, S. & BUDHIONO, A. 2000. Bacterial cellulose—a masterpiece of nature's arts. *Journal of Materials Science*, 35, 261-270.
- IZANO, E. A., SHAH, S. M. & KAPLAN, J. B. 2009. Intercellular adhesion and biocide resistance in nontypeable *Haemophilus influenzae* biofilms. *Microbial pathogenesis*, 46, 207-213.
- JEFFERSON, B., LAINE, A., JUDD, S. & STEPHENSON, T. 2000. Membrane bioreactors and their role in wastewater reuse. *Water Science and Technology*, 41, 197-204.
- JEN, A. C., WAKE, M. C. & MIKOS, A. G. 1996. Review: Hydrogels for cell immobilization. *Biotechnology and bioengineering*, 50, 357-364.
- JIANG, B. & LIU, Y. 2010. Energy uncoupling inhibits aerobic granulation. *Applied microbiology and biotechnology*, 85, 589-595.
- JIANG, W., XIA, S., LIANG, J., ZHANG, Z. & HERMANOWICZ, S. W. 2013. Effect of quorum quenching on the reactor performance, biofouling and biomass characteristics in membrane bioreactors. *Water research*, 47, 187-196.
- JO, S., KWON, H., JEONG, S., LEE, S., OH, H., YI, T., LEE, C. & KIM, T. 2016. Effects of Quorum Quenching on the Microbial Community of Biofilm in an Anoxic/Oxic MBR for Wastewater Treatment. *Journal of microbiology and biotechnology*, 26, 1593.
- JOHIR, M., ARYAL, R., VIGNESWARAN, S., KANDASAMY, J. & GRASMICK, A. 2011. Influence of supporting media in suspension on membrane fouling reduction in submerged membrane bioreactor (SMBR). *Journal of membrane science*, 374, 121-128.
- JUDD, S. 2008. The status of membrane bioreactor technology. *Trends in biotechnology*, 26, 109-116.
- JUDD, S. 2010. *The MBR book: principles and applications of membrane bioreactors for water and wastewater treatment*, Elsevier.
- K SE-MUTLU, B., ERG N-CAN, T., KOYUNCU, İ. & LEE, C.-H. 2015. Quorum quenching MBR operations for biofouling control under different operation conditions and using different immobilization media. *Desalination and Water Treatment*, 1-11.
- KAI, K., FUJII, H., IKENAKA, R., AKAGAWA, M. & HAYASHI, H. 2014. An

- acyl-SAM analog as an affinity ligand for identifying quorum sensing signal synthases. *Chemical Communications*, 50, 8586-8589.
- KAPLAN, J. 2010. Biofilm dispersal: mechanisms, clinical implications, and potential therapeutic uses. *Journal of dental research*, 89, 205-218.
- KAPLAN, J. B., RAGUNATH, C., VELLIYAGOUNDER, K., FINE, D. H. & RAMASUBBU, N. 2004. Enzymatic detachment of *Staphylococcus epidermidis* biofilms. *Antimicrobial agents and chemotherapy*, 48, 2633-2636.
- KHAN, R., SHEN, F., KHAN, K., LIU, L., WU, H., LUO, J. & WAN, Y. 2016. Biofouling control in a membrane filtration system by a newly isolated novel quorum quenching bacterium, *Bacillus methylotrophicus* sp. WY. *RSC Advances*, 6, 28895-28903.
- KHIL, M. S., BHATTARAI, S. R., KIM, H. Y., KIM, S. Z. & LEE, K. H. 2005. Novel fabricated matrix via electrospinning for tissue engineering. *Journal of Biomedical Materials Research Part B: Applied Biomaterials*, 72, 117-124.
- KIM, C., CHOI, Y.-O., LEE, W.-J. & YANG, K.-S. 2004a. Supercapacitor performances of activated carbon fiber webs prepared by electrospinning of PMDA-ODA poly (amic acid) solutions. *Electrochimica Acta*, 50, 883-887.
- KIM, C., PARK, S.-H., LEE, W.-J. & YANG, K.-S. 2004b. Characteristics of supercapacitor electrodes of PBI-based carbon nanofiber web prepared by electrospinning. *Electrochimica Acta*, 50, 877-881.
- KIM, H.-W., OH, H.-S., KIM, S.-R., LEE, K.-B., YEON, K.-M., LEE, C.-H., KIM, S. & LEE, J.-K. 2013a. Microbial population dynamics and proteomics in membrane bioreactors with enzymatic quorum quenching. *Applied microbiology and biotechnology*, 97, 4665-4675.
- KIM, J.-H., CHOI, D.-C., YEON, K.-M., KIM, S.-R. & LEE, C.-H. 2011. Enzyme-immobilized nanofiltration membrane to mitigate biofouling based on quorum quenching. *Environmental science & technology*, 45, 1601-1607.
- KIM, S.-R., LEE, K.-B., KIM, J.-E., WON, Y.-J., YEON, K.-M., LEE, C.-H. & LIM, D.-J. 2015. Macroencapsulation of quorum quenching bacteria by polymeric membrane layer and its application to MBR for biofouling control. *Journal of Membrane Science*, 473, 109-117.
- KIM, S.-R., OH, H.-S., JO, S.-J., YEON, K.-M., LEE, C.-H., LIM, D.-J., LEE, C.-H. & LEE, J.-K. 2013b. Biofouling control with bead-entrapped quorum quenching bacteria in membrane bioreactors: physical and biological effects. *Environmental science & technology*, 47, 836-842.
- KJELLEBERG, S. & GIVSKOV, M. 2007. *The biofilm mode of life: mechanisms and adaptations*, Horizon Scientific Press.
- KLAUSEN, M., AAES-JORGENSEN, A., MOLIN, S. & TOLKER-NIELSEN, T. 2003. Involvement of bacterial migration in the development of complex multicellular structures in *Pseudomonas aeruginosa* biofilms. *Molecular Microbiology*, 50, 61-68.
- KLEEREBEZEM, M., QUADRI, L. E., KUIPERS, O. P. & DE VOS, W. M. 1997. Quorum sensing by peptide pheromones and two-component signal-transduction systems in Gram-positive bacteria. *Molecular microbiology*, 24, 895-904.

- KOSTAKIOTI, M., HADJIFRANGISKOU, M. & HULTGREN, S. J. 2013. Bacterial biofilms: development, dispersal, and therapeutic strategies in the dawn of the postantibiotic era. *Cold Spring Harbor perspectives in medicine*, 3, a010306.
- LABBATE, M., QUEEK, S. Y., KOH, K. S., RICE, S. A., GIVSKOV, M. & KJELLEBERG, S. 2004. Quorum sensing-controlled biofilm development in *Serratia liquefaciens* MG1. *Journal of Bacteriology*, 186, 692-698.
- LASARRE, B. & FEDERLE, M. J. 2013. Exploiting quorum sensing to confuse bacterial pathogens. *Microbiology and Molecular Biology Reviews*, 77, 73-111.
- LE CLECH, P., JEFFERSON, B., CHANG, I. S. & JUDD, S. J. 2003. Critical flux determination by the flux-step method in a submerged membrane bioreactor. *Journal of membrane science*, 227, 81-93.
- LEADBETTER, J. R. & GREENBERG, E. 2000. Metabolism of acyl-homoserine lactone quorum-sensing signals by *Variovorax paradoxus*. *Journal of Bacteriology*, 182, 6921-6926.
- LEE, J.-H., KAPLAN, J. B. & LEE, W. Y. 2008. Microfluidic devices for studying growth and detachment of *Staphylococcus epidermidis* biofilms. *Biomedical microdevices*, 10, 489-498.
- LEE, J. M., HEITMANN, J. A. & PAWLAK, J. J. 2007. Rheology of carboxymethyl cellulose solutions treated with cellulases. *BioResources*, 2, 20-33.
- LEE, S., LEE, S. H., LEE, K., KWON, H., NAHM, C. H., LEE, C. H., PARK, P. K., CHOO, K. H., LEE, J. K. & OH, H. S. 2016a. Effect of the Shape and Size of Quorum-Quenching Media on Biofouling Control in Membrane Bioreactors for Wastewater Treatment. *J Microbiol Biotechnol*, 26, 1746-1754.
- LEE, S., PARK, S.-K., KWON, H., LEE, S. H., LEE, K., NAHM, C. H., JO, S. J., OH, H.-S., PARK, P.-K. & CHOO, K.-H. 2016b. Crossing the Border between Laboratory and Field: Bacterial Quorum Quenching for Anti-Biofouling Strategy in an MBR. *Environmental science & technology*, 50, 1788-1795.
- LEE, S. H., LEE, S., LEE, K., NAHM, C. H., KWON, H., OH, H.-S., WON, Y.-J., CHOO, K.-H., LEE, C.-H. & PARK, P.-K. 2016c. More Efficient Media Design for Enhanced Biofouling Control in a Membrane Bioreactor: Quorum Quenching Bacteria Entrapping Hollow Cylinder. *Environmental Science & Technology*, 50, 8596-8604.
- LEQUETTE, Y., BOELS, G., CLARISSE, M. & FAILLE, C. 2010. Using enzymes to remove biofilms of bacterial isolates sampled in the food-industry. *Biofouling*, 26, 421-431.
- LEROY, C., DELBARRE, C., GHILLEBAERT, F., COMPERE, C. & COMBES, D. 2008a. Effects of commercial enzymes on the adhesion of a marine biofilm-forming bacterium. *Biofouling*, 24, 11-22.
- LEROY, C., DELBARRE, C., GHILLEBAERT, F., COMPERE, C. & COMBES, D. 2008b. Influence of subtilisin on the adhesion of a marine bacterium which produces mainly proteins as extracellular polymers. *Journal of applied microbiology*, 105, 791-799.
- LI, D., WANG, R. & CHUNG, T.-S. 2004. Fabrication of lab-scale hollow fiber

- membrane modules with high packing density. *Separation and purification technology*, 40, 15-30.
- LI, J., ATTILA, C., WANG, L., WOOD, T. K., VALDES, J. J. & BENTLEY, W. E. 2007. Quorum sensing in *Escherichia coli* is signaled by AI-2/LsrR: Effects on small RNA and Biofilm architecture. *Journal of Bacteriology*, 189, 6011-6020.
- LINDUM, P. W., ANTHONI, U., CHRISTOPHERSEN, C., EBERL, L., MOLIN, S. & GIVSKOV, M. 1998. N-Acyl-L-homoserine lactone autoinducers control production of an extracellular lipopeptide biosurfactant required for swarming motility of *Serratia liquefaciens* MG1. *Journal of bacteriology*, 180, 6384-6388.
- LOISELLE, M. & ANDERSON, K. W. 2003. The use of cellulase in inhibiting biofilm formation from organisms commonly found on medical implants. *Biofouling*, 19, 77-85.
- LOWERY, C. A., DICKERSON, T. J. & JANDA, K. D. 2008. Interspecies and interkingdom communication mediated by bacterial quorum sensing. *Chemical Society Reviews*, 37, 1337-1346.
- LU, T. K. & COLLINS, J. J. 2007. Dispersing biofilms with engineered enzymatic bacteriophage. *Proceedings of the National Academy of Sciences*, 104, 11197-11202.
- LYNCH, M. J., SWIFT, S., KIRKE, D. F., KEEVIL, C. W., DODD, C. E. R. & WILLIAMS, P. 2002. The regulation of biofilm development by quorum sensing in *Aeromonas hydrophila*. *Environmental Microbiology*, 4, 18-28.
- MA, Z., KOTAKI, M., INAI, R. & RAMAKRISHNA, S. 2005. Potential of nanofiber matrix as tissue-engineering scaffolds. *Tissue engineering*, 11, 101-109.
- MAARTENS, A., SWART, P. & JACOBS, E. 1996. An enzymatic approach to the cleaning of ultrafiltration membranes fouled in abattoir effluent. *Journal of membrane science*, 119, 9-16.
- MAH, T.-F., PITTS, B., PELLOCK, B., WALKER, G. C., STEWART, P. S. & O'TOOLE, G. A. 2003. A genetic basis for *Pseudomonas aeruginosa* biofilm antibiotic resistance. *Nature*, 426, 306-310.
- MAIRA-LITR N, T., KROPEC, A., ABEYGUNAWARDANA, C., JOYCE, J., MARK, G., GOLDMANN, D. A. & PIER, G. B. 2002. Immunochemical properties of the staphylococcal poly-N-acetylglucosamine surface polysaccharide. *Infection and Immunity*, 70, 4433-4440.
- MANEFIELD, M., DE NYS, R., NARESH, K., ROGER, R., GIVSKOV, M., PETER, S. & KJELLEBERG, S. 1999. Evidence that halogenated furanones from *Delisea pulchra* inhibit acylated homoserine lactone (AHL)-mediated gene expression by displacing the AHL signal from its receptor protein. *Microbiology*, 145, 283-291.
- MANEFIELD, M., RASMUSSEN, T. B., HENZTER, M., ANDERSEN, J. B., STEINBERG, P., KJELLEBERG, S. & GIVSKOV, M. 2002. Halogenated furanones inhibit quorum sensing through accelerated LuxR turnover. *Microbiology*, 148, 1119-1127.
- MANUAL, I. Quick Start™ Bradford Protein Assay.
- MAQBOOL, T., KHAN, S. J., WAHEED, H., LEE, C.-H., HASHMI, I. & IQBAL, H. 2015. Membrane biofouling retardation and improved sludge



- characteristics using quorum quenching bacteria in submerged membrane bioreactor. *Journal of Membrane Science*, 483, 75-83.
- MASHBURN, L. M. & WHITELEY, M. 2005. Membrane vesicles traffic signals and facilitate group activities in a prokaryote. *Nature*, 437, 422-425.
- MASUKO, T., MINAMI, A., IWASAKI, N., MAJIMA, T., NISHIMURA, S.-I. & LEE, Y. C. 2005. Carbohydrate analysis by a phenol-sulfuric acid method in microplate format. *Analytical biochemistry*, 339, 69-72.
- MATSUKAWA, M. & GREENBERG, E. 2004. Putative exopolysaccharide synthesis genes influence *Pseudomonas aeruginosa* biofilm development. *Journal of bacteriology*, 186, 4449-4456.
- MATTHYSSE, A. G. & MCMAHAN, S. 1998. Root colonization by *Agrobacterium tumefaciens* is reduced in cel, attB, attD, and attR mutants. *Applied and environmental microbiology*, 64, 2341-2345.
- MATTHYSSE, A. G., WHITE, S. & LIGHTFOOT, R. 1995. Genes required for cellulose synthesis in *Agrobacterium tumefaciens*. *Journal of bacteriology*, 177, 1069-1075.
- MC GRATH, S. & VAN SINDEREN, D. 2007. *Bacteriophage: genetics and molecular biology*, Horizon Scientific Press.
- MCADAM, E., EUSEBI, A. & JUDD, S. 2010a. Evaluation of intermittent air sparging in an anoxic denitrification membrane bioreactor. *Water Science and Technology*, 61, 2219-2225.
- MCADAM, E. J., PAWLETT, M. & JUDD, S. J. 2010b. Fate and impact of organics in an immersed membrane bioreactor applied to brine denitrification and ion exchange regeneration. *Water research*, 44, 69-76.
- MCCLEAN, K. H., WINSON, M. K., FISH, L., TAYLOR, A., CHHABRA, S. R., CAMARA, M., DAYKIN, M., LAMB, J. H., SWIFT, S. & BYCROFT, B. W. 1997. Quorum sensing and *Chromobacterium violaceum*: exploitation of violacein production and inhibition for the detection of N-acylhomoserine lactones. *Microbiology*, 143, 3703-3711.
- MCDUGALD, D., RICE, S. A., BARRAUD, N., STEINBERG, P. D. & KJELLEBERG, S. 2012. Should we stay or should we go: mechanisms and ecological consequences for biofilm dispersal. *Nature Reviews Microbiology*, 10, 39-50.
- MENG, F., CHAE, S.-R., DREWS, A., KRAUME, M., SHIN, H.-S. & YANG, F. 2009. Recent advances in membrane bioreactors (MBRs): membrane fouling and membrane material. *Water research*, 43, 1489-1512.
- MILLER, M. B. & BASSLER, B. L. 2001. Quorum sensing in bacteria. *Annual Reviews in Microbiology*, 55, 165-199.
- MONCLUS, H., ZACHARIAS, S., SANTOS, A., PIDOU, M. & JUDD, S. 2010. Criticality of flux and aeration for a hollow fiber membrane bioreactor. *Separation Science and Technology*, 45, 956-961.
- MU OZ, C., HIDALGO, C., ZAPATA, M., JEISON, D., RIQUELME, C. & RIVAS, M. 2014. Use of cellulolytic marine bacteria for enzymatic pretreatment in microalgal biogas production. *Applied and environmental microbiology*, 80, 4199-4206.
- N EZ, M. & LEMA, J. 1987. Cell immobilization: Application to alcohol production. *Enzyme and microbial technology*, 9, 642-651.
- NADELL, C. D., XAVIER, J. B., LEVIN, S. A. & FOSTER, K. R. 2008. The

- evolution of quorum sensing in bacterial biofilms. *PLoS Biol*, 6, e14.
- NAGAOKA, H., UEDA, S. & MIYA, A. 1996. Influence of bacterial extracellular polymers on the membrane separation activated sludge process. *Water Science and Technology*, 34, 165-172.
- NAPOLI, C., DAZZO, F. & HUBBELL, D. 1975. Production of cellulose microfibrils by *Rhizobium*. *Applied microbiology*, 30, 123-131.
- NG, W. L. & BASSLER, B. L. 2009. Bacterial Quorum-Sensing Network Architectures. *Annual Review of Genetics*, 43, 197-222.
- NGUYEN, L. N., HAI, F. I., KANG, J., PRICE, W. E. & NGHIEM, L. D. 2012. Removal of trace organic contaminants by a membrane bioreactor–granular activated carbon (MBR–GAC) system. *Bioresource technology*, 113, 169-173.
- NIJLAND, R., HALL, M. J. & BURGESS, J. G. 2010. Dispersal of biofilms by secreted, matrix degrading, bacterial DNase. *PLoS One*, 5, e15668.
- NOVICK, R. P. & MUIR, T. W. 1999. Virulence gene regulation by peptides in staphylococci and other Gram-positive bacteria. *Current opinion in microbiology*, 2, 40-45.
- O'TOOLE, G. A. 2011. Microtiter dish biofilm formation assay. *JoVE (Journal of Visualized Experiments)*, e2437-e2437.
- OH, H.-S., KIM, S.-R., CHEONG, W.-S., LEE, C.-H. & LEE, J.-K. 2013. Biofouling inhibition in MBR by *Rhodococcus* sp. BH4 isolated from real MBR plant. *Applied microbiology and biotechnology*, 97, 10223-10231.
- OH, H.-S., YEON, K.-M., YANG, C.-S., KIM, S.-R., LEE, C.-H., PARK, S. Y., HAN, J. Y. & LEE, J.-K. 2012. Control of membrane biofouling in MBR for wastewater treatment by quorum quenching bacteria encapsulated in microporous membrane. *Environmental science & technology*, 46, 4877-4884.
- PARADOSSI, G., CAVALIERI, F., CHIESSI, E., SPAGNOLI, C. & COWMAN, M. K. 2003. Poly (vinyl alcohol) as versatile biomaterial for potential biomedical applications. *Journal of Materials Science: Materials in Medicine*, 14, 687-691.
- PARSEK, M. R. & GREENBERG, E. P. 2000. Acyl-homoserine lactone quorum sensing in Gram-negative bacteria: A signaling mechanism involved in associations with higher organisms. *Proceedings of the National Academy of Sciences of the United States of America*, 97, 8789-8793.
- PARSEK, M. R., VAL, D. L., HANZELKA, B. L., CRONAN, J. E. & GREENBERG, E. 1999. Acyl homoserine-lactone quorum-sensing signal generation. *Proceedings of the National Academy of Sciences*, 96, 4360-4365.
- PARVEEN, N. & CORNELL, K. A. 2011. Methylthioadenosine/S-adenosylhomocysteine nucleosidase, a critical enzyme for bacterial metabolism. *Molecular microbiology*, 79, 7-20.
- PAUL, D., KIM, Y. S., PONNUSAMY, K. & KWEON, J. H. 2009. Application of quorum quenching to inhibit biofilm formation. *Environmental Engineering Science*, 26, 1319-1324.
- PAUL, K., ERHARDT, M., HIRANO, T., BLAIR, D. F. & HUGHES, K. T. 2008. Energy source of flagellar type III secretion. *Nature*, 451, 489-492.
- PERSSON, T., HANSEN, T. H., RASMUSSEN, T. B., SKINDERSO, M. E.,

- GIVSKOV, M. & NIELSEN, J. 2005. Rational design and synthesis of new quorum-sensing inhibitors derived from acylated homoserine lactones and natural products from garlic. *Organic & Biomolecular Chemistry*, 3, 253-262.
- PESCI, E. C., MILBANK, J. B. J., PEARSON, J. P., MCKNIGHT, S., KENDE, A. S., GREENBERG, E. P. & IGLEWSKI, B. H. 1999. Quinolone signaling in the cell-to-cell communication system of *Pseudomonas aeruginosa*. *Proceedings of the National Academy of Sciences of the United States of America*, 96, 11229-11234.
- POLLICE, A., BROOKES, A., JEFFERSON, B. & JUDD, S. 2005. Sub-critical flux fouling in membrane bioreactors—a review of recent literature. *Desalination*, 174, 221-230.
- RIBOLDI, S. A., SAMPAOLESI, M., NEUENSCHWANDER, P., COSSU, G. & MANTERO, S. 2005. Electrospun degradable polyesterurethane membranes: potential scaffolds for skeletal muscle tissue engineering. *Biomaterials*, 26, 4606-4615.
- ROBLEDO, M., RIVERA, L., JIM NEZ-ZURDO, J. I., RIVAS, R., DAZZO, F., VEL ZQUEZ, E., MART NEZ-MOLINA, E., HIRSCH, A. M. & MATEOS, P. F. 2012. Role of *Rhizobium* endoglucanase CelC2 in cellulose biosynthesis and biofilm formation on plant roots and abiotic surfaces. *Microbial cell factories*, 11, 1.
- ROSENBERGER, S., HELMUS, F., KRAUSE, S., BARETH, A. & MEYER-BLUMENROTH, U. 2011. Principles of an enhanced MBR-process with mechanical cleaning. *Water Science and Technology*, 64, 1951-1958.
- ROSS, P., MAYER, R. & BENZIMAN, M. 1991. Cellulose biosynthesis and function in bacteria. *Microbiological reviews*, 55, 35-58.
- RUBY, E. G. & LEE, K.-H. 1998. The *Vibrio fischeri*-*Euprymna scolopes* light organ association: current ecological paradigms. *Applied and environmental microbiology*, 64, 805-812.
- RYAN, R. P. & DOW, J. M. 2011. Communication with a growing family: diffusible signal factor (DSF) signaling in bacteria. *Trends in microbiology*, 19, 145-152.
- RYAN, R. P., FOUHY, Y., LUCEY, J. F., CROSSMAN, L. C., SPIRO, S., HE, Y.-W., ZHANG, L.-H., HEEB, S., C MARA, M. & WILLIAMS, P. 2006. Cell-cell signaling in *Xanthomonas campestris* involves an HD-GYP domain protein that functions in cyclic di-GMP turnover. *Proceedings of the National Academy of Sciences*, 103, 6712-6717.
- SACHIDANANDHAM, R., YEW-HOONG GIN, K. & LAA POH, C. 2005. Monitoring of active but non-culturable bacterial cells by flow cytometry. *Biotechnology and bioengineering*, 89, 24-31.
- SAGHI, H., MORADI, F., MOHSENI, R., ABADI, A. H., ATAEE, R. A., ZADEH, P. B., MESKINI, M. & ESMAEILI, D. 2015. Quorum Sensing in Bacterial Pathogenesis. *Global Journal of Infectious Diseases and Clinical Research*, 1, 004-009.
- SALALHA, W., KUHN, J., DROR, Y. & ZUSSMAN, E. 2006. Encapsulation of bacteria and viruses in electrospun nanofibres. *Nanotechnology*, 17, 4675.
- SANTOS, A., MA, W. & JUDD, S. J. 2011. Membrane bioreactors: two decades of research and implementation. *Desalination*, 273, 148-154.

- SCHAEFER, A. L., HANZELKA, B. L., EBERHARD, A. & GREENBERG, E. P. 1996. Quorum sensing in *Vibrio fischeri*: Probing autoinducer-LuxR interactions with autoinducer analogs. *Journal of Bacteriology*, 178, 2897-2901.
- SCHREUDER-GIBSON, H., GIBSON, P., WADSWORTH, L., HEMPHILL, S. & VONTORCIK, J. 2002. Effect of filter deformation on the filtration and air flow for elastomeric nonwoven media. *Adv Filtr Sep Technol*, 15, 525-537.
- SCHREUDER-GIBSON, H. L., GIBSON, P., TSAI, P., GUPTA, P. & WILKES, G. 2005. Cooperative charging effects of fibers from electrospinning of electrically dissimilar polymers. DTIC Document.
- SCOTT JR, T. A. & MELVIN, E. H. 1953. Determination of dextran with anthrone. *Analytical Chemistry*, 25, 1656-1661.
- SERRA, D. O., RICHTER, A. M. & HENGGE, R. 2013. Cellulose as an architectural element in spatially structured *Escherichia coli* biofilms. *Journal of bacteriology*, 195, 5540-5554.
- SHAW, P. D., PING, G., DALY, S. L., CHA, C., CRONAN, J. E., RINEHART, K. L. & FARRAND, S. K. 1997. Detecting and characterizing N-acyl-homoserine lactone signal molecules by thin-layer chromatography. *Proceedings of the National Academy of Sciences*, 94, 6036-6041.
- SHEU, S.-Y., LIN, Y.-S., CHEN, J.-C., KWON, S.-W. & CHEN, W.-M. 2014. *Undibacterium squillarum* sp. nov., isolated from a freshwater shrimp culture pond. *International journal of systematic and evolutionary microbiology*, 64, 3459-3466.
- SIMÕES, M., SIMES, L. C. & VIEIRA, M. J. 2010. A review of current and emergent biofilm control strategies. *LWT-Food Science and Technology*, 43, 573-583.
- SLATER, H., ALVAREZ-MORALES, A., BARBER, C. E., DANIELS, M. J. & DOW, J. M. 2000. A two-component system involving an HD-GYP domain protein links cell-cell signalling to pathogenicity gene expression in *Xanthomonas campestris*. *Molecular microbiology*, 38, 986-1003.
- SMITH, D. J., RENEKER, D. H., MCMANUS, A. T., SCHREUDER-GIBSON, H. L., MELLO, C. & SENNETT, M. S. 2004. Electrospun fibers and an apparatus therefor. Google Patents.
- SOLANO, C., GARCIA, B., VALLE, J., BERASAIN, C., GHIGO, J. M., GAMAZO, C. & LASA, I. 2002. Genetic analysis of *Salmonella enteritidis* biofilm formation: critical role of cellulose. *Molecular microbiology*, 43, 793-808.
- SPIERS, A. J., DEENI, Y. Y., FOLORUNSO, A. O., KOZA, A., MOSHYNETS, O. & ZAWADZKI, K. 2013. Cellulose expression in *Pseudomonas fluorescens* SBW25 and other environmental pseudomonads. *Cellulose*.
- SPIERS, A. J. & RAINEY, P. B. 2005. The *Pseudomonas fluorescens* SBW25 wrinkly spreader biofilm requires attachment factor, cellulose fibre and LPS interactions to maintain strength and integrity. *Microbiology*, 151, 2829-2839.
- STEIDLE, A., SIGL, K., SCHUHEGGER, R., IHRING, A., SCHMID, M., GANTNER, S., STOFFELS, M., RIEDEL, K., GIVSKOV, M. & HARTMANN, A. 2001. Visualization of N-acylhomoserine lactone-mediated cell-cell communication between bacteria colonizing the tomato

- rhizosphere. *Applied and Environmental Microbiology*, 67, 5761-5770.
- STEINDLER, L. & VENTURI, V. 2007. Detection of quorum-sensing N-acyl homoserine lactone signal molecules by bacterial biosensors. *FEMS Microbiology Letters*, 266, 1-9.
- SUTHERLAND, I. W. 2001. The biofilm matrix—an immobilized but dynamic microbial environment. *Trends in microbiology*, 9, 222-227.
- SWEITY, A., YING, W., ALI-SHTAYEH, M. S., YANG, F., BICK, A., ORON, G. & HERZBERG, M. 2011. Relation between EPS adherence, viscoelastic properties, and MBR operation: Biofouling study with QCM-D. *Water research*, 45, 6430-6440.
- SWIFT, S., KARLYSHEV, A. V., FISH, L., DURANT, E. L., WINSON, M. K., CHHABRA, S. R., WILLIAMS, P., MACINTYRE, S. & STEWART, G. 1997. Quorum sensing in *Aeromonas hydrophila* and *Aeromonas salmonicida*: identification of the LuxRI homologs AhyRI and AsaRI and their cognate N-acylhomoserine lactone signal molecules. *Journal of bacteriology*, 179, 5271-5281.
- TAKEI, T., IKEDA, K., IJIMA, H. & KAWAKAMI, K. 2011. Fabrication of poly (vinyl alcohol) hydrogel beads crosslinked using sodium sulfate for microorganism immobilization. *Process Biochemistry*, 46, 566-571.
- TE POELE, S. & VAN DER GRAAF, J. 2005. Enzymatic cleaning in ultrafiltration of wastewater treatment plant effluent. *Desalination*, 179, 73-81.
- TEATHER, R. M. & WOOD, P. J. 1982. Use of Congo red-polysaccharide interactions in enumeration and characterization of cellulolytic bacteria from the bovine rumen. *Applied and environmental microbiology*, 43, 777-780.
- TEPLITSKI, M., EBERHARD, A., GRONQUIST, M. R., GAO, M., ROBINSON, J. B. & BAUER, W. D. 2003. Chemical identification of N-acyl homoserine lactone quorum-sensing signals produced by *Sinorhizobium meliloti* strains in defined medium. *Archives of microbiology*, 180, 494-497.
- THIEL, V., VILCHEZ, R., SZTAJER, H., WAGNER-D BLER, I. & SCHULZ, S. 2009. Identification, Quantification, and Determination of the Absolute Configuration of the Bacterial Quorum-Sensing Signal Autoinducer-2 by Gas Chromatography–Mass Spectrometry. *ChemBioChem*, 10, 479-485.
- TOMASZ, A. 1965. Control of the competent state in *Pneumococcus* by a hormone-like cell product: an example for a new type of regulatory mechanism in bacteria.
- TRIVEDI, A., MAVI, P. S., BHATT, D. & KUMAR, A. 2016. Thiol reductive stress induces cellulose-anchored biofilm formation in *Mycobacterium tuberculosis*. *Nature communications*, 7.
- TSUYUHARA, T., HANAMOTO, Y., MIYOSHI, T., KIMURA, K. & WATANABE, Y. 2010. Influence of membrane properties on physically reversible and irreversible fouling in membrane bioreactors. *Water Science and Technology*, 61, 2235-2240.
- UDE, S., ARNOLD, D. L., MOON, C. D., TIMMS-WILSON, T. & SPIERS, A. J. 2006. Biofilm formation and cellulose expression among diverse environmental *Pseudomonas* isolates. *Environmental Microbiology*, 8, 1997-2011.
- UPDEGRAFF, D. M. 1969. Semimicro determination of cellulose in biological

- materials. *Analytical biochemistry*, 32, 420-424.
- UROZ, S., CHHABRA, S. R., CAMARA, M., WILLIAMS, P., OGER, P. & DESSAUX, Y. 2005. N-Acylhomoserine lactone quorum-sensing molecules are modified and degraded by *Rhodococcus erythropolis* W2 by both amidolytic and novel oxidoreductase activities. *Microbiology*, 151, 3313-3322.
- VASSEUR, P., VALLET-GELY, I., SOSCIA, C., GENIN, S. & FILLOUX, A. 2005. The *pel* genes of the *Pseudomonas aeruginosa* PAK strain are involved at early and late stages of biofilm formation. *Microbiology*, 151, 985-997.
- VENTURI, V. 2006. Regulation of quorum sensing in *Pseudomonas*. *FEMS microbiology reviews*, 30, 274-291.
- VU, B., CHEN, M., CRAWFORD, R. J. & IVANOVA, E. P. 2009. Bacterial extracellular polysaccharides involved in biofilm formation. *Molecules*, 14, 2535-2554.
- WANG, J., QUAN, C., WANG, X., ZHAO, P. & FAN, S. 2011. Extraction, purification and identification of bacterial signal molecules based on N-acyl homoserine lactones. *Microbial biotechnology*, 4, 479-490.
- WANG, L. H., HE, Y., GAO, Y., WU, J. E., DONG, Y. H., HE, C., WANG, S. X., WENG, L. X., XU, J. L. & TAY, L. 2004a. A bacterial cell-cell communication signal with cross-kingdom structural analogues. *Molecular microbiology*, 51, 903-912.
- WANG, R., LI, D., ZHOU, C., LIU, M. & LIANG, D. 2004b. Impact of DEA solutions with and without CO<sub>2</sub> loading on porous polypropylene membranes intended for use as contactors. *Journal of Membrane Science*, 229, 147-157.
- WANG, X., KIM, Y.-G., DREW, C., KU, B.-C., KUMAR, J. & SAMUELSON, L. A. 2004c. Electrostatic assembly of conjugated polymer thin layers on electrospun nanofibrous membranes for biosensors. *Nano Letters*, 4, 331-334.
- WANG, Z., WU, Z. & TANG, S. 2009. Extracellular polymeric substances (EPS) properties and their effects on membrane fouling in a submerged membrane bioreactor. *Water research*, 43, 2504-2512.
- WANNATONG, L. & SIRIVAT, A. 2004. Electrospun fibers of polypyrrole/polystyrene blend for gas sensing applications. *Polymeric Materials Science and Engineering*, 91.
- WATERS, C. M. & BASSLER, B. L. 2005. Quorum sensing: cell-to-cell communication in bacteria. *Annu. Rev. Cell Dev. Biol.*, 21, 319-346.
- WEERASEKARA, N. A., CHOO, K.-H. & LEE, C.-H. 2014. Hybridization of physical cleaning and quorum quenching to minimize membrane biofouling and energy consumption in a membrane bioreactor. *Water research*, 67, 1-10.
- WHITE, A., GIBSON, D., KIM, W., KAY, W. & SURETTE, M. 2006. Thin aggregative fimbriae and cellulose enhance long-term survival and persistence of *Salmonella*. *Journal of bacteriology*, 188, 3219-3227.
- WIATER, A., SZCZODRAK, J. & ROGALSKI, J. 2004. Hydrolysis of mutan and prevention of its formation in streptococcal films by fungal  $\alpha$ -D-glucanases. *Process Biochemistry*, 39, 1481-1489.
- WILLIAMS, W. S. & CANNON, R. E. 1989. Alternative environmental roles for

- cellulose produced by *Acetobacter xylinum*. *Applied and environmental microbiology*, 55, 2448-2452.
- WINSON, M. K., SWIFT, S., FISH, L., THROUP, J. P., J RGENSEN, F., CHHABRA, S. R., BYCROFT, B. W., WILLIAMS, P. & STEWART, G. S. 1998. Construction and analysis of luxCDABE-based plasmid sensors for investigating N-acyl homoserine lactone-mediated quorum sensing. *FEMS microbiology letters*, 163, 185-192.
- WITHERS, H., SWIFT, S. & WILLIAMS, P. 2001. Quorum sensing as an integral component of gene regulatory networks in Gram-negative bacteria. *Current opinion in microbiology*, 4, 186-193.
- WOOD, D. W., GONG, F., DAYKIN, M. M., WILLIAMS, P. & PIERSON, L. 1997. N-acyl-homoserine lactone-mediated regulation of phenazine gene expression by *Pseudomonas aureofaciens* 30-84 in the wheat rhizosphere. *Journal of Bacteriology*, 179, 7663-7670.
- XIE, S., TAI, S., SONG, H., LUO, X., ZHANG, H. & LI, X. 2016. Genetically engineering of *Escherichia coli* and immobilization on electrospun fibers for drug delivery purposes. *Journal of Materials Chemistry B*, 4, 6820-6829.
- XIONG, Y. & LIU, Y. 2010. Biological control of microbial attachment: a promising alternative for mitigating membrane biofouling. *Applied microbiology and biotechnology*, 86, 825-837.
- XU, H. & LIU, Y. 2010. Control of microbial attachment by inhibition of ATP and ATP-mediated autoinducer-2. *Biotechnology and bioengineering*, 107, 31-36.
- YAMAMOTO, K., HIASA, M., MAHMOOD, T. & MATSUO, T. 1989. Direct solid-liquid separation using hollow fiber membrane in an activated sludge aeration tank. *Water Science and Technology*, 21, 43-54.
- YANG, F., MURUGAN, R., WANG, S. & RAMAKRISHNA, S. 2005. Electrospinning of nano/micro scale poly (L-lactic acid) aligned fibers and their potential in neural tissue engineering. *Biomaterials*, 26, 2603-2610.
- YANG, Q., LI, Z., HONG, Y., ZHAO, Y., QIU, S., WANG, C. & WEI, Y. 2004. Influence of solvents on the formation of ultrathin uniform poly (vinyl pyrrolidone) nanofibers with electrospinning. *Journal of Polymer Science Part B: Polymer Physics*, 42, 3721-3726.
- YEOM, I-T., NAH, Y-M. & AHN, K-H. 1999. Treatment of household wastewater using an intermittently aerated membrane bioreactor. *Desalination*, 124, 193-203.
- YEON, K.-M., CHEONG, W.-S., OH, H.-S., LEE, W.-N., HWANG, B.-K., LEE, C.-H., BEYENAL, H. & LEWANDOWSKI, Z. 2008. Quorum sensing: a new biofouling control paradigm in a membrane bioreactor for advanced wastewater treatment. *Environmental science & technology*, 43, 380-385.
- YEON, K.-M., LEE, C.-H. & KIM, J. 2009. Magnetic enzyme carrier for effective biofouling control in the membrane bioreactor based on enzymatic quorum quenching. *Environmental science & technology*, 43, 7403-7409.
- YIGIT, N., HARMAN, I., CIVELEKOGLU, G., KOSEOGLU, H., CICEK, N. & KITIS, M. 2008. Membrane fouling in a pilot-scale submerged membrane bioreactor operated under various conditions. *Desalination*, 231, 124-132.
- YOON, K., KIM, K., WANG, X., FANG, D., HSIAO, B. S. & CHU, B. 2006. High

- flux ultrafiltration membranes based on electrospun nanofibrous PAN scaffolds and chitosan coating. *Polymer*, 47, 2434-2441.
- YOON, S.-H. 2015. *Membrane bioreactor processes: Principles and applications*, CRC Press.
- YUNIARTO, A., NOOR, Z. Z., UJANG, Z., OLSSON, G., ARIS, A. & HADIBARATA, T. 2013. Bio-fouling reducers for improving the performance of an aerobic submerged membrane bioreactor treating palm oil mill effluent. *Desalination*, 316, 146-153.
- ZHANG, C., YUAN, X., WU, L., HAN, Y. & SHENG, J. 2005. Study on morphology of electrospun poly (vinyl alcohol) mats. *European polymer journal*, 41, 423-432.
- ZHANG, H., JIE, X., YANG, Y., ZIXING, W. & FENGLIN, Y. 2009. Mechanism of calcium mitigating membrane fouling in submerged membrane bioreactors. *Journal of Environmental Sciences*, 21, 1066-1073.
- ZHANG, J., CHUA, H. C., ZHOU, J. & FANE, A. 2006a. Factors affecting the membrane performance in submerged membrane bioreactors. *Journal of Membrane Science*, 284, 54-66.
- ZHANG, K., CHOI, H., DIONYSIOU, D. D., SORIAL, G. A. & OERTHER, D. B. 2006b. Identifying pioneer bacterial species responsible for biofouling membrane bioreactors. *Environmental Microbiology*, 8, 433-440.
- ZHANG, S., YANG, F., LIU, Y., ZHANG, X., YAMADA, Y. & FURUKAWA, K. 2006c. Performance of a metallic membrane bioreactor treating simulated distillery wastewater at temperatures of 30 to 45 C. *Desalination*, 194, 146-155.
- ZOGAJ, X., NIMTZ, M., ROHDE, M., BOKRANZ, W. & RMLING, U. 2001. The multicellular morphotypes of *Salmonella typhimurium* and *Escherichia coli* produce cellulose as the second component of the extracellular matrix. *Molecular microbiology*, 39, 1452-1463.